RECEIVED 11-6-67

MS-DV V SE000148 5R C01

MISSILE AND SPACE DIVISION

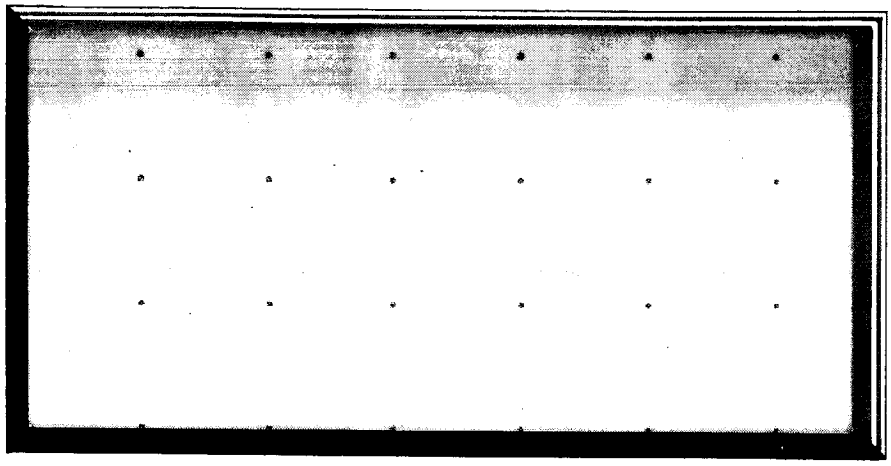

VOYAGER

GENERAL ELECTRIC

GPO PRICE $ _____

CFSTI PRICE(S) $ _____

Hard copy (HC) 3.00

Microfiche (MF) .65

ff 653 July 65

MAR 1968
RECEIVED
NASA STI FACILITY
INPUT BRANCH

N68-19093

(ACCESSION NUMBER)	(THRU)
114 (PAGES)	1 (CODE)
CR-93537 (NASA CR OR TMX OR AD NUMBER)	30 (CATEGORY)

FACILITY FORM 602

GENERAL ELECTRIC

DIN 67SD4379
16 OCTOBER 1967

FINAL REPORT

VOYAGER SPACECRAFT

PHASE B, TASK D

VOLUME IV (BOOK 4 OF 5)

MARS ATMOSPHERE DEFINITION

PREPARED FOR

GEORGE C. MARSHALL SPACE FLIGHT CENTER

UNDER MSFC CONTRACT NO. NAS8-22603

GENERAL ELECTRIC
MISSILE AND SPACE DIVISION
Valley Forge Space Technology Center
P.O. Box 8555 • Philadelphia 1, Penna.

VOLUME SUMMARY

The Voyager Phase B, Task D Final Report is contained in four volumes. The volume numbers and titles are as follows:

Volume I	Summary
Volume II	System Description
Book 1	Guidelines and Study Approach, System Functional Description
Book 2	Telecommunication
Book 3	Guidance and Control Computer and Sequencer Power Subsystem Electrical System
Book 4	Engineering Mechanics Propulsion Planet Scan Platform
Book 5	Design Standards Operational Support Equipment Mission Dependent Equipment
Volume III	Implementation Plan
Volume IV	Engineering Tasks
Book 1	Effect of Capsule RTG's on Spacecraft
Book 2	Applicability of Apollo Checkout Equipment
Book 3	Central Computer
Book 4	Mars Atmosphere Definition
Book 5	Photo-Imaging

TABLE OF CONTENTS

Section		Page
1	INTRODUCTION	1-1
	1.1 Objective	1-1
	1.2 Scope	1-1
	1.3 Reports	1-1
2	SUMMARY	2-1
	2.1 Physical Data	2-1
	2.2 Atmospheric Parameters Near the Surface	2-1
	2.3 Entry Atmosphere	2-2
	2.4 Outer Atmosphere Structure	2-2
	2.5 Clouds and Haze	2-3
	2.6 Chemical Kinetics and Composition	2-3
3	PHYSICAL DATA	3-1
4	ATMOSPHERIC PARAMETER NEAR SURFACE	4-1
	4.1 Introduction	4-1
	4.2 Composition and Pressure	4-2
	4.3 Temperature	4-3
	4.3.1 Diurnal Variation of Surface Temperature	4-5
	4.3.2 Latitudinal and Seasonal Variation of Surface Temperature	4-6
	4.3.3 Relations of Surface to Near-Surface Temperature	4-11
	4.4 Winds	4-13
	4.4.1 General Circulation	4-13
	4.4.2 Drift of Martian Clouds	4-15
	4.4.3 Dust Transport	4-19
	4.4.4 Design Wind Speeds	4-22
	4.5 Conclusions	4-22
	4.6 References	4-23
5	ENTRY ATMOSPHERE MODELS	5-1
	5.1 Introduction	5-1
	5.2 Near Surface Atmosphere	5-1
	5.2.1 Temperature	5-1
	5.2.2 Pressure	5-4

TABLE OF CONTENTS (Cont'd)

Section		Page
	5.3 Troposphere Characteristics	5-4
	5.3.1 Thermal Gradient	5-4
	5.3.2 Tropopause Altitude	5-5
	5.4 Discussion of Results	5-5
	5.5 Conclusions	5-8
	5.6 References	5-8
6	OUTER ATMOSPHERE STRUCTURE	6-1
	6.1 Introduction	6-1
	6.2 Predicted Solar Flux	6-1
	6.3 Exosphere	6-3
	6.3.1 Temperature Variation	6-3
	6.3.2 Altitude of Exosphere Base	6-4
	6.4 Thermosphere	6-5
	6.4.1 Altitude of Base	6-5
	6.4.2 Thermal Gradient	6-5
	6.4.3 Altitude of Top Thermosphere	6-6
	6.5 Outer Atmosphere Models	6-9
	6.5.1 VM-3 Model Extension	6-10
	6.5.2 GE Voyager Reference Atmosphere	6-12
	6.5.3 MSFC Atmosphere Model	6-14
	6.6 Variation of Atmospheric Density	6-17
	6.6.1 Diurnal Variation	6-17
	6.6.2 Solar Cyclic Variations	6-17
	6.7 Conclusions	6-20
	6.8 References	6-21
7	CLOUDS AND HAZE	7-1
	7.1 Introduction	7-1
	7.2 Blue Haze	7-1
	7.3 Blue Clouds	7-2
	7.4 White Clouds	7-2
	7.5 Yellow Clouds	7-3
	7.6 Conclusions	7-3
	7.7 References	7-4

TABLE OF CONTENTS (Cont'd)

Section		Page
8	CHEMICAL KINETICS AND COMPOSITION	8-1
8.1	Introduction	8-1
8.2	Atmospheric Data	8-1
8.3	Chemical System and Chemical Kinetics	8-4
8.3.1	Chemical Species	8-4
8.3.2	The Chemical Processes	8-5
8.3.3	Kinetics of Individual Species	8-8
8.4	Method of Calculation	8-8
8.5	Atmospheric Composition	8-11
8.5.1	Neutral Species	8-11
8.5.2	Charged Species	8-16
8.5.3	The Solar Flux	8-20
8.5.4	The Diffusion Problem	8-23
8.6	Conclusions	8-28
8.7	References	8-28

LIST OF ILLUSTRATIONS

Figure		Page
4-1	Observed Hourly Variation of Surface Temperature Near the Equator of Mars	4-5
4-2	Diurnal Variation of Surface Temperature on the Martian Equator at Perihelion	4-7
4-3	Hourly Variation of Surface Temperature Near the Equator of Mars	4-7
4-4	Spring-Autumn Latitudinal Variation of Temperature on Mars - Summary	4-9
4-5	Winter-Summer Variation of Temperature on Mars - Summary	4-9
4-6	Temperature Versus Time at the Equator of Mars at the Surface and at Z = 0.5 Meters	4-12
4-7	Schematic Diagrams of Solstice Circulation on Mars	4-14
4-8	Motion of Yellow (Dust) Clouds on Mars	4-16
4-9	Latitudinal Profile of Mean Zonal Wind for the Four Martian Seasons	4-18
4-10	Motion of Projections on Mars	4-20
5-1	Density Profile Variation with Season and Latitude	5-7
6-1	GE Voyager Reference Atmospheric Density Profile	6-14
6-2	Idealized Martian Molecular Weight Profiles	6-15
6-3	Perliminary Mean Profile and Confidence Envelopes for Martian Atmosphere Density	6-15
8-1	Density of Martian Atmosphere as a Function of Altitude	8-3
8-2	Schematic Representation of CO_2 Kinetics in Martian Atmosphere	8-9
8-3	Schematic Representation of CO Kinetics in Martian Atmosphere	8-9
8-4	Schematic Representation of Chemical Kinetics of Atomic Oxygen in Martian Atmosphere	8-10
8-5	Schematic Representation of Chemical Kinetics of N_2 in Martian Atmosphere	8-10
8-6	Flow Diagram of Computer Program Used for Martian Atmosphere Composition Calculations	8-12
8-7	Calculated Neutral Species Concentrations (80% CO_2, 20% N_2)	8-13
8-8	Calculated Neutral Species Concentrations (90% CO_2, 10% N_2)	8-14
8-9	Calculated Neutral Species Concentrations (100% CO_2)	8-15
8-10	Ion Concentrations Relative to Electron Density (80% CO_2, 20% N_2)	8-17
8-11	Ion Concentrations Relative to Electron Density (90% CO_2, 10% N_2)	8-18
8-12	Ion Concentrations Relative to Electron Density (100% CO_2)	8-19
8-13	Flux at Various Altitudes as a Function of Wavelength (80% CO_2, 20% N_2)	8-21
8-14	Flux/Incident Flux Versus Altitude	8-22

LIST OF TABLES

Table		Page
3-1	Physical Data for Mars	3-2
3-2	Physical Characteristics of Martian Moons.	3-3
4-1	Estimates of Atmospheric Pressure at the Surface Mars	4-4
4-2	Mean Temperature (°K) as a Function of Latitude and Season on Mars	4-10
4-3	Comparison of Surface to Near-Surface Temperature Differential	4-13
5-1	Voyager and Mars Entry Atmosphere Models	5-2
5-2	Mean Temperature (°K) as a Function of Latitude and Season on Mars	5-3
5-3	Latitude Variation of the Tropopause on Mars and Earth	5-6
5-4	Latitudinal Variation of Pressure and Density at 100 Kilometers on Mars and Earth	5-7
6-1	Predicted Values of the 10.7 cm Flux	6-2
6-2	Martian Exospheric Temperature (°K) as a Function of the 10.7 cm Solar Flux (S)	6-3
6-3	Comparison of the Harris and Priester Model Temperatures at 2000 km and 420 km	6-4
6-4	Altitude Variation of the Thermal Gradient (°K/km) in the Earth's Thermosphere as a Function of Solar Activity	6-7
6-5	Altitude Variation of the Thermal Gradient (°K/km) in the Martian Thermosphere as a Function of Solar Activity	6-8
6-6	Integrated Thermal Gradients (°K/km) in the Martian Thermosphere as a Function of Solar Activity	6-10
6-7	Comparison of Mean Atmosphere Parameter Values at 1000 Kilometers	6-16
6-8	Distribution of Density at 1000 Kilometers in Models of the Terrestrial and Martian Atmospheres	6-18
6-9	Variation of the Martian Atmospheric Density at 700 Kilometers as a Function of Solar Activity	6-19
8-1	Chemical Reactions and Rate Constants Used in the Chemical Kinetics Calculations	8-7
8-2	Comparison of Diffusion and Chemical Dominance	8-27

SECTION 1

INTRODUCTION

SECTION 1

INTRODUCTION

1.1 OBJECTIVE

The objective of the atmosphere definition study was to provide definition of the Martian atmospheric characteristics required by spacecraft designers. The categories of interest are: physical data, atmospheric parameters near the surface, entry atmosphere structure, outer atmosphere structure, clouds and haze, and chemical kinetics and composition. Emphasis was placed on the characteristics of the outer atmosphere and on the chemical kinetics and composition of the atmosphere.

1.2 SCOPE

The atmosphere definition task consisted of utilizing existing Martian atmosphere guides and updating these to incorporate the more recent information. The latter including the findings based on: the Mariner IV data, the spectroscopic data obtained during the recent opposition, theoretical studies, and empirical studies. In providing information on the atmospheric parameters of interest for which the present level of knowledge was inadequate or totally lacking, empirical methods were developed to provide an estimate of parameter values required. In addition, a theoretical analysis of the chemical kinetics and the composition of the atmosphere was made in order to gain a better understanding of the probable time-space characteristics of the upper atmosphere.

1.3 REPORTS

This document summarizes and extends the studies included in the following Milestone Reports issued during Task D:

a. "Survey of Present Knowledge on the Martian Atmsophere with Application to Spacecraft Design," Parts I, II and III, VOY-D4-TM-4, 28 July 1967.

b. "A Preliminary Estimate of the Solar Cyclic Variation of the Atmosphere of Mars Above 100 Kilometers", VOY-D4-TM-17, 28 August 1967.

c. "On the Latitudinal and Seasonal Variation of the Martian Atmosphere Below 100 Kilometers," VOY-D4-TM-18, 28 August 1967.

SECTION 2

SUMMARY

2.1 PHYSICAL DATA

A selection of Martian atmosphere mean and extreme physical data values was compiled based primarily upon the JPL Voyager Environmental Predictions Document and a number of MSFC reports. An analysis of these reports, and other Martian atmosphere guides, indicate that there is not a generally accepted standard set of values, adoption of such a standard set is recommended.

2.2 ATMOSPHERIC PARAMETERS NEAR THE SURFACE

A survey of the information available on the composition, pressure, temperature and winds in the Martian atmosphere is summarized in this final report.

Based on recent interpretations of the spectroscopic and Mariner IV occultation data, the near surface atmosphere is expected to be rich in CO_2 and to have a total pressure of less than 25 millibars.

Based on theoretical analyses, the near surface temperature is expected to be $20^{\circ}K$ to $50^{\circ}K$ less than the surface temperature over the equatorial regions. Over the polar regions it is expected that the near surface temperature is perhaps 10 to 20 degrees greater than the surface temperature. The maximum wind speed at the surface, based on observed cloud motions, is on the order of 30 meters per second. However, based on theoretical studies of dust transport, the maximum wind may be in excess of 60 meters per second for a low pressure (5 mbs) atmosphere.

2.3 ENTRY ATMOSPHERE

The existing Voyager-Mars (VM) model atmospheres appear adequate to define the lower atmosphere structure; that is, below 100 kms. However, since these do not account for time-space variations, a model of the latitudinal and seasonal variation of the atmosphere was developed for Mars. The results indicate that the density at 100 kilometers may vary by as much as 65 percent from the equator to 60 degrees latitude. Density variations of about 45 percent are normally encountered in models of the Earth's atmosphere at 100 kilometers over this latitude spread.

The tropopause altitude variation from equator to 60 degrees latitude, resulting from the model assumptions, was found to be 75 percent for Mars. This variation is comparable to that encountered in Models of the Earth's atmosphere, where the tropopause altitude variation is normally about 65 percent over the same latitude range.

2.4 OUTER ATMOSPHERE STRUCTURE

Based on the Mariner IV ionospheric experiment data, the base of the thermosphere may be as low as 105 km. The thermal gradient is expected to range in value for 0.5° to 3.0° K/km during periods of low to high solar activity respectively. The MSFC maximum density envelope compares favorably with the maximum density profile from the VM3 extension. The MSFC density at 1000 kms being less than one order of magnitude below the VM3 extended model value. The MSFC mean density profile compares favorably with the older GE Voyager reference atmosphere. The MSFC mean density value at 1000 kms is approximately one order of magnitude greater than that obtained from the GE Voyager reference model. The MSFC mean density profile and associated confidence envelopes were found to be consistent with most models presently available.

Estimates of the variations of the atmospheric structure as a function of solar activity were prepared and indicate:

a. The density at altitudes of about 1,000 kilometers is likely to exhibit a diurnal (day-night) variation of an order of magnitude.

b. The atmospheric density at 1,000 kilometers during a period of high solar activity is likely to be three orders of magnitude greater than it is during a period of low solar activity.

c. Solar cyclic variations of the atmosphere's density at 1,000 kilometers of five and six orders of magnitude are expected to result more from uncertainties in the models than from probable variations of the atmosphere itself.

d. The MSFC mean-to-maximum density profiles appear reasonable for periods of high solar activity.

e. The MSFC mean-to-minimum density profiles appear adequate to define the density likely to be encountered during a period of moderate to low solar activity.

2.5 CLOUDS AND HAZE

The characteristics of the various cloud and haze layers presented in the final report were obtained from a survey of the existing literature. Based on the observed cloud motions, there appear to exist preferential regions over which the white and yellow clouds occur, as well as preferential time periods during which they are most likely to be observed. An analysis of a selected data sample of observed motions of clouds, which are thought to exist at different altitudes on Mars, was performed. The results indicate that even a limited sample of observed motions of white and yellow clouds may provide a means of assessing the horizontal and vertical circulation characteristics of the atmosphere.

2.6 CHEMICAL KINETICS AND COMPOSITION

The composition of the Martian atmosphere as a function of altitude is dependent upon the chemical kinetics. A complex chemical system has been developed and calculations made of the chemical kinetics involved. These calculations resulted in a predicted steady-state atmosphere which gives the concentrations of eighteen species as a function of altitude. (The calculations involved fifty chemical reactions, ten of which were photochemical).

A total density distribution and three elemental compositions (corresponding to those given by 80% CO_2, 20% N_2; 90% CO_2, 10% N_2; and 100% CO_2) were assumed. Mean and extreme solar flux values were used to evaluate the effect of solar activity on the atmosphere. Although no account was taken of diffusion, it is an important factor which should be considered in a subsequent study.

Based on the results obtained for the neutral species, it is found that CO_2 is more than 50 percent dissociated at all altitudes above 60 km. Above this CO and O are major constituents. Ozone is present in mole fractions comparable to those in the Earth's atmosphere. Nitrogen oxides probably do not build up in large concentrations.

Charged species are more difficult to predict. Above 80 km electrons are the only important negatively charged species. Below this, negative ions, expecially CO_3^-, become important but none build up to large concentrations. The major positive ions are O^+, N^+ and CO^+ at high altitudes and NO^+ at lower altitudes.

SECTION 3

PHYSICAL DATA

SECTION 3

PHYSICAL DATA

The physical data for the planet Mars can be obtained from numerous sources. Since varying degrees of uncertainty exist on the parameters of interest, a variety of numerical values can be obtained, any of which is as valid as the other. Thus, it is important to select a single set of physical data values, giving the parameter mean and extremes which are to be used throughout the Voyager program. To this end, the physical data values given in Table 3-1 were obtained from the Voyager Environmental Predictions document (Hess and Pounder, 1966).

The physical characteristics of the Martian moons presented in Table 3-2, were obtained from Evans, et.al.(1967).

Table 3-1. Physical Data for Mars (from Hess and Pounder, 1966)

Parameter	Units	Minimum	Mean	Maximum
Planetary Radius				
Equatorial	kms	3320	3375 ± 20	3443
Polar	kms	3272	3350 ± 10	3360
Gravitational Constant	km^3/sec^2	-	4.297780×10^4	-
Planetary Mass	Earth Mass	0.1073	0.10745 ± 0.001	0.1080
Planetary Density	g/cc	3.95	4.0	4.24
Rotation Period of Mars	hr:min:sec	-	24:37:22.6	-
Length of Year	Earth 24-hr days	-	687	-
Orbital Characteristics of Mars (abbreviated form - 1973)				
Semimajor Axis	AU		1.52369	
Eccentricity			0.09338	
Inclination to Ecliptic	deg:min		1:51	
Mean Longitude of Ascending Node	deg:min:sec		49:21:6	
Mean Longitude of Perihelion	deg:min:sec		335:33:43	

Table 3-2. Physical Characteristics of Martian Moons
(From Evans, et. al., 1967)

Parameter	Unit	Phobos	Deimos
Diameter	km	16 to 19	6 to 10
Mean Distance from Center of Mars	km	9,350	23,400
Orbital Inclination to Equator of Mars	deg	1.1	0.9 to 2.7
Orbital Inclination to Orbit of Mars	deg	27.5	27.5
Period of Revolution	hr:min:sec.	7:39:13	30:17:17
Eccentricity	-	0.0170	0.0031

SECTION 4

ATMOSPHERIC PARAMETER NEAR SURFACE

SECTION 4

ATMOSPHERIC PARAMETERS NEAR SURFACE

4.1 INTRODUCTION

In developing models for the upper atmosphere of Mars for spacecraft design consideration, it is necessary to define the near surface atmosphere characteristics because they represent the initial or boundary conditions used in the various models. The parameters of particular interest in this instance are composition, pressure and temperature of the near surface atmosphere.

These near surface parameters are also of interest in the development of scientific experiments to be conducted from an orbiter. In this latter regard, the characteristics of the near surface wind field are also of interest. Knowledge of the characteristics of the wind field is valuable in planning scientific experiments designed to better define the wind field, and in assessing the possible influence of the winds on certain other experiments. For example, the likelihood of encountering turbulent eddies, wind entrained dust, etc., is of particular importance to photo-imaging experiments.

4.2 COMPOSITION AND PRESSURE

The present knowledge of the composition of the Martian atmosphere is based on gases observed spectroscopically and on gases theoretically deduced as being present. Additionally, there exists the polarization and occultation measurements which provide information on the total amount of gases present. Of the expected major constituents (N_2, CO_2, and A), only CO_2 has been observed spectroscopically. In general, the amount of CO_2 reported will be found to lie within the limits given by Kaplan, et. al. (1964) of 55 atm-m $\pm$20 atm-m. (The units of atm-m represent the total thickness of a column of gas reduced to STP.) This abundance of CO_2 leads to a partial pressure of about 4 $\pm$2 mbs.

Unfortunately, general agreement does not exist on the amount of N_2 and A. The amount of radiogenic argon may be derived from several approaches of which the following method is

commonly used to obtain an upper limit. The presence of argon 40 is inferred as a decay product of potassium 40 in the planet crust. Assuming that the concentration of potassium in the crust is the same as it is on Earth, and further assuming that weathering is equally rapid on Mars, then the atmospheric mass of argon per unit area should be the same as that of the Earth's atmosphere, i.e., 74 meters at STP. The argon partial pressure on Mars would then be about 5 millibars. In general, it is thought that weathering is less severe on Mars; thus, the total amount of argon would be much less than that present in the Earth's atmosphere. Consequently, an upper limit to the amount of argon can be assumed equal to the amount present in the Earth's atmosphere, i.e., having a partial pressure of 5 millibars on Mars.

Based on the Mariner IV occultation data, Spencer (1966) has shown that, for mean temperatures above the occultation point of 140 to 180°K, the "allowable" mean molecular weight could range from 33.1 to 50. Similarly, Hess and Pounder (1966) indicate that while the mean molecular weight is estimated as 33.2 to 39.2 based on the Mariner IV data, a range of 31.2 to 44 is consistent with reliable spectroscopic data. Thus, it is seen that the more recent data interpretations strongly favor a CO_2 rich atmosphere.

The case for N_2 is quite uncertain and is largely dependent upon the inferred total thickness or pressure of the atmosphere. The total pressure of the atmosphere has in the last 3 years been inferred as being as low as 4 mbs and as high as 165 mbs. Taking the upper limit of the partial pressures of CO_2 and A one obtains 11 mbs. Thus, it would be possible to conclude that the atmosphere is composed entirely of CO_2 on one end of the scale; while on the other, the atmosphere would be largely composed of N_2. The more recent analyses of the measurements of absorption by strongly pressure dependent CO_2 bands, suggests that the upper bound on total pressure is less than 45 mbs. In the last two years, analyses of the spectroscopic data together with the Mariner IV occultation data, has led to a reduction of this upper limit down to perhaps 25 mbs.

Hess and Pounder noted that while the Mariner IV occultation and 1965 Mars opposition spectroscopic measurement results suggest a mean surface pressure in the range of from 4 to 16 mbs, uncertainties in these limits allow for a possible range of from 2 to 30 mbs. Recent analysis by Leighton and Murray (1966), which showed the feasibility of the Martian ice caps being CO_2 (dry ice), present the possibility that the partial pressure of CO_2 and therefore the total pressure may vary by ± 1 mb on a seasonal basis due to the precipitation of CO_2 from the atmosphere. Another consequence of their analysis is that the equilibrium vapor pressure of CO_2 in the atmosphere would be 3 to 5 mb since the north polar ice cap does not disappear.

At present, the most commonly used values of total pressure values are 5, 7, and 10 millibars. These low pressure values would also suggest that the atmosphere of Mars is rich in CO_2 and may have very little, if any, N_2.

A brief survey of Martian surface pressure estimates is given in Table 4-1. The impact of the findings of Kaplan, Munch, Spinrad and of Kuiper and Owen are very much in evidence. Similarly, the occultation findings as well as the recent spectroscopic analyses are also quite evident in the reduced pressure estimates made in the last two years.

4.3 TEMPERATURE

A considerable amount of information exists on the surface temperature of Mars and on its variation in time and space. Indeed, the available data are sufficiently abundant to permit description of the seasonal and latitudinal variation of surface temperature along with its diurnal variation. This is not to say that general agreement exists on the actual time-space variation of surface temperature, but rather that enough data are available to allow such depictions to be made without indulging in too much speculation.

Although data on the surface temperature are abundant, it is questionable whether such data ought to be used in developing vertical temperature profiles. The problem encountered is quite simply that the temperature a few feet above the surface likely decreases at a

Table 4-1. Estimates of Atmospheric Pressure at The Surface of Mars

Year	Total Pressure	Reference	Remarks
1961	90	Dollfus	Outdated
	85	Kellogg/Sagan	Outdated
	81 - 89	deVaucouleurs	Outdated
	56 - 132	Deirmendjian	Outdated
1962-63	41 - 133	Schilling	Outdated
1964	37 - 162	Evans/Wasko	Outdated
	10 - 40	Kaplan/Munch/Spinrad	Spectroscopic
	10 - 20	Kuiper	Spectroscopic
	14 - 20	Owen/Kuiper	Spectroscopic
1965	24 - 82	Hanst/Swan	Spectroscopic
	8 - 36	Spencer	Spectroscopic
	5 - 10	Aviation Week	Engineering Models
	4.3 - 6.6 (Estimated Extreme 25)	Vachon	Preliminary Mariner IV
	7 - 13	Hunten	Spectroscopic
	4 - 14	Spinrad	Spectroscopic
	4.1 - 6.0	Kliore, et. al.	Preliminary Mariner IV
	8 - 10	Munch	Reevaluation of Mariner IV
1966	4 - 6.2	Fjeldbo, et. al.	Mariner IV Occult.
	4.2 - 13.5	Spencer	Spectroscopic
	3.7 - 11.0 (13.8 Extreme)	Spencer	Mariner IV
	3.8 - 5 (CO_2 Partial Pressure 3-5 mb)	Leighton/Murray	Equilibrium Vapor Pressure

superadiabatic rate in daytime, while at night a temperature inversion may be experienced. This very characteristic is generally the rule on Earth (Sutton, 1953), and for this reason free air temperature is obtained from a thermometer which is four feet above ground and located in an instrument shelter. This temperature value is then used as the "surface temperature" when a temperature versus altitude profile is generated. From the aspect of providing a vertical profile of the temperature in the Martian atmosphere, it is not the surface temperature which ought to be used, but rather the near surface temperature. Thus, in addition to presenting information on the time-space variation of surface temperature, one must also give attention to the relationship of surface to near-surface temperature.

4.3.1 DIURNAL VARIATION OF SURFACE TEMPERATURE

The observed hourly variation of temperatures near the equator of Mars, as reported by Gifford (1956) and by Sinton and Strong (1960), is shown in Figure 4-1. The data of Sinton and Strong indicate the presence of a larger diurnal variation than does Gifford's data, and additionally would indicate that peak surface temperature only lags peak insolation by one hour.

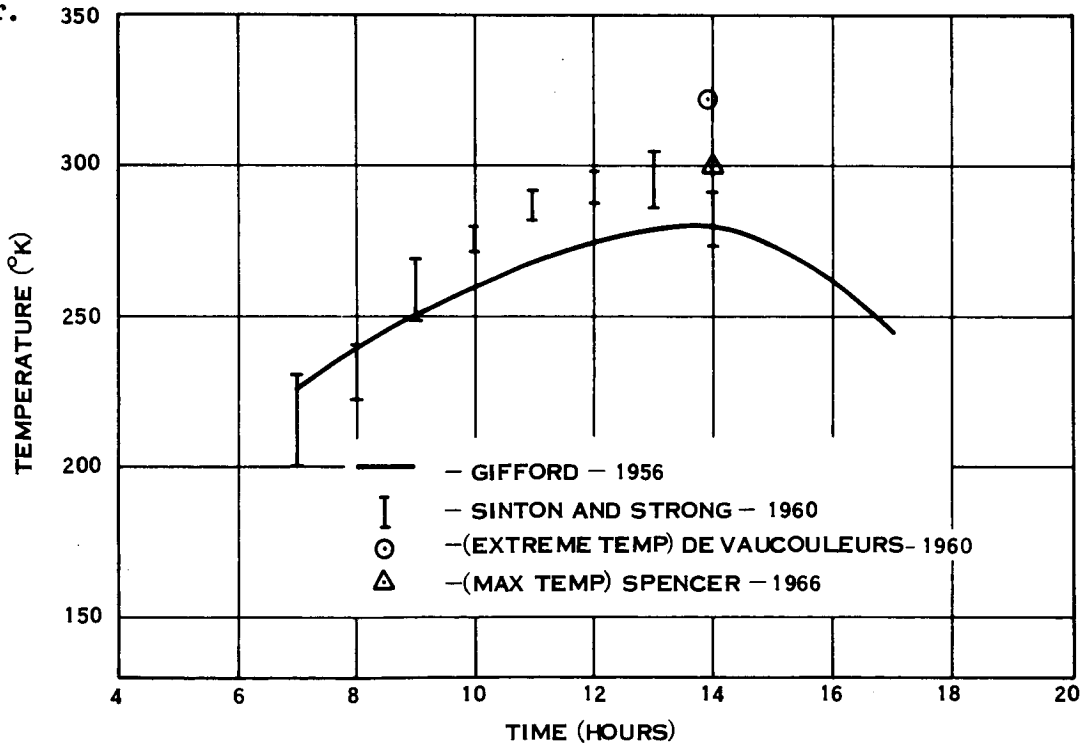

Figure 4-1. Observed Hourly Variation of Surface Temperature Near the Equator of Mars

Hess and Pounder (1966), favor the hourly distribution shown in Figure 4-2 which is based on Opik's correction of the data of Sinton and Strong to allow for the fact that Mars is not a perfect blackbody emitter. Regardless of which hourly temperature distribution is accepted, the observations and their interpretations suggests very strongly that the maximum temperature lag is on the order of one to one and a half hour.

The question of the range of the diurnal temperature variation is not so easily resolved. From Figure 4-1, it is noticed that the observed temperature data are restricted to the hours of 0700 to 1700. Since the minimum temperature should occur in the predawn hours ($\approx$0600), one could infer a diurnal temperature range of 60°K (Rasool-1963), 80°K (Vachon-1966), 103°K (Evans et. al., 1967), or as high as 150°K (Leighton and Murray, 1966). The diurnal temperature range obtained depends heavily upon which observed temperature data are used, and what assumptions are made in regards to the surface thermal conductivity. The influence of the thermal conductivity on the derived diurnal temperature range is shown in Figure 4-3 which is based on the findings of Leighton and Murray (1966). The thermal conductivity, according to Hess and Pounder (1966), is expected to range from 0.8×10^{-4} to 4.2×10^{-4} cal/cm-sec-^{o}K. The diurnal temperature range for these latter values of thermal conductivity are obtained from Figure 4-3 as being on the order of 100°K or slightly less. A similar diurnal surface temperature range (95°K) was obtained from the theoretical analysis of Neubauer (1966). On the basis of the more recent observational data and subsequent theoretical analyses, it appears that the diurnal range of surface temperature near the equator of Mars is quite consistent with the hourly temperature distribution given in Figure 4-2.

4.3.2 LATITUDINAL AND SEASONAL VARIATION OF SURFACE TEMPERATURE

The variation of the surface temperature of Mars, as a function of latitude and season, has been determined by theoretical analyses. These analyses are generally based on considerations of radiative and convective equilibrium conditions for the atmosphere and surface. The findings of House-1966, Ohring and Mariano (1967) and Leovy (1966) are all in general accord. The major difference between the results of Ohring and Mariano and the results

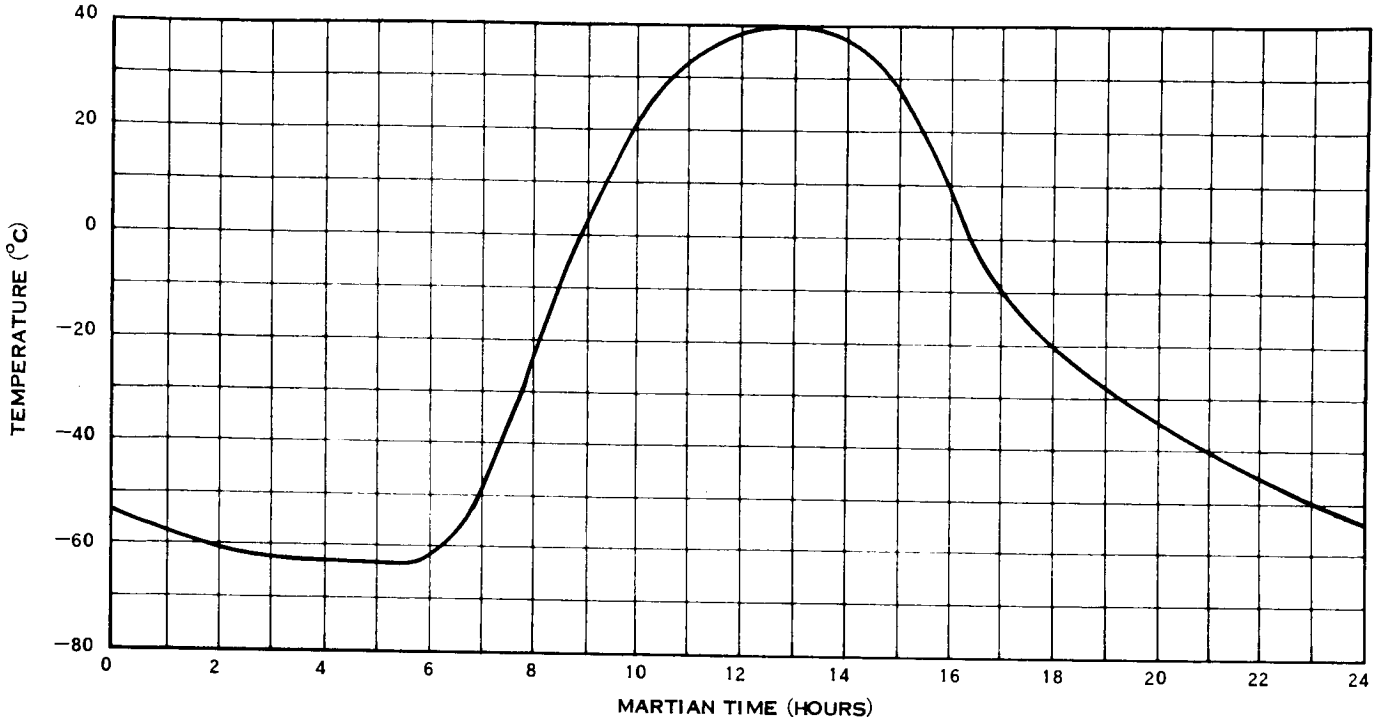

Figure 4-2. Diurnal Variation of Surface Temperature on the Martian Equator at Perihelion

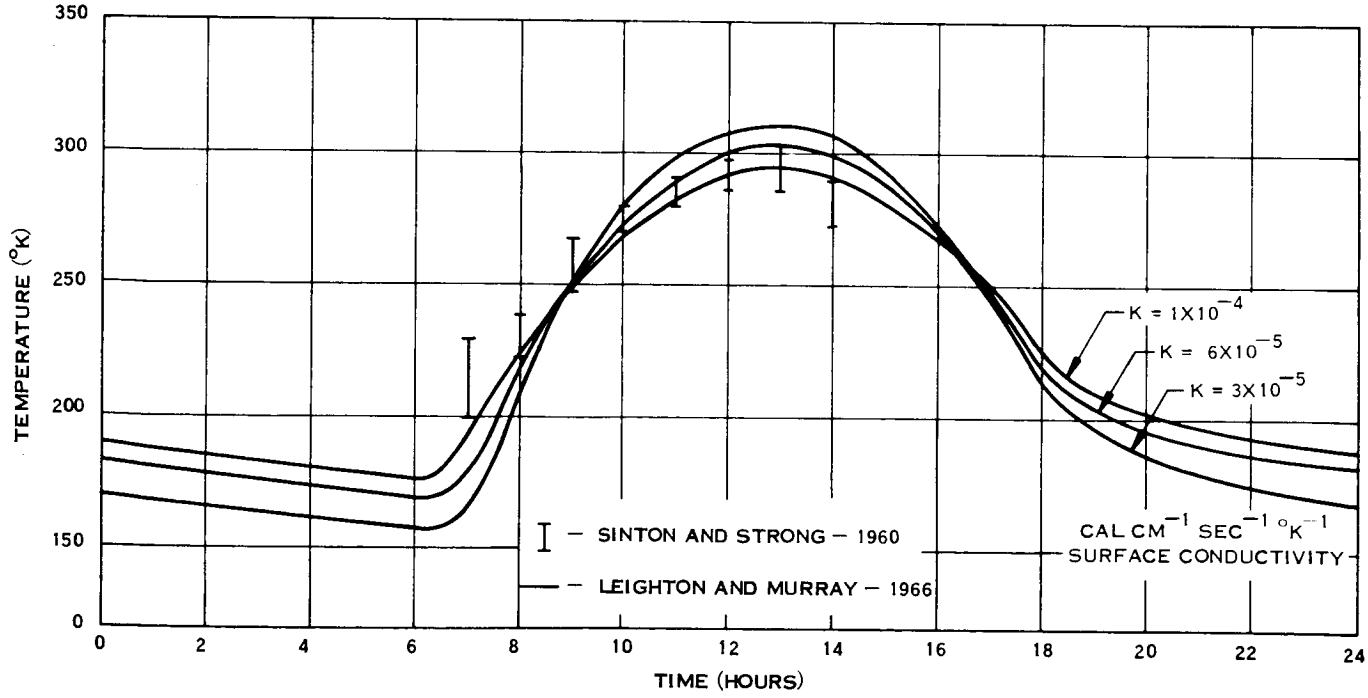

Figure 4-3. Hourly Variation of Surface Temperature Near the Equator of Mars

of Leovy is found for latitudes in excess of 50 degrees in the winter hemisphere. By considering the possible condensation of CO_2, Leovy derives a minimum temperature of $145^{o}K$ for latitudes in excess of sixty degrees. Such a consideration was not considered by Ohring and Mariano with the result that their temperatures are allowed to decrease below $145^{o}K$. Indeed, their calculations would indicate that the mean temperature could be as low as $110^{o}K$ at sixty degrees latitude.

The mean surface temperature values given in Figure 4-4 and 4-5 are based on the values given by Ohring and Mariano (1967), with modification for the polar latitudes. Interestingly, in an earlier treatment on the subject by Mintz (1961), temperature values derived from the observed temperature variation along the noon meridian were presented which agree with the more recent theoretical analyses.

In contrast, the latitudinal and seasonal surface mean temperature values derived from the data presented by Gifford (1956), given in Table 4-2 and plotted on Figure 4-4, are consistently higher than the values given by any of the preceding authors.

Since Gifford's maps of the seasonal average isotherms across the Martian surface are utilized to define the latitudinal and seasonal temperature variation by both Hess and Pounder (1966), and Weidner and Hasseltine (1967), it appears that the values presented in Table 4-2 are likely to be favored as a design reference. Obviously, an effort should be made in the near future to resolve the disagreement which is clearly apparent from a comparison of the mean temperature values shown in Figure 4-4.

The maximum temperature at any latitude during any given season is not expected to have a simple linear relation to the mean. Thus merely taking a diurnal variation of $100^{o}K$ and assuming that the maximum temperature is $50^{o}K$ greater than the mean at any latitude for any season would not be a valid approach. The maximum temperatures shown in Figures 4-4 and 4-5 were obtained from Mintz (1961) for the summer-winter seasons, and from Tilson (1964) for the spring-autumn seasons.

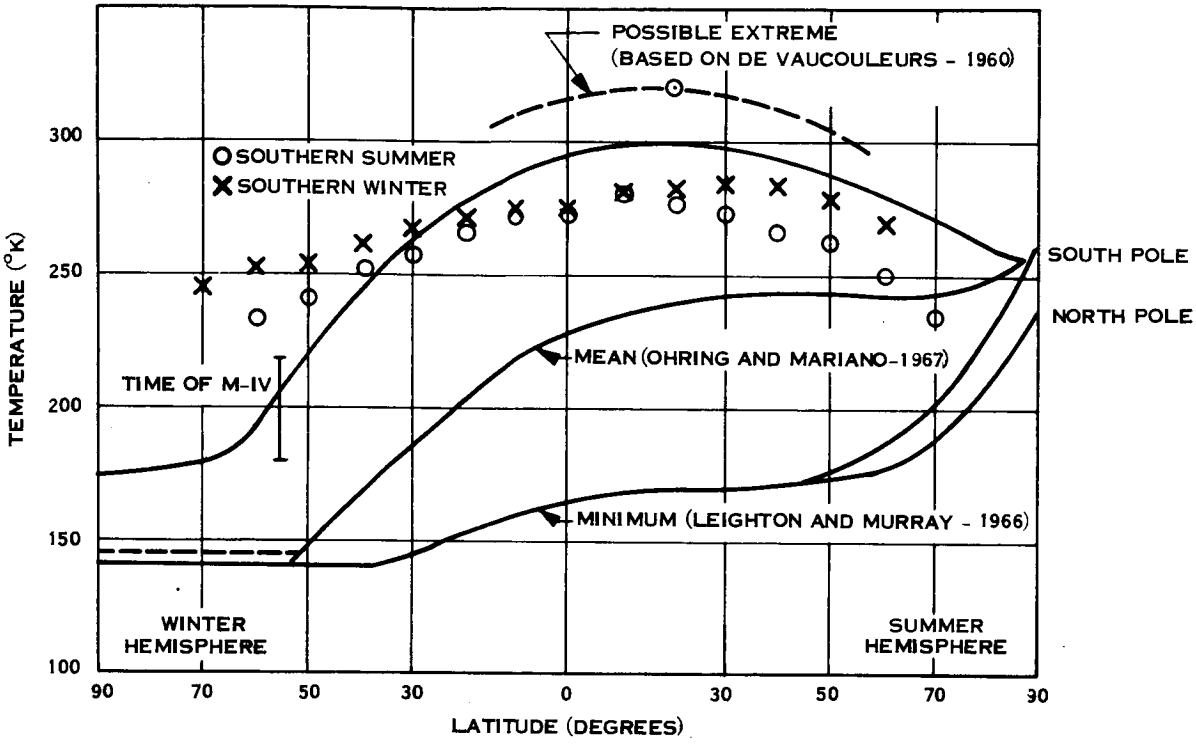

Figure 4-4. Spring-Autumn Latitudinal Variation of Temperature of Mars-Summary

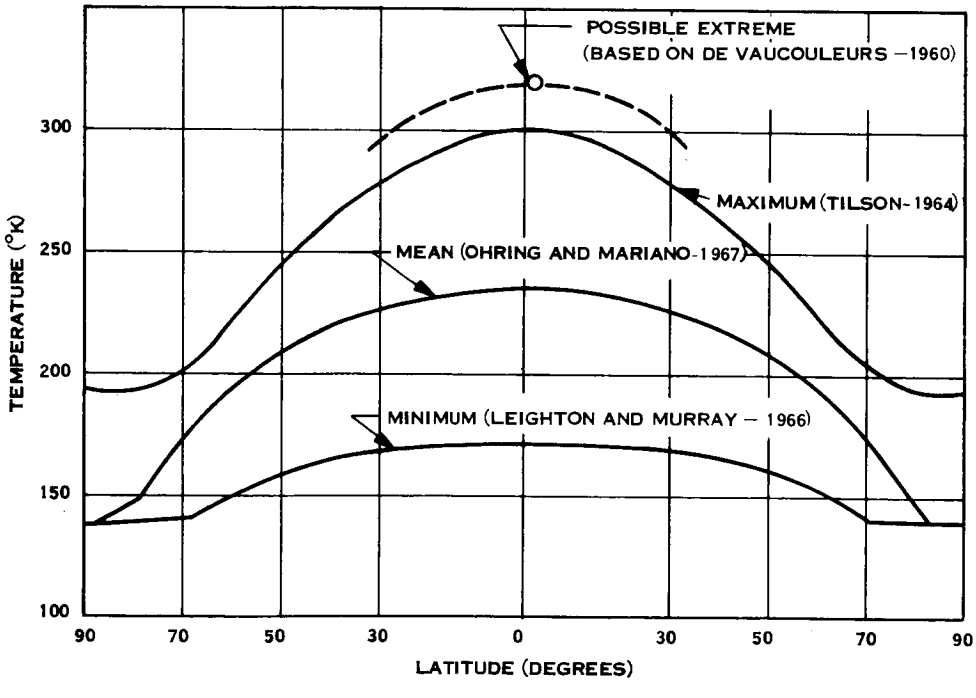

Figure 4-5. Winter-Summer Variation of Temperature on Mars Summary

Table 4-2. Mean Temperature (^{o}K) as a Function of Latitude and Season on Mars

Latitude / Season	-70	-60	-50	-40	-30	-20	-10	0	10	20	30	40	50	60
Southern Summer	235	250	261	266	273	277	280	277	272	266	258	251	241	232
Southern Winter	245	252	254	262	268	272	275	278	280	283	284	283	278	269

The temperature maxima shown, when compared with the mean temperature distribution of Ohring and Mariano, provide a relation of the maximum to mean temperature as a function of latitude and season.

The mean winter hemisphere temperatures obtained from the data of Gifford (1956) are found to exceed the maximum values given by Mintz (1961) at latitudes greater than forty degrees.

From the viewpoint of relating the probable maximum temperature associated with the values derived from Gifford's data, suffice it to say that the maximum temperature would be less than 50°K greater than the mean temperature at any latitude.

The minimum surface temperature variation with latitude and season shown in Figures 4-4 and 4-5 were based on the findings of Leighton and Murray (1966). In general, the temperature minima obtained from the theoretical study of Leighton and Murray result is lower temperatures than are reported by other researchers, e.g., Mintz (1961). From the viewpoint of design studies, the more conservative environment definition is desirable, and as a consequence the surface temperature minima values given in Figures 4-4 and 4-5 are

probably to be preferred. However, it is important to note that the temperature minima values given should not be used in conjunction with the mean temperature values based on Gifford's data, since this will result in a temperature differential which far exceeds the observed temperature range.

The minimum temperature at polar latitudes in summer is not the same for the northern and southern hemispheres. The minimum surface temperature values obtained from Leighton and Murray (1966) (see Figure 4-4), reflect this hemispheric influence.

The temperature derived from the Mariner IV data (Spencer, 1965) is shown in Figure 4-4 and compares favorably with the expected temperatures. Unfortunately, the derived temperature would agree with the upper ranges based on recent theoretical studies, and would also agree with the lower range based on values derived from Gifford's data. Thus, the derived temperature does not by itself provide a means of evaluating the merits of the two proposed distributions.

4.3.3 RELATION OF SURFACE TO NEAR-SURFACE TEMPERATURE

The relation between surface and near-surface temperature was considered in a recent theoretical analysis by Neubauer (1966). Specifically, Neubauer finds that while the surface may experience a diurnal temperature variation of about 95°K, the atmosphere at 0.5 meters might experience only a variation of 20° Kelvin. The findings of Neubauer are shown on Figure 4-6 and indicate that the difference between the surface temperature maximum and the near-surface maximum may be 42°K.

The difference between the maximum surface and maximum near-surface temperature was shown by Mintz (1961) to be related to the amplitude of the diurnal variation of surface temperature. The relationship being:

$$T^{s}_{max} - T^{a}_{max} = 0.54\,(T^{s}_{max} - T^{s}_{min})$$

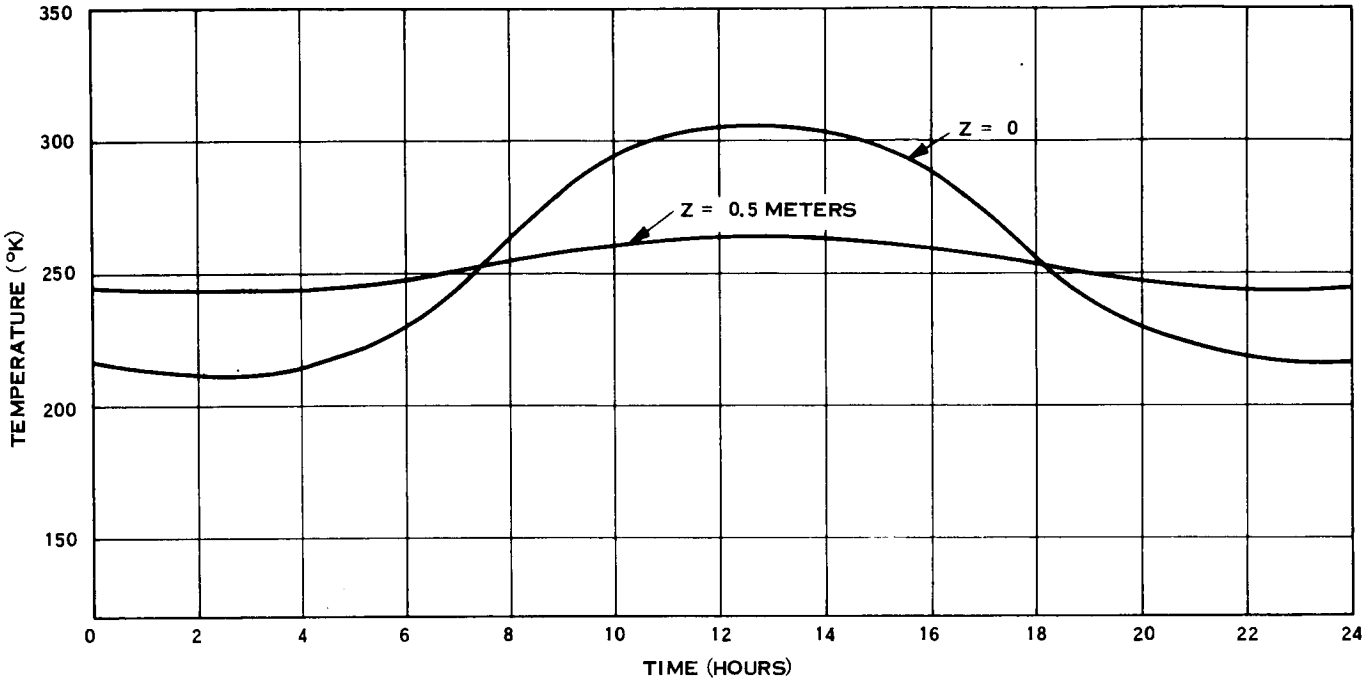

Figure 4-6. Temperature Versus Time at the Equator of Mars at the Surface and at Z = 0.5 Meters (Neubauer - 1966)

Assuming this relationship to be valid, it is of interest to compare the surface to near-surface temperature differential using the diurnal temperature range suggested by various authors (Table 3-1). It is seen that the relationship suggested by Mintz (1961) agrees reasonably well with the findings of Neubauer (1966). The minimum temperature differential (30°K) between the maximum surface and near-surface temperatures is found to be obtained from the theoretical analyses of House (1966). On the basis of presently available theoretical studies on the subject, it appears that the maximum near-surface temperature will be from 30 to 50°K less than the maximum surface temperature. Thus, if the maximum surface temperature observed is 320 to 325°K (deVaucouleurs, 1960), then it is unlikely that the near-surface temperature will exceed 295°K. Spencer (1965), in providing an estimate of the maximum atmospheric temperature at the surface for design purposes recommended a value of 300°K. In light of the findings from the more recent theoretical studies, Spencer's recommended near-surface temperature maximum appears reasonably conservative.

Table 4-3. Comparison of Surface to Near-Surface Temperature Differential

Diurnal Surface Temperature Range (^{o}K)	Surface to Near-Surface Maximum Temperature Differential (^{o}K)	References
103	(56)	Evans et. al. (1967)
101	(54)	Hess & Pounder (1966)
100	(54)	--
95	(51)	Neubauer (1966)
80	(43)	Vachon (1966)
60	(32)	Rasool (1963)
(56)	30	House (1966)
(78)	42	Neubauer (1966)

Values in parenthesis calculated using the relationship of Mintz (1961)

The question of the relationship between the surface and near-surface minimum temperature is deferred for future treatment, i.e., other than this study. For the present, it is noted that the near surface minimum temperature is perhaps from 10° to 20°K greater than the surface minimum temperature. However, if the hypothesis of CO_2 polar caps is accepted, then over the polar regions the near-surface temperature may be equal to the surface temperature.

4.4 WINDS

4.4.1 GENERAL CIRCULATION

The distribution of the Martian wind field can be approximated through the use of general circulation models (e.g., Mintz 1961; Leovy, 1965). As stated by Mintz (1961), general circulation models are developed to provide two basic functions: first, to maintain thermal equilibrium by transporting heat from the heat sources (often the equatorial regions) to the

cold sinks (often the polar regions); and second, to produce the kinetic energy necessary to maintain the circulation against frictional dissipation. The seasonal change in the planetary heat differential is expected to be more on Mars than it is on Earth due to the expected small heat capacity of the Martian surface. The latter is expected to result in extreme cooling at the poles in winter and possibly warming at the poles in summer. Thus, in theory, one would expect the winter circulation to become unstable and to lead to the development of waves in the general circulation. As reported by Mintz (1961), a symmetrical circulation regime (where air rises at the equator, flows poleward aloft, sinks at the poles, and flows equatorward at the lower levels) would have lower surface winds ($\approx$ 1 m/sec) than would a wave regime ($\approx$ 10 m/sec). The probable general circulation of the Martian atmosphere given by Leovy (1965) is shown in Figure 4-7. Since the winter hemisphere is expected to conform to a wave circulation regime, one would expect to encounter the highest winds during this season. Additionally, one would expect dust storms to be more common during the winter. How well the theory agrees with the observations of the drift of clouds will now be considered.

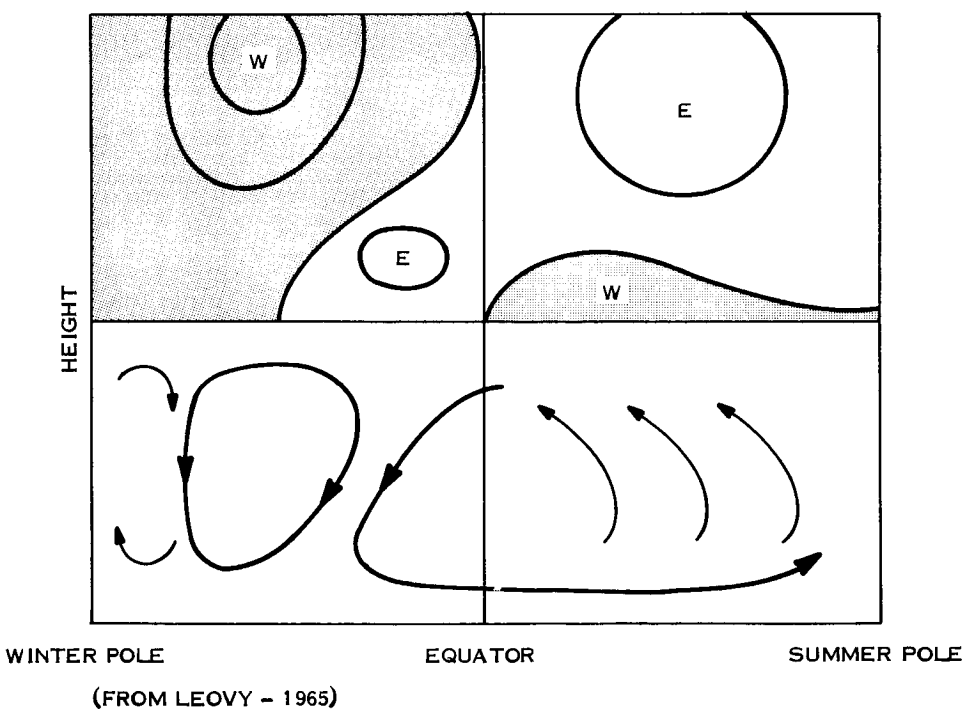

Figure 4-7. Schematic Diagram of Solstice Circulation on Mars

4.4.2 DRIFT OF MARTIAN CLOUDS

In general, upper air winds are larger than surface winds both in theory and based on observations in the Earth's atmosphere. Consequently, clouds which exist at upper altitudes, as well as those which develop to upper levels, will tend to move faster than low level clouds. Additionally, dust brought to upper levels by convective processes would tend to disperse rapidly and to cover a wider area than is likely from low level dust clouds. Thus, if one wishes to infer surface winds from observations of cloud motion, it is necessary to consider only the low level yellowish clouds. These data are somewhat limited in quantity and are comprised of 53 cases covering an 87-year period (Gifford 1964).

The average daily drift of yellowish clouds across the surface of Mars has already been discussed by a number of researchers, (e.g., Gifford, 1964, Hess 1950, Spencer 1965, Dollfus 1965). Of particular value in this section is the paper by Gifford (1964) in which considerable information is provided on the motion of the yellow clouds. Significantly, Gifford has separated the cloud data into two classes: one dealing with low altitude yellow or dust clouds, and the other dealing with the yellow clouds which extend to fairly high altitudes termed "projections" by Gifford. This separation is of considerable merit because the cloud characteristics of the two classes appear to differ.

4.4.2.1 Dust Clouds

Using Gifford's data, clouds considered in this class, and termed dust clouds, may be characterized as follows:

a. The clouds tend to originate over the Martian equatorial regions; 68 percent are first observed within 30 degrees of the equator, and 87 percent within 40 degrees of the equator.

b. The clouds tend to be restricted to motion within the equatorial belt; 56 percent terminate within 30 degrees of the equator, and 81 percent terminate within 40 degrees of the equator.

c. The velocity distribution of yellow (dust) clouds, based on sixteen cases observed since 1873, may be defined as a normal circular distribution with a mean vector direction of 321 degrees, vector module 5.9 m/sec, and standard vector deviation of 8.2 m/sec. Such a distribution leads to a 3σ value of the wind speed of 31 m/sec.

d. The clouds seem to originate preferentially over light areas and in regions of high surface temperature.

e. The clouds are likely "composed of wind-driven sand grains moving by saltation within a few meters of the Martian surface, accompanied by an overlying dust cloud, of much smaller particles, extending, perhaps, to many thousands of meters" (Gifford, 1964).

f. The clouds appear to be devoid of moisture. The movement of this class of clouds is shown in Figure 4-8 from which the first, second, and fourth characteristics noted above are clearly evident. It is worth noting that the velocity distribution (c above) refers only to the average daily cloud motions. The variability of the velocity of the cloud system can be appreciable and as reported by deVaucouleurs (1961) "velocities up to 60 km/hr or more have been recorded in the early phases of a dust storm, later subsiding to about 10 km/hr." It is also quite likely that actual wind velocities within the cloud system could differ from the system velocity.

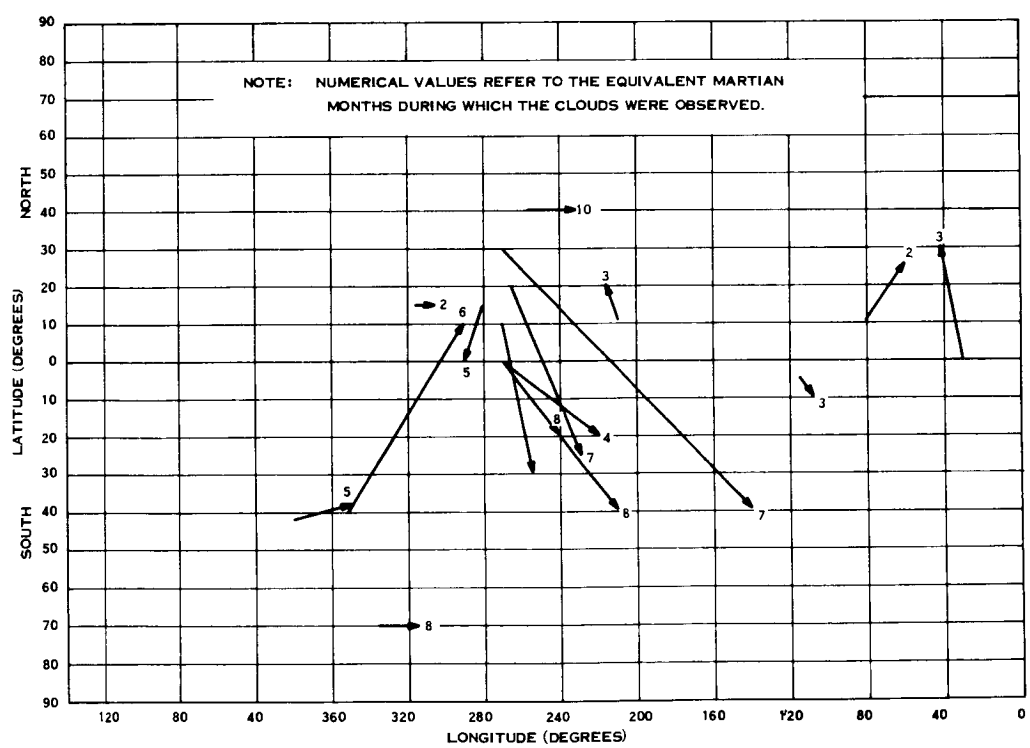

Figure 4-8. Motion of Yellow (Dust) Clouds on Mars

Lastly, in comparing the observed cloud motions to general circulation models one encounters what appear to be inconsistencies. Several explanations have been offered to resolve these inconsistencies within the framework of symmetric and wave circulation regimes. The general equatorward drift of the yellow (dust) clouds could be associated with polar outbreaks, similar to northers on Earth (Gifford, 1964). Alternatively, the apparent inconsistencies could be related to the breakdown of a symmetric regime of the circulation into a wave regime (Miyamoto, 1964). This latter possibility was predicted theoretically by Mintz (1961). The above two explanations would account for certain inconsistencies associated respectively with the motions of individual storm systems, lasting a few days, and hemispheric disturbances, lasting for over a month. Two separate explanations appear necessary for as noted by Gifford (1963), "the yellow (dust) clouds are generally speaking too small to be related to large-scale baroclinic wave instability". On the other hand, large disturbances such as the 1956 and 1963 storms are large enough to correspond to the expected wave number on Mars which Mintz (1961) calculated as being equal to three. More recently, detailed theoretical analyses of the general circulation of the Martian atmosphere have been made by Tang (1966 and 1967). Tang's first analysis was of the steady symmetrical regime for the equinoctial seasons. The results showed that the mean zonal wind was two m/sec and the mean meridional wind was 10 m/sec at the surface in the middle latitudes. In his analysis, however, he states that since the computed magnitudes of the atmospheric pole-to-equator temperature difference produced by the symmetrical circulation are greater than those inferred from observations, the observed average temperature difference cannot be explained by a symmetrical circulation regime. The symmetric regime, thus, should be replaced by a wave regime. Although the symmetrical regime is not the prevailing regime in the Martian atmosphere, he suggests that the velocities he computed should be first approximations of the average zonal and meridional velocities of the atmosphere at middle latitudes. On his second analysis (1967) Tang considers another model based on Adem's (1962) simple general circulation model for the Earth's atmosphere. Using this model, Tang calculated the seasonal mean zonal winds at the middle of the Martian atmosphere. The zonal wind as a function of season and latitude is shown in Figure 4-9. The maximum mean zonal winds occur at latitudes 35°N

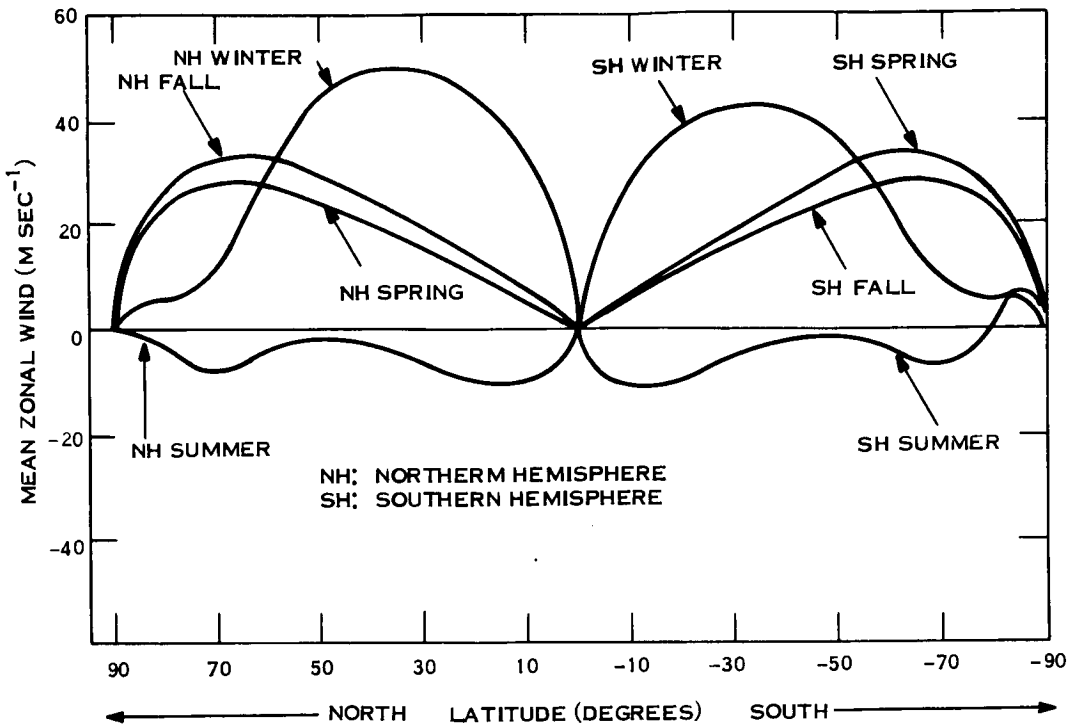

Figure 4-9. Latitudinal Profile of Mean Zonal Wind for the Four Martian Seasons (From Tang, 1967)

and 35°S during the Northern Hemisphere winter solstice, and are about 50 and 40 M/sec, respectively. The winds are westerly except during the summer season of each hemisphere when they are easterly. The easterlies have peaks of 10 m/sec at 10°N and 10°S and secondary peaks of 5 m/sec at 70°N and 70°S. The wind profiles suggest a wave regime during winter, late spring and early fall.

In summary, the observed cloud motions suggest the possible existence of two separate circulation regimes consisting of a symmetric regime in summer and a wave regime in winter. On occasion the symmetric regime may break down into a wave regime. From the more recent theoretical analyses it would appear that the symmetric regime only exists for a short period during the summer months.

4.4.2.2 Projections

The clouds considered in this class and termed "projections" may be characterized as follows:

a. The clouds tend to originate at temperate latitudes: 70 percent are first observed within the latitudes of 30 to 50 degrees (see Figure 4-10).

b. The clouds tend to move within the temperate latitudes: 60 percent terminate within the latitudes of 30 to 50 degrees.

c. The reported velocities of the projections, based on 20 cases observed since 1890, result in a time averaged mean speed of 8.6 m/sec with a maximum reported value of 39 m/sec. Assuming a normal distribution of wind speeds, and determining the standard deviation from the range of the twenty reported values, one obtains a value of 9.1 m/sec which would lead to a 3σ value of about 36 m/sec.

d. The clouds probably are in part aqueous condensations. Dollfus (1965) suggests that the preferential appearance in temperate latitudes in spring may result from an increase in the available water vapor due to vaporization of the caps.

e. The clouds have been reported as extending to great elevations (over 50 kms) and at times observed to be detached from the Martian surface. Since the wind speed will generally increase with altitude one would expect to find higher velocities associated with projections than are reported for the low level yellow (dust) clouds.

Comparing the motion of the projections with circulation models, and recalling that the cloud altitudes are much more variable than those of the dust clouds, the reported motions tend to conform to a symmetric regime (see Figure 4-10) if the cloud altitudes are fairly low. However, if the clouds extend to fairly high altitudes, then the motions conform to a wave regime circulation.

4.4.3 DUST TRANSPORT

If one assumes the yellow clouds to be composed of wind blown dust, as seems the case for the low level clouds, it is then possible to calculate the velocity required to raise dust particles from the surface of the planet. Such calculations have been performed [e.g., Ryan (1964), Galbraith (1966)] and indicate that the required surface winds could be quite high, especially if the surface pressure is as low as 5 millibars. However, it is important to note that a variety of required velocity values can be obtained by making various assumptions. The required velocities are a function of a number of variables any of which would serve to alter the results. For example, the threshold velocity, sufficient to cause particles

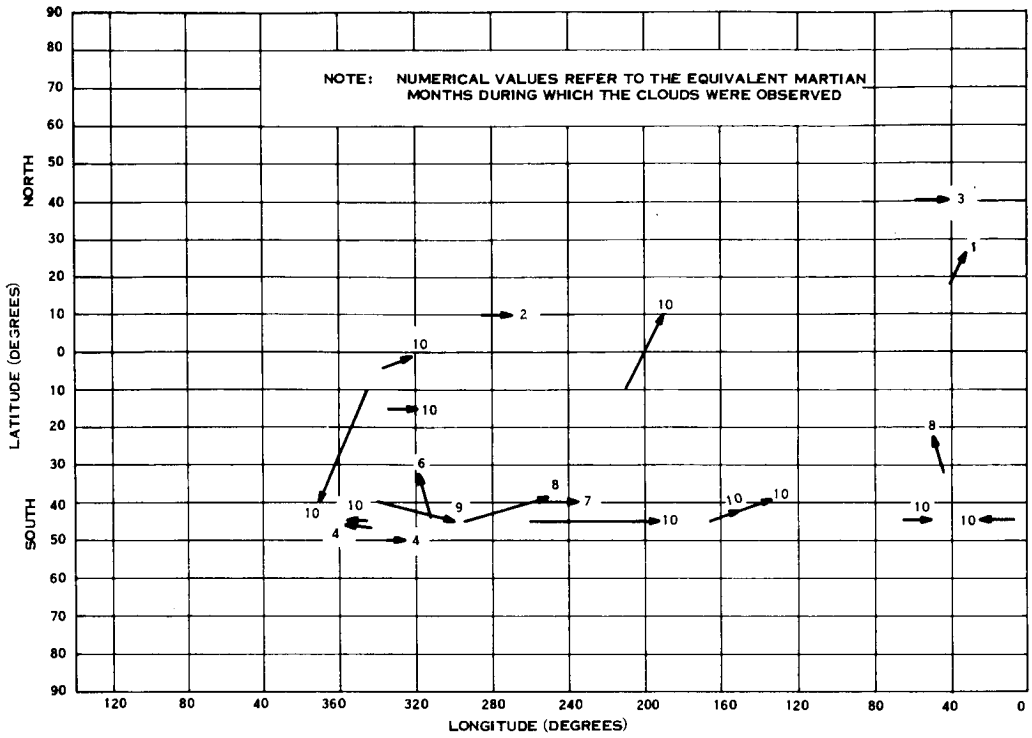

Figure 4-10. Motion of Projections on Mars

of a given diameter to move, is a function of: the particle density, particle diameter, angle between the vertical and the line joining adjacent particle centers, air density, and the gravitational acceleration. Since the air densities at the surface given in the six VM model atmospheres (5, 7, and 10 mbs) varies from 0.68×10^{-5} gm/cc to 2.57×10^{-5} gm/cc, considerable variation can be obtained in the threshold velocity.

In addition, in calculating the wind speed required for particle motion, the customary approach is to use Prandtl's logarithmic velocity profile distribution and to determine the velocity at one meter above the surface. The velocity profile distribution is in this case dependent on the threshold velocity, the altitude above ground, and the surface roughness. The latter variable requires an estimate which will vary with the researchers, although most commonly assumed to be some fraction of the value assigned to terrestrial deserts.

The end result of these calculations of dust transport is to provide a range of required velocities for a range of dependent parameter values. Thus, one can find calculations which show that the wind speeds required to initiate motion of the probable particle sizes on Mars are comparable with the drift velocities of yellow clouds ≈ 8 m/sec, Gifford (1964). However, one can also find values of 67 m/sec which are based on similar calculations, Hess and Pounder (1966).

One solution is to assume that the wind speeds obtained from the general circulation models and cloud motions represent the large scale conditions. The wind speed for particle motion is then defined, and one can then determine what values should be assigned to the dependent parameters. On a small scale, possibly in the form of dust devils, speeds in excess of those obtained from circulation models or cloud motions could exist and the magnitude of these winds might be determined from considerations of particle transport. Neubauer (1966) has done a study of dust devils as the possible source of the dust clouds. His calculations show that the Martian atmosphere is more favorable for the initiation of dust devils than the Earth's atmosphere and that dust devils larger than 100 meters in diameter are a distinct possibility. Once aloft the dust would spread out in large clouds. The fact that dust clouds are observed in equatorial regions which are most prone to generating dust devils and the small size of the clouds (relative to the planet) lends additional support to this theory. On the other hand, it is difficult to explain the giant dust storms of 1956 and 1963 by this mechanism. In general, the theory appears to explain the observed phenomenon quite well.

This model would permit much lower velocity surface winds consistent with observed motions of the clouds, while allowing for dust to be raised from the surface. Goody (1967) has estimated from radiative transfer theory that surface winds of only 6 m/sec would be predicted and these would be of a diurnal nature. He also indicates that an additional zonal flow may exist as well as a meridional flow to transport CO_2 to and from the poles if they are in fact composed of carbon dioxide. He points out further that Leovy and Mintz estimate wind speeds to be 100 m/sec.

Opik (1966) has suggested as an alternate explanation that the clouds are generated by meteroid impacts which he estimates could even generate the planet wide dust clouds of 1956 and 1963. Although volcanic eruptions are sometimes suggested as a cause of the clouds, Opik states this is very unlikely because of the lack of a larger nitrogen atmosphere on Mars which is one of the gases released in a volcanic eruption.

4.4.4 DESIGN WIND SPEEDS

From the viewpoint of providing design wind speeds, it is not possible at this time to justify rejecting the very high values given in the VM atmosphere table (Section 5.2). The preceding discussion on the wind field, with particular regard to providing lower wind speed values, may be of use in system-cost tradeoff studies with associated calculated risks.

It is worth noting that the near-surface wind speed is scaled as $p\ v^2$ = constant. Thus if the surface pressure is shown to be higher than five millibars, the design wind speeds will be reduced. The magnitude of this reduction can be adjudged from the wind speed values given for each VM model atmosphere in Section 5.2.

4.5 CONCLUSIONS

Based on recent interpretations of the spectroscopic and Mariner IV occultation data, the near surface atmosphere is expected to be rich in CO_2 and to have a total pressure of less than 25 millibars.

Based on theoretical analyses, the near surface temperature is expected to be 20° to 50°K less than the surface temperature over the equatorial regions. Over the polar regions, it is expected that the near surface temperature is perhaps 10 to 20 degrees greater than the surface temperature. The maximum wind speed at the surface, based on observed cloud motions, is on the order of 30 meters per second. However, based on theoretical studies of dust transport, the maximum wind may be in excess of 60 meters per second for a low pressure (5 mbs) atmosphere.

4.6 REFERENCES

Adem, J., "On the Theory of the General Circulation of the Atmosphere," Tellus, 14, 102-105, 1962.

Aviation Week, "Voyager-Mars Engineering Model Atmospheres," 22 November 1965.

Deirmendjian, D., "Notes on the Surface Pressure Estimates of the Martian Atmosphere," Rand Corporation Quard. Tech. Program Report (3), RM-2769-JPL, Section XI, April 1961.

deVaucouleurs, G., "The Physical Environment of Mars," in Physics and Medicine of the Atmosphere and Space, Eds. O. O. Benson and H. Strughold, John Wiley and Sons, 1960.

deVaucouleurs, G., "Reconnaissance of the Nearer Planets," AFOSR/DRA-61-1, November 1961.

Dollfus, A., "Polarization Studies of the Planets," in Planets and Satellites, Volume 3, Solar System, Eds. G.P. Kuiper and B.M. Middlehurst, University of Chicago Press, 1961.

Dollfus, A., Étude de la Planète Mars de 1954 a 1958, Ann. D' Astrophys., 28, November 4, 1965.

Evans, D.C., and Wasko, P.E., "Model Atmospheres for the Planet Mars," Aerospace Sciences Meeting, New York, AIAA preprint No. 64-67, January 1964.

Fjeldbo, G., Fjeldbo, W.C., and Eshleman, Von R., "Models for the Atmosphere of Mars Based on the Mariner IV Occultation Experiments," J.G.R., 71, No. 9, May 1966.

Galbraith, T.L., "Particle Transport in the Martian Atmosphere," GE-TM-8126-4, May 1966.

Gifford, F., "The Surface-Temperature Climate of Mars," Ap. J., 123, 1956.

Gifford, F., "The Problem of the Martian Yellow Clouds," Monthly Weather Rev., 91, 1963.

Gifford, F., "A Study of Martian Yellow Clouds that Display Movement," Monthly Weather Review, 92, October 1964.

Goody, R., "Seminar on the Lower Atmosphere of Mars," University of Colorado, March 30, 1967.

Hanst, P.L., and Swan, P.R., "The Absorption Intensity of the $5\nu_3$ Band of Carbon Dioxide and the Martian CO_2 Abundance and Atmospheric Pressure," Icarus, 4, September 1965.

Hess, S.L., "Some Aspects of the Meteorology of Mars," Jrnl. of Meteorology, 7, February 1950.

Hess, D.S., and Pounder, E., "Voyager Environmental Predictions Document," SE003BB001-1B28, NASA-JPL, October 1966.

House, F.B., "The Seasonal Climatology of Mars," Contributions to Planetary Meteorology GCA Technical Report No. 66-8-N, March 1966.

Hunten, D., "CO Bands and the Martian Surface Pressure," Proceedings of the Caltech-JPL Lunar and Planetary Conference, September 13-18, 1965.

Kaplan, L.D., Munch, G., and Spinrad, H., "An Analysis of the Spectrum of Mars," Ap. J. 139, 1964.

Kellogg, W.W., and Sagan, C., "The Atmospheres of Mars and Venus," NAS-NRC-Publ. 944, 1961.

Kliore, A.J.; Cain, D.L.; Levy, G.S.; Eshleman, V.R., Fjeldbo, G.; Drake, F.D.; "Preliminary Results of the Mariner IV Occultation Measurements of the Atmosphere of Mars," Proceedings of the Caltech-JPL Lunar and Planetary Conference, September 13-18 1965.

Kuiper, G.P., "Infrared Spectra of Stars and Planets, IV: The Spectrum of Mars, 1 - 2.5 Microns, and the Structure of its Atmosphere," Comm. of the Lunar and Planet. Lab., 2, No. 31, pp 79-112, University of Arizona, 1964.

Leighton, R.B., Murray, B.C., "Behavior of Carbon Dioxide and Other Volatiles on Mars," Science, 153, p. 136 July 1966.

Leovy, C., "Some Aspects of the Circulation of Mars," Rand Corporation paper P-3262, November 1965.

Leovy, C., "Radiative - Convective Equilibrium Calculations for a Two-Layer Mars Atmosphere," Rand Memo RM-5017, 1966.

Mintz, Y., "The General Circulation of Planetary Atmospheres," Appendix 8, pp 107-146, in "The Atmospheres of Mars and Venus," NAS-NRC-Publ. 944, 1961.

Miyamoto, S., "Meteorological Observations of Mars During the 1962-1963 Opposition, and Observational Study on the General Circulation of Mars," Contr. Nos. 124 and 125, University of Kyoto, 1964.

Munch, G., "Summary Remarks on Mars," Proceedings of the Caltech-JPL Lunar and Planetary Conference, September 13-18, 1965.

Neubauer, F.M., "Thermal Convection in the Martian Atmosphere," JGR, 71, p. 2419, May 15, 1966.

Ohring, G. and Mariano, J., "Seasonal and Latitudinal Variations of the Average Surface Temperature Profile of Mars," GCA Technical Report 67-5-N, March 1967.

Opik, E.J., "The Martian Surface," Science, 153, July 15, 1966.

Owen, T.C., and Kuiper, G.P., "A Determination of the Composition and Surface Pressure of the Martian Atmosphere," Comm. of the Lunar and Planet. Lab., 2, No. 32, University of Arizona, 1964.

Owen, T.C., "A Determination of the Martian CO_2 Abundance," Comm. of the Lunar and Planet. Lab. 2, No. 33, University of Arizona, 1964.

Rasool, S.L., "Structure of Planetary Atmospheres", AIAA Journal, I., No. 1, January 1963.

Ryan, J.A., "Notes on the Martian Yellow Clouds," JGR, 69, September 1964.

Schilling, G.F., "Limiting Model Atmospheres of Mars," Rand Corporation, Report R-402-JPL, August 1962.

Sinton, W.M., Strong, J., Astrophysical Journal, 131, p. 459, 1960.

Spencer, D.F., "Engineering Models of the Martian Atmosphere and Surface," NASA-JPL-TM No. 33-234, July 1965.

Spencer, D.F., "Our Present Knowledge of the Martian Atmosphere," AIAA/AAS Stepping Stones to Mars Meeting, Baltimore, Maryland, March 1966.

Spinrad, H., "Spectroscopic Observations of Mars, 1964-5," Proceedings of the Caltech-JPL Lunar and Planetary Conference, September 13-18, 1965.

Sutton, O.G., Micrometeorology, McGraw Hill, 1953.

Tang, W., "On the Steady Symmetrical Regime of the General Circulation of the Martian Atmosphere" in Contributions to Planetary Meteorology, GCA Technical Report No. 66-8-N, March 1966.

Tang, W., "The General Circulation of the Martian Atmosphere" in Planetary Meteorology, GCA Technical Report 67-5-N, March 1967.

Tilson, S., "Planet Mars," Space/Aeronautics, July 1964.

Vachon, D.N., "Influence of the Mariner IV Findings on the NASA Engineering Models of the Atmosphere of Mars," GE-PIR-8123-755, September 1965.

Vachon, D. N., "Statistical Sampling of Winds on Mars," GE-TM-8126-7, July 1966.

Vachon, D. N., "Design Environments for Missions to Mars," GE-TM-8126-8, August 1966.

Weidner, D. K., and Hasseltine, C. L., "Natural Environment Design Criteria Guidelines for MSFC Voyager Spacecraft for Mars 1973 Mission," NASA-TMX-53616, June 1967.

SECTION 5

ENTRY ATMOSPHERE MODELS

SECTION 5
ENTRY ATMOSPHERE MODELS

5.1 INTRODUCTION

The entry atmosphere models most commonly used in design studies are the Voyager Mars (VM) series. The basic characteristics of the 10 VM models were taken from Hess and Pounder (1966) and are given in Table 5-1. The GE atmosphere modeling computer program was utilized to provide parameter values up to an altitude of 200 kilometers. The automatic plot subroutine was then utilized to provide profiles of the parameters of interest. Tabulations and graphical presentations of each of the 10 VM models for altitudes up to 200 kilometers are provided in milestone report VOY-D4-TM-4 (Jewett and Vachon, 1967).

It is the purpose of this section of the report to provide a modification of a selected VM model atmosphere, whereby an estimate of the probable latitudinal and seasonal variation of the atmosphere below 100 kilometers can be obtained.

The VM-4 model atmosphere was selected as the reference model, since the initial conditions are similar to those of the MSFC mean model (Weidner and Hasseltine, 1967).

5.2 NEAR SURFACE ATMOSPHERE

In order to simplify the construction of a latitudinal-seasonal model of the Martian atmosphere, only the two extreme seasons are considered.

5.2.1 TEMPERATURE

The latitudinal-seasonal variation of temperature was obtained by calculating the mean temperature for every 10 degrees of latitude from the isotherm maps prepared by Gifford-1956, which were also utilized by Hess and Pounder, as well as Weidner and Hasseltine. The eccentricity of the orbit of Mars was expected to result in a lack of symmetry in the surface temperature distribution. However, if a degree of symmetry existed, then the

Table 5-1. Voyager Mars Entry Atmosphere Models

Property	Symbol	Dimension	VM-1	VM-2	VM-3	VM-4	VM-5	VM-6	VM-7	VM-8	VM-9	VM-10
Surface pressure	P_o	mb	7.0	7.0	10.0	10.0	14.0	14.0	5.0	5.0	20.0	20.0
		lb/ft^2	14.6	14.6	20.9	20.9	29.2	29.2	10.4	10.4	41.7	41.7
Surface density	ρ_o	$(gm/cm^3)10^5$	0.955	1.85	1.365	2.57	1.91	3.08	0.68	1.32	2.73	3.83
		$(slugs\ ft^3)10^5$	1.85	3.59	2.65	4.98	3.7	5.97	1.32	2.56	5.30	7.44
Surface temperature	T_o	^oK	275	200	275	200	275	200	275	200	275	200
		^oR	495	360	495	360	495	360	495	360	495	360
Stratospheric temperature	T_s	^oK	200	100	200	100	200	100	200	100	200	100
		^oR	360	180	360	180	360	180	360	180	360	180
Acceleration of gravity at surface	g	cm/sec^2	375	375	375	375	375	375	375	375	375	375
		ft/sec^2	12.3	12.3	12.3	12.3	12.3	12.3	12.3	12.3	12.3	12.3
Composition (percent)												
CO_2 (by mass)			28.2	100.0	28.2	70.0	28.2	35.7	28.2	100.0	28.2	13.0
CO_2 (by volume)			20.0	100.0	20.0	68.0	20.0	29.4	20.0	100.0	20.0	9.5
N_2 (by mass)			71.8	0.0	71.8	0.0	71.8	28.6	71.8	0.0	71.8	62.0
N_2 (by volume)			80.0	0.0	80.0	0.0	80.0	32.2	80.0	0.0	80.0	70.5
A (by mass)			0.0	0.0	0.0	30.0	0.0	35.7	0.0	0.0	0.0	25.0
A (by volume)			0.0	0.0	0.0	32.0	0.0	38.4	0.0	0.0	0.0	20.0
Molecular weight	M	mol^{-1}	31.2	44.0	31.2	42.7	31.2	36.6	31.2	44.0	31.2	31.9
Specific heat of mixture	C_p	cal/gm^oC	0.230	0.166	0.230	0.1530	0.23	0.174	0.230	0.166	0.230	0.207
Specific heat ratio	α		1.38	1.37	1.38	1.43	1.38	1.45	1.38	1.37	1.38	1.41
Adiabatic lapse rate	Γ	$^oK/km$	-3.88	-5.39	-3.88	-5.85	-3.88	-5.14	-3.88	-5.39	-3.88	-4.33
		$^oR/1000\ ft$	-2.13	-2.96	-2.13	-3.21	-2.13	-2.82	-2.13	-2.96	-2.13	-2.38
Tropopause altitude	h_T	km	19.3	18.6	19.3	17.1	19.3	19.4	19.3	18.6	19.3	23.1
		kilo ft	63.3	61.0	63.3	56.1	63.3	63.6	63.3	61.0	63.3	75.8
Inverse scale height (stratosphere)	β	km^{-1}	0.0705	0.199	0.070	0.193	0.0705	0.1655	0.0705	0.199	0.0705	0.145
		$ft^{-1} \times 10^5$	2.15	6.07	2.15	5.89	2.15	5.05	2.15	6.07	2.15	4.41
Continuous surface wind speed	$\bar{v}$	ft/sec	186.0	186.0	155.5	155.5	131.5	131.5	220.0	220.0	110.0	110.0
Maximum surface wind speed	v_{max}	ft/sec	470.0	470.0	390.0	390.0	330.0	330.0	556.0	556.0	278.0	278.0
Design vertical wind gradient	$\frac{d\bar{v}}{dh}$	ft/sec/1000 ft	2	2	2	2	2	2	2	2	2	2
Design gust speed	v_g	ft/sec	200	200	150.0	150.0	150.0	150.0	200.0	200.0	100.0	100.0

northern summer could be taken as representative of the southern summer and vice versa. It was therefore desirable to determine the latitudinal variation of temperature for the southern hemisphere in both summer and winter. The calculated mean temperatures are given in Table 5-2, along with a comparison of the temperature values.

From the temperature differences obtained in comparing the southern hemisphere winter and summer temperatures, it is obvious that a marked seasonal variation exists. When the comparison is made between the southern hemisphere summer and the northern hemisphere summer, the latter obtained by reversing the southern winter distribution, the temperature differences remain fairly large. Thus it is concluded that the temperature across the Martian surface is not symmetrical, and that the influence of the planet's orbital eccentricity is the dominant cause of the lack of symmetry.

Table 5-2. Mean Temperature (^{o}K) as a Function of Latitude and Season on Mars

Season	Latitude (degrees)													
	-70	-60	-50	-40	-30	-20	-10	0	10	20	30	40	50	60
Southern summer	235	250	261	266	273	277	280	277	272	266	258	251	241	232
Southern winter	245	252	254	262	268	272	275	278	280	283	284	283	278	269
Δ T	10	2	7	4	5	5	5	1	8	17	26	32	37	37
Southern summer	235	250	261	266	273	277	280	277	272	266	258	251	241	232
Northern summer (reverse of southern winter)	-	269	278	283	284	283	280	278	275	272	268	262	254	252
Δ T	-	19	17	17	11	6	0	1	3	6	10	11	13	20

Since the Voyager 1973 mission is understood to be primarily concerned with the time period coinciding with the southern summer, the southern hemisphere summer temperature distribution was selected.

5.2.2 PRESSURE

The latitudinal and seasonal variation of surface pressure is expected to be quite small. For example, at the earth's surface the pressure variation with latitude and season is on the order of 1 percent (Vachon, 1964). By analogy with the Earth's atmosphere, it is expected that the latitudinal and seasonal variations of the mean surface pressure is of secondary importance.

5.3 TROPOSPHERE CHARACTERISTICS

5.3.1 THERMAL GRADIENT

The troposhere is assumed to be characterized by a thermal gradient which is equal to the adiabatic lapse rate. For the VM-4 model atmosphere, the adiabatic lapse rate is equal to -5.85°K/km.

The probable existence of super-adiabatic gradients near the surface over equatorial regions is neglected as it is not expected to be greatly significant, since the highest mean temperature given in Table 5-2 is as much as 30 degrees less than the highest mean temperature expected over certain equatorial regions.

The neglect of temperature inversions over polar regions is likewise not particularly critical. Indeed, since the latitudinal models were only to be constructed for latitudes of less than 60 degrees, the neglect of temperature inversions over polar regions is of secondary importance at this time.

For present purposes, it is assumed that the adiabatic temperature lapse rate is an acceptable means of defining the temperature profile. It is further assumed that the adiabatic lapse rate is equally valid at any latitude or during any season.

5.3.2 TROPOPAUSE ALTITUDE

The tropopause altitude, top of the troposphere, is defined as the altitude at which the troposphere temperature reaches a value equal to the stratosphere temperature. The VM-4 stratosphere temperature is given as 100°K (Hess and Pounder, 1966) which for a surface temperature of 280°K and a thermal gradient of -5.85°K/km, would yield a tropopause altitude of 30.8 kilometers. On the other hand, if a stratosphere temperature of 150°K is used for the same conditions, then a tropopause altitude of 22.2 kilometers is obtained. The latter altitude is more in keeping with the tropopause altitudes of the VM models, which range from 17.1 to 23.1 kilometers. Since the Martian stratosphere temperature is expected to be in the range of 100 to 150°K, the use of a stratosphere temperature of 150°K appears easily justifiable.

Assuming the stratosphere temperature to remain relatively constant in time and space, the tropopause altitude must then vary with latitude and season. In order to determine whether the resultant Martian tropopause altitude variations were reasonable, a comparison with the Earth's tropopause altitude variations was made. The mean tropopause altitude over equatorial regions and over a latitude of 60 degrees in winter is given in Table 5-3 for both Mars and Earth. The comparison of the percent variation in the tropopause altitude from equatorial regions to 60 degrees north appears reasonable. Certainly one would expect a higher tropopause altitude over the equatorial regions than over the subpolar regions.

5.4 DISCUSSION OF RESULTS

Discussing the merits of the empirically derived latitudinal and seasonal models is somewhat difficult, since one does not have any corresponding measurements against which the

Table 5-3. Latitude Variation of the Tropopause Altitude on Mars and Earth

Latitude	Tropopause Altitude (km)	Percent Variation
Earth		
Equatorial regions	16	75
60° north - winter	12	
Mars		
Equatorial regions	22	64
60° north - winter	14	

models could be checked. It is therefore necessary to draw on analogies with the Earth's atmosphere in order to discuss the probable validity of the models.

As a basis for comparison, the latitudinal variation of pressure and density at 100 kilometers was selected for both Earth and Mars. Such a comparison does not necessarily prove the derived models, but should serve to determine if they are reasonable. The pressure and density at 100 kilometers for the Earth's atmosphere (Vachon, 1964) and for the Martian atmosphere are given in Table 5-4 for 0 and 60 degrees north latitude.

Comparison of the percent variation values of pressure and density for Earth and Mars given in Table 5-4 suggests that the latitudinal variations inherent in the Martian models are reasonable. Further, the profiles of the vertical distribution of density, shown in Figure 5-1, for 0 and 60 degrees latitude are also in keeping with the distribution which would be expected, based on analogy with the Earth's atmosphere.

Table 5-4. Latitudinal Variation of Pressure and Density at 100 Kilometers on Mars and Earth

Parameter	Latitude		
	60° North Winter	0° Latitude	Percent Variation
Mars			
Pressure (mb)	5.3×10^{-5}	8.0×10^{-5}	66
Density (g/cc)	1.9×10^{-10}	2.9×10^{-10}	66
Earth			
Pressure (mb)	3.7×10^{-4}	8.1×10^{-4}	46
Density (kg/m^3)	4.9×10^{-7}	1.1×10^{-6}	45

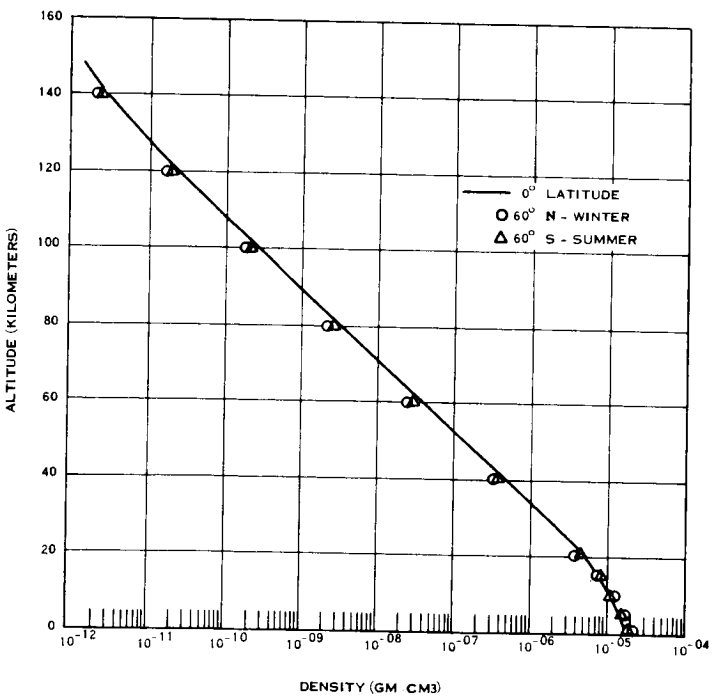

Figure 5-1. Density Profile Variation with Season and Latitude

Profiles of the parameters of interest are provided in milestone report VOY-D4-TM-18 (Vachon, 1967) for a number of latitudes during summer and winter.

5.5 CONCLUSIONS

The existing Voyager-Mars (VM) model atmospheres appear adequate to define the lower atmosphere structure, that is, below 100 kilometers. Since these models do not account for time-space variations, it is necessary to modify them in order to provide an estimate of the latitudinal and seasonal variation of the atmosphere. The method presented is considered adequate, since it makes maximum use of the VM model characteristics, as well as being consistent with the latitudinal and seasonal surface temperature variations recommended for use by Hess and Pounder (1966) and Weidner and Hasseltine (1967). The results indicate that the density at 100 kilometers may vary by as much as 65 percent from the equator to 60 degrees latitude. Density variations of about 45 percent are normally encountered in models of the Earth's atmosphere at 100 kilometers over this latitude spread.

The tropopause altitude variation from equator to 60 degrees latitude, resulting from the model assumptions, was found to be 75 percent for Mars. This variation is comparable to that encountered in models of the Earth's atmosphere, where the tropopause altitude variation is normally about 65 percent over the same latitude range.

5.6 REFERENCES

Hess, D. S., and Pounder, E., "Voyager Environmental Predictions Document," SE-003-BB001-1B28, NASA-JPL, October 1966.

Vachon, D.N., "A Model of the Latitudinal and Seasonal Variation of the Atmosphere Below 100 Kilometers," GE-TIS-64SD275, September 1964.

Vachon, D.N., "On the Latitudinal and Seasonal Variation of the Martian Atmosphere Below 100 Kilometers," GE-VOY-D4-TM-18, August 1967.

Vachon, D.N. and Jewett, J., "Survey of Present Knowledge on the Martian Atmosphere with Application to Spacecraft Design, Part II. Entry Atmosphere Models," VOY-D4-TM-4, 1967.

Weidner, D.K., and Hasseltine, C.L., "Natural Environment Design Criteria Guidelines for MSFC Voyager Spacecraft for Mars 1973 Mission," NASA-TM-X-53616, June 1967.

SECTION 6

OUTER ATMOSPHERE STRUCTURE

SECTION 6
OUTER ATMOSPHERE STRUCTURE

6.1 INTRODUCTION

The orbital lifetime of a body placed in orbit around Mars can be calculated by considering the atmospheric density likely to be experienced at orbital altitudes.

Defining the density profile is somewhat of a problem, however, since it can be expected that the structure of the outer atmosphere will be greatly influenced by solar variations in much the same manner as the Earth's atmosphere. It is expected that the density at orbital altitudes will be greatest during periods of high solar activity, as is the case in the Earth's upper atmosphere. Thus, an estimate of the probable solar cyclic related variation of the upper atmosphere of Mars can be of assistance in reducing the uncertainty range of density variation likely to be experienced in any given year. In addition, such an estimate would provide a means of relating derived density profiles from fly-by experiments made at different periods of time.

The purpose of this section is to provide (1) a brief discussion of the probable time-space variations of the outer atmosphere of Mars; (2) present several models of the outer atmosphere which have been developed; and (3) to develop, by empirical means, a method of reducing density uncertainties associated with a given model by allowing for solar cyclic variations.

6.2 PREDICTED SOLAR FLUX

Before discussing the probable solar cyclic variations of the upper atmosphere of Mars, an estimate of the probable variation of solar activity should be made. Of particular interest is the time variation of the 10.7 cm radiation flux for the years 1964, 1969, 1971, 1973, and 1975.

The predicted mean and extreme values of the 10.7 cm flux (Galbraith, 1967), together with the observed mean and extreme values for 1964 are given in Table 6-1.

Table 6-1. Predicted Values of the 10.7 cm Flux
(in units of 10^{-22} watts/cm^2)

Year	Mean	Extreme
1964	70	75 - 85
1969	205 - 225	280 - 310
1971	150 - 160	205 - 225
1973	110 - 135	140 - 175
1975	70 - 80	85 - 110

From the values given in Table 6-1, it is seen that the Mariner IV fly-by occurred during a period of low solar activity, while the Mars'69 fly-by should occur during a period of high solar activity. Consequently, if the upper atmosphere of Mars behaves in a manner similar to the Earth's atmosphere, then the derived densities from the Mars'69 fly-by experiments should be considerably greater than those derived from the Mariner IV experiments.

A period of relatively low solar activity is expected in 1973 with a minimum of activity occurring in 1976. Thus, it is likely that the atmospheric density encountered at orbital altitudes by the Voyager spacecraft in 1973 will be closer to that derived from the Mariner IV experiments than to that derived from the Mars'69 experiments. Significantly, the atmospheric densities derived from the Mars'69 experiments should provide a close estimate of the maximum density likely to be encountered in the upper atmosphere of Mars.

6.3 EXOSPHERE

6.3.1 TEMPERATURE VARIATION

The empirical relation between the exospheric temperature and solar activity, (Vachon and Homsey, 1963), was found to be consistent with the temperature values derived from the Mariner IV data (Vachon, 1966). On the basis of this agreement, the empirical relation appears acceptable at this time. Data from the Mars '69 fly-by may provide an opportunity to check the relative validity of the relation for periods of high solar activity. For the present, it is assumed that the empirical relation will provide a reasonable estimate of the exospheric temperature variation as a function of solar activity.

The temperature minima (T_n) are taken to occur at 0400 while the maxima (T_x) occur at 1400 for any value of the 10.7 cm solar flux (S). The minima and maxima are obtained by the following formulation:

$$T_n = 1.94S + 275$$

$$T_x = 3.05S + 372$$

where T_n and T_x are in degrees Kelvin, while the 10.7 cm solar flux is in units of 10^{-22} watts/m^2-cps. The values of exospheric temperature as a function of solar activity are given in Table 6-2:

Table 6-2. Martian Exospheric Temperature (^oK) as a Function of the 10.7 cm Solar Flux (S)

T (^oK)	Solar Flux (S)				
	70	100	150	200	250
Minima	411	469	566	663	760
Maxima	586	677	829	982	1134

6.3.2 ALTITUDE OF EXOSPHERE BASE

The base of the exosphere (i.e., top of the thermosphere) was initially proposed as a variable dependent on the thermosphere thermal gradient and the exosphere temperature. More recent evaluations indicate that for all practical purposes the altitude of the base of the exosphere may be relatively constant in time, although intimately related to the selected values of the thermosphere thermal gradient. A comparison between the Harris and Priester (1962) temperature values at 420 kilometers and the temperature value at 2000 kilometers, well within the Earth's exosphere, is given in Table 6-3.

It thus appears that the base of the exosphere is relatively insensitive to variations in solar activity.

The base altitude of the Martian exosphere is intuitively expected to be lower than it is in the Earth's atmosphere. The upper atmosphere models presented by Hess and Pounder (1967) would suggest an exosphere base altitude of 250 km. Similarly, the model of Smith and Beutler (1967) would suggest an exosphere base altitude of about 340 kilometers.

The empirically derived base altitude of the exosphere will be discussed in Section 6.4.3 since, as noted above, it is expected to be related to the selected values of the thermosphere thermal gradient.

Table 6-3. Comparison of the Harris and Priester Model Temperatures at 2000 km and 420 km

	Solar Flux (S)				
T (^{o}K)	250	200	150	100	70
Minima					
2000 km	1392	1163	944	737	612
420 km	1383	1155	938	732	609
Maxima					
2000 km	2121	1768	1409	1046	827
420 km	2068	1739	1394	1039	822

6.4 THERMOSPHERE

6.4.1 ALTITUDE OF BASE

The atmosphere of Mars at high altitudes is expected to exhibit a region of temperature increase due to recombination heating. The altitude at which this heat source occurs has recently been estimated at about 90 kilometers (Gross, et. al. - 1966), 100 km (Donahue, 1966), and <140 km (Chamberlain and McElroy, 1966). Based on our own evaluations of the Mariner IV data (Vachon, 1966) the base of the thermosphere was evaluated as being around 103 kilometers. For our purposes, the base of the thermosphere is taken as being at an altitude of 100 kilometers. To simplify further calculations, it is assumed that conditions at 100 kilometers remain constant in time and space. Thus, we introduce a fixed boundary condition at 100 kilometers, which contains all of the inherent limitations contained in the same assumption made in regards to the Earth's upper atmosphere, e.g., the density at the boundary altitude is held constant in time and space, although it is known to vary substantially. In the Harris and Priester model (1962), it is found that a fixed boundary exists at an altitude of 120 kilometers. Considering that the Harris and Priester model provides a reasonable fit to the observed conditions at altitudes in excess of 200 kilometers, the assumption of a fixed boundary condition appears permissable as a means of developing models of the atmospheric structure above 200 kilometers for use in orbit decay evaluations.

6.4.2 THERMAL GRADIENT

The thermal gradient in the thermosphere would be expected to be greatest near the base and to diminish with altitude. The magnitude of the gradient itself is dependent upon the chemical kinetics of the atmosphere. Although it is doubtful that one can use the thermal gradients of the Earth's thermosphere to derive the probable gradients in the Martian thermosphere, it would be interesting to compare such empirically derived values with those from existing models of the Martian upper atmosphere.

The intensity of solar radiation at the Martian orbital distance is about half that incident at the Earth's distance. Since the thermosphere is a byproduct of photodissociation or recombination, it will be assumed that the Martian thermosphere thermal gradients are equal to

half the value of the Earth's thermosphere thermal gradients. This is an admittedly crude assumption for it totally neglects the differences in the chemical kinetics of the two atmospheres. The thermal gradients for three selected altitude intervals, as well as the equivalent over the three intervals, is given in Table 6-4 for the Earth, and in Table 6-5 for Mars as a function of solar activity.

From the values presented in Table 6-5, it is obvious that the estimates of the altitude variation of the Martian thermal gradients, based on values for the Earth's thermosphere, decrease much more rapidly than those used in Martian atmosphere models. However, based on our own evaluation of the Mariner IV data (Vachon, 1966), the thermal gradient over the altitude range of 105 to 138 kilometers, during a period of low solar activity, was found to lie within the limits of $1 \pm 0.5^{o}K/km$.

From the viewpoint of establishing empirical relationships, it would appear more prudent at this time to only use the integrated gradient values between 400 and 100 kilometers. Since the integrated thermal gradients obtained from evaluations of the chemical kinetics (Smith and Beutler, 1967) are in reasonable agreement with the empirically derived values, the latter may then provide a relatively reasonable means of relating variations of the thermal gradients as a function of solar activity.

6.4.3 ALTITUDE OF TOP OF THERMOSPHERE

As noted in Section 6.3.2, the altitude of the top of the thermosphere; i.e., base of the exosphere, is expected to be relatively constant. However, if one uses the integrated thermal gradients of Section 6.4.2, together with the exospheric temperature values of Section 6.3 and a fixed boundary at the base of the thermosphere, then it is found that the altitude of the base of the exosphere must vary. Thus, it is found that either the altitude of the top of the thermosphere must be made variable or the integrated thermal gradients must be changed, in order to fit the condition of a fixed base altitude for the exosphere. Since the thermal gradients are dependent upon the chemical kinetics of the atmosphere, which were largely ignored, it is felt that modifying the gradient values would be better than introducing

Table 6-4. Altitude Variation of the Thermal Gradient (^{o}K/km) in the Earth's Thermosphere as a Function of Solar Activity

Altitude (km)	Solar Flux (S)				
	250	200	150	100	70
220 - 120					
Minima	8.72	6.83	4.94	3.13	2.06
Maxima	12.65	10.58	8.28	5.70	3.99
320 - 220					
Minima	1.32	0.98	0.74	0.53	0.40
Maxima	3.52	2.64	1.76	0.97	0.58
420 - 320					
Minima	0.24	0.19	0.15	0.11	0.08
Maxima	0.96	0.65	0.35	0.17	0.10
420 - 120					
Minima	3.42	2.67	1.94	1.26	0.85
Maxima	5.70	4.61	3.46	2.28	1.56

Table 6-5. Altitude Variation of the Thermal Gradient (^{o}K/km) in the Martian Thermosphere as a Function of Solar Activity

Altitude (km)	Solar Flux (S)						
	250	200	150	100	70	Smith/ Beutler 1967	Weidner/ Hasseltine 1967-Mean
200 - 100							
Minima	4.36	3.42	2.47	1.56	1.03	2.40	*2.84
Maxima	6.33	5.29	4.14	2.85	2.00	2.40	*2.84
300 - 200							
Minima	0.66	0.49	0.37	0.27	0.20	1.06	1.02
Maxima	1.76	1.32	0.88	0.49	0.29	1.06	1.02
400 - 300							
Minima	0.12	0.09	0.07	0.06	0.04	0.28	1.36
Maxima	0.48	0.31	0.17	0.09	0.05	0.28	1.36
400 - 100							
Minima	1.71	1.33	0.97	0.63	0.42	1.27	1.63
Maxima	2.85	2.30	1.73	1.14	0.78	1.27	1.63

* Gradient value given is for an altitude interval of 200-150 km

a variable exosphere base altitude. Using the integrated gradient values from Table 6-5 together with the exosphere temperature from Table 6-2, the lowest altitude of the exosphere (460 km) was found to be associated with the highest integrated thermal gradient (2.85^{o}K/km), and the highest exosphere temperature (1134°K). Since there is doubt that the exosphere temperature could be this high, and that the integrated thermal gradient is itself much higher than the Smith and Beutler value based on evaluation of the chemical kinetics, it was decided to reject this condition as the basis for scaling. The next lowest altitude of the exosphere (482 km) was found to be associated with an integrated thermal gradient of 1.7^{o}K/km, and an exosphere temperature of 760°K. The relative agreement between the integrated gradient of this case and the model of Weidner and Hasseltine (1967) was taken as a favorable aspect, since their model is based in part on an evaluation of the chemical kinetics. Further, the exosphere temperature value of 760°K is not out of accord with most studies of the chemical kinetics of the Martian upper atmosphere. Although intuitively the top of the thermosphere is expected to be lower than it is in the Earth's atmosphere, for the present it is assumed that the top of the thermosphere on Mars is at an altitude of 482 kilometers.

The introduction of a fixed altitude for the top of the thermosphere, with a fixed boundary at 100 kilometers and for the given exospheric temperatures, requires a change in the integrated thermal gradient values. The integrated thermal gradient values for a variable exosphere altitude and for a fixed exosphere altitude are given in Table 6-6.

6.5 OUTER ATMOSPHERE MODELS

Several models of the outer atmosphere of Mars have been developed in the past year and utilized in orbital lifetime and planetary quarantine studies. The first of these, identified as the VM-3 extension, is an empirical model intended as an estimate of the maximum density likely to be encountered at orbital altitudes. The second, identified as the GE Voyager reference atmosphere, is based on a theoretical model which represented the mean atmospheric structure consistent with the Mariner IV fly-by results. The third, identified as the

Table 6-6. Integrated Thermal Gradients (^{o}K/km) in the Martian Thermosphere as a Function of Solar Activity

T (^{o}K)	Solar Flux (S)				
	250	200	150	100	70
Variable Exosphere					
Minima	1.71	1.33	0.97	0.63	0.42
Maxima	2.85	2.30	1.73	1.14	0.78
Fixed Exosphere					
Minima	1.71	1.46	1.20	0.95	0.80
Maxima	2.69	2.29	1.89	1.49	1.26

MSFC model, is a semi-empirical model which provides a preliminary estimate of the mean density profile and associated confidence envelopes.

6.5.1 VM-3 MODEL EXTENSION

The probable characteristics of the thermosphere and exosphere of Mars were utilized in extending the VM-3 model atmosphere (Vachon, 1966). As the main purpose of the model was to provide an estimate of the maximum density likely at orbital altitudes, the VM-3 model atmosphere was selected for extension, since it provided the highest density at altitudes of 100 kilometers.

The VM-3 atmosphere density profile was extended as follows:

a. The altitude of the base of the thermosphere was taken as equal to 103 kilometers.

b. The solar flux index was taken as 250 units.

c. The thermal gradient in the thermosphere was taken as 1°K/km for the night side and 1.5^{o}K/km for the day side.

d. The exosphere temperature was taken as 760°K on the night side and 1134°K on the day side.

e. The molecular weight was assumed constant with altitude. In testing the influence of molecular weight variations, the molecular weight above 103 kilometers was assumed to decrease by one-half its value below 103 kilometers. This latter condition resulted in a four-order-of-magnitude increase in the density at 1,000 kilometers.

f. The density of interplanetary space during high solar activity was assumed to be on the order of 10^{-21} to 10^{-22} gms/cc.

g. In order to simplify the calculations, the geopotential altitude concept was used which resulted in reducing the thermal gradients cited above.

The density in the thermosphere was calculated by use of the following formula:

$$\rho = \rho_o \left(\frac{T}{T_o}\right)^{-\left(1 + \frac{M_o g_o}{R\, dT/dh}\right)}$$

The density in the exosphere was calculated by use of the more common exponential decay formula:

$$\rho = \rho_o \exp\left[\left(-\frac{M_o g_o}{R T}\right) h - h_o\right]$$

The density at 1000 kilometers during a period of high solar activity was thus calculated as ranging from a diurnal minimum of 9×10^{-18} g/cc to a diurnal maximum of 3×10^{-15} g/cc. On the basis of the theoretical studies being performed at JPL (Newburn, 1966), the maximum density profile appeared quite conservative. Indeed, the maximum exospheric temperature consistent with Gunn's model (of JPL) is 700°K as compared with our empirically derived value of 760 to 1134°K for periods of high solar activity.

Thus the VM-3 model extension, daytime density profile, is expected to represent what should prove to be a very conservative density profile.

6.5.2 GE VOYAGER REFERENCE ATMOSPHERE

The description of the Martian upper atmosphere recently provided by Hess and Pounder (1966) was used as the basis for a proposed Voyager Mars reference atmosphere (Vachon, 1967). The reference atmosphere was intended not as an extreme atmosphere model, but rather as a probable mean.

In order to provide a complete profile of the atmospheric structure up to 900 kilometers, the upper limit of Figure 9 in Hess and Pounder (1966), it was necessary to extrapolate the data downward below 100 kilometers. The assumptions made in extrapolating the JPL model downward were discussed with D. Spencer of JPL (1966) and are considered reasonable. The following approach was used in extrapolating the JPL model downwards.

The atmospheric structure between 100 and 900 kilometers is given in graphical form (Hess and Pounder, 1966) and provide (a) the number density of the various constituents, (b) the kinetic temperature up to 300 kilometers, and (c) the free electron concentration up to about 200 kilometers. The constituent number densities were obtained from Figure 9 (Hess and Pounder, 1966) for altitude increments of 50 kilometers up to 300 kilometers, and thereafter at 100 kilometer intervals. The molecular weight and mass density was then calculated from the extracted values of number density. These latter values were in turn replotted and curve-fitted to obtain smooth profiles.

The temperature values were extracted from Figure 9 of the referenced report for a number of altitude values required to closely fit the profile given.

The atmospheric structure below 100 kilometers consistent with the definition of the structure above 100 kilometers was quickly found not to fit any of the VM atmosphere models. Thus in order to obtain a self-consistent model it was necessary to extrapolate the atmosphere downward. The conditions at 100 kilometers obtained from Figure 9 of the referenced report are:

$T = 150^{o}K$; $\rho = 1.9 \times 10^{-10}$ g/cc

$M = 43$ or 44; $p = 5.4 \times 10^{-5}$ millibars

Assuming the surface temperature to be $275^{o}K$ (which corresponds to the value used in VM-1, 3, 5, 7, and 9) and the troposphere temperature gradient equal to the adiabatic, then for a CO_2 rich atmosphere with $M = 44$, $dT/dZ = -5.39^{o}K/km$. The tropopause is taken as occurring at an altitude where the temperature reaches a value of $150^{o}K$ (equal to the value at 100 km). The tropopause altitude is thus obtained as 23.2 kilometers. Using this temperature profile, the pressure at 100 kilometers is then extrapolated downward and yields a surface pressure value of 7.5 millibars.

The density values above 100 kilometers selected for this reference atmosphere are those which correspond to the model developed using an eddy diffusivity value of 10^{-3} km^2/sec. This latter value corresponds to a diffusion time on the order of a few hours. This model was selected since it contains the higher densities of the two models given.

The vertical structure of this reference atmosphere is provided in Figure 6-1 and includes the density values obtained directly from Figure 9 in Hess and Pounder. The computer printout and associated automatic plots for this model are provided in milestone report VOY-D4-TM-4 (Vachon, 1967).

Comparing the density at 1000 kilometers obtained from this model ($\approx 2 \times 10^{-20}$ g/cc) with that obtained in the VM-3 extension (9×10^{-18} to 3×10^{-15} g/cc), it is seen that the VM-3 extension is indeed very conservative. However, since the reference model is not necessarily intended as a mean during periods of high solar activity, while the VM-3 extension is restricted to that period, comparisons between the two models require a degree of latitude.

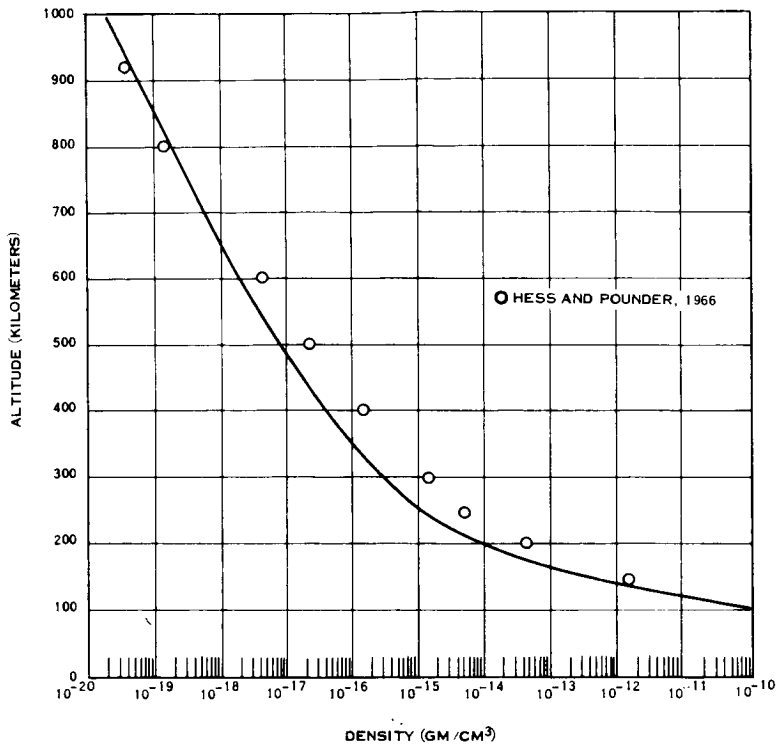

Figure 6-1. GE Voyage Reference Atmosphere Density Profile

6.5.3 MSFC ATMOSPHERE MODEL

The MSFC mean model and 99 percent confidence envelopes for the Mars atmosphere were recently prepared by Weidner (1967). These models contain the attractive feature of having a molecular weight variation with altitude (Figure 6-2) which does not asymptote at 16 as in models based on the chemical kinetics of the Martian atmosphere. Although the minimum, mean, and maximum density models (Figure 6-3) are semi-empirical, they appear reasonable at this time, pending further studies of the chemical kinetics of the upper atmosphere.

Comparisons of the mean atmosphere parameter values from Weidner (1967) and from the GE Voyager reference atmosphere are given in Table 6-7.

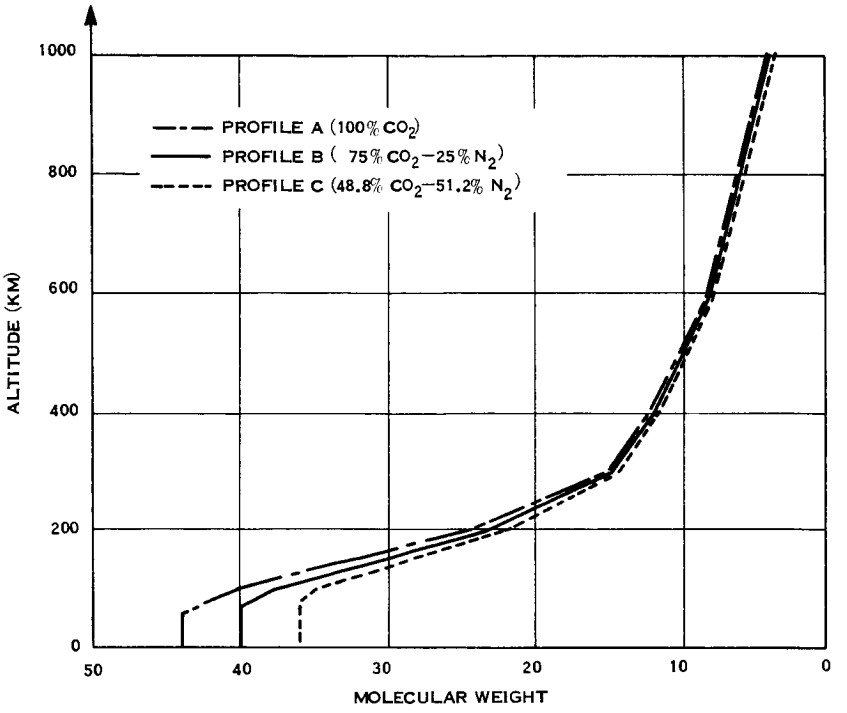

Figure 6-2. Idealized Martian Molecular Weight Profiles (from Weidner, 1967)

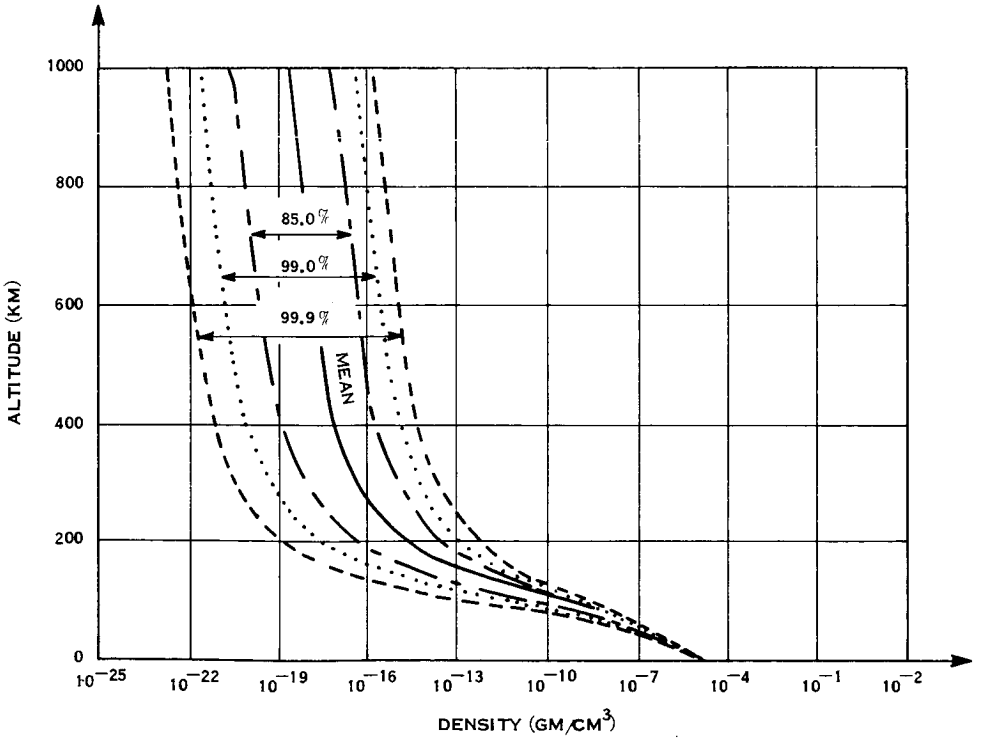

Figure 6-3. Preliminary Mean Profile and Confidence Envelopes for Martian Atmospheric Density (From Weidner, 1967)

Table 6-7. Comparison of Mean Atmosphere Parameter Values at 1000 Kilometers

Parameter	Weidner (1967)	GE Reference Atmosphere
Kinetic temperature (^{o}K)	914	412
Pressure (dynes/cm^{2})	7.7×10^{-9}	4.6×10^{-9}
Density (g/cc)	6×10^{-19}	2×10^{-20}
Molecular weight	5.9	16

The comparison of the parameter values indicates that while the density values do not differ appreciably, there exists considerable conflict in the temperature and molecular weight values. Based on the theoretical studies of Gunn at JPL it is unlikely that the kinetic temperature will exceed 700°K. On the other hand, it is intuitively unlikely that the molecular weight will asymptote at 16. Future studies of the chemical kinetics of the upper atmosphere which includes the probable concentrations of hydrogen and helium may well resolve this quandary. For the present, the mean density model of Weidner-1967 is preferred, since associated with this mean density model are a family of density profiles representing various confidence levels which include the GE reference atmosphere profile.

The maximum density given by Weidner (1967) for 1000 kilometers (1×10^{-16} g/cc) compares favorably with the maximum from the VM-3 extension (3×10^{-15} g/cc). Recalling that the latter was thought to be quite conservative, the difference between the two values is perhaps to be expected. In addition, since the VM-3 extension totally neglects variations of molecular weight with altitude, while the MSFC maximum density model accounts for such variations, the latter appears to be reasonable.

From the viewpoint of providing a common reference atmosphere and associated extremes, the preliminary models of Weidner (1967) should be utilized. Tabulations of the minimum, mean, and maximum density models were included in milestone report VOY-D4-TM-4 (Vachon, 1967) and are also available in the recent report by Weidner and Hasseltine (1967).

6.6 VARIATION OF ATMOSPHERIC DENSITY

6.6.1 DIURNAL VARIATION

The atmospheric density in the Earth's upper atmosphere at 1000 kilometers varies by about one order of magnitude from a minimum at 0400 hours to a maximum at 1400 hours during maximum solar activity periods. Although the magnitude of the dirunal variation of density is about a factor of 3 during periods of low solar activity, occasionally larger variations are encountered even during these periods.

In regards to the Martian atmosphere, it is likely that diurnal variations of density of an order of magnitude are likely to be encountered at orbital altitudes around 1000 kilometers. In a previous estimate of the variation of density on Mars (Vachon, 1966), diurnal variations of about two orders of magnitude were suggested as being probable during periods of high solar activity. However, based on more recent evaluations of the probable density variations as a function of solar activity, which are discussed in the following section, it appears that this earlier estimate was overly pessimistic. Indeed, from the density values given in Table 6-9 (presented in Section 6.6.2), it is seen that the diurnal density variation is about one order of magnitude.

6.6.2 SOLAR CYCLIC VARIATIONS

The range of density values at 1000 kilometers given by Weidner and Hasseltine (1967) is expected to reflect the range of variation likely to be experienced over the full solar cycle. The full range of the Martian density variations at 1000 kilometers is about 3×10^5, according to the models of Weidner and Hasseltine.

In order to relate the probable distribution of density as a function of solar activity within this range, the Harris and Priester models of the Earth's atmosphere are again considered. The range of density variation at 1000 kilometers from a period of low solar activity (S = 70) to a period of high solar activity (S = 250) is found to be about three orders of magnitude. The distribution of density at 1000 kilometers in models of the terrestrial and Martian atmospheres is given in Table 6-8.

Table 6-8. Distribution of Density at 1000 Kilometers in Models of the Terrestrial and Martian Atmospheres

S	Density (g/cc)	Range	Remarks
200 to 250	3×10^{-18} to 1.3×10^{-16}	$\sim 10^{2}$	Priester and Harris
70 to 100	2×10^{-19} to 1.7×10^{-18}	$\sim 10^{1}$	Models of Earth's
70 to 250	2×10^{-19} to 1.3×10^{-16}	$\sim 10^{3}$	atmosphere at 1000 km
Mean to maximum	5.97×10^{-19} to 1.4×10^{-16}	$\sim 2\text{-}3 \times 10^{2}$	Weidner and Hasseltine models of Mars atmosphere at 1000 km
Minimum to mean	5.03×10^{-22} to 5.97×10^{-19}	$\sim 10^{3}$	
Minimum to maximum	5.03×10^{-22} to 1.4×10^{-16}	$\sim 3 \times 10^{5}$	

From a comparison of the density values and the range of variation given in Table 6-8, several possibilities are suggested. First, the range of density variation in the Martian mean-to-maximum model agrees closely with that expected during a period of high solar activity. Second, the range of density variation in the Martian minimum-to-mean model is much greater than would be expected during a period of low solar activity. Third, the full range of density variation in the Martian atmosphere models is almost twice as large as that expected in the Earth's atmosphere. On the basis of the above comparisons it would appear reasonable to assume the mean-to-maximum density models to be representative of periods of high solar activity. On the other hand, assuming the minimum-to-mean density models to be representative of periods of low solar activity, would appear to introduce a greater range of variation than would be encountered by analogy with the Harris and Priester models.

In order to provide an estimate of the probable variation of the atmospheric structure as a function of solar activity, the mean atmosphere model of Weidner and Hasseltine (1967) was modified. The modification consisted of altering the thermal structure above 100 kilometers by substitution of the thermosphere thermal gradient values given in Table 6-6, together with the exosphere temperature values given in Table 6-2. This rather simple modification

provides a means of estimating the probable variation of the atmosphere as a function of solar activity for any given model. In the case of the Weidner and Hasseltine mean model, the resulting range of density variation as a function of solar activty (Table 6-9) was found to closely agree with that obtained from the Harris and Priester (1962) models.

Table 6-9. Variation of the Martian Atmospheric Density at 700 Kilometers as a Function of Solar Activity

	Solar Flux (S)				
	250	200	150	100	70
Minima	5×10^{-17}	2.2×10^{-17}	7×10^{-18}	1.8×10^{-18}	6.2×10^{-19}
Maxima	4.2×10^{-16}	2.2×10^{-16}	8×10^{-17}	2.4×10^{-17}	8.2×10^{-18}

From the values in Table 6-9, it is seen that the density at 700 kilometers during a period of high solar activity is likely to be almost three orders of magnitude greater than during a period of low solar activity. At an altitude of 1000 kilometers, the calculated density variations indicate a three-order-of-magnitude spread over the full solar cycle. As noted in the preceding section, the diurnal variation of density is seen from Table 6-9 to amount to about one order of magnitude.

Based on the calculated values for the modified Weidner and Hasseltine mean model, as well as similar calculations using other models, it appears unlikely that the density at 1000 kilometers will vary by much more than three orders of magnitude over the full solar cycle. However, since the composition of the upper atmosphere is uncertain, the range of density variations must be increased to allow for this uncertainty. As noted previously, the Weidner maximum density profile was in reasonable agreement with the expected highly conservative VM-3 model extension. Thus, if the uncertainty in the composition is to produce an increase in the range of density values at any given altitude, then the range should be increased to include less dense atmospheres.

MSFC's (Weidner and Hasseltine models) mean to maximum density profiles would thus provide a reasonable range of density values for periods of high solar activity. The MSFC mean to minimum density profiles would, by the same token, provide a reasonable range of density values for periods of moderate to low solar activity.

6.7 CONCLUSIONS

Based on the Mariner IV ionospheric experiment data, the base of the thermosphere may be as low as 105 km. The thermal gradient is expected to range in value for 0.5° to 3.0°K/km during periods of low to high solar activity respectively. The MSFC maximum density envelope compares favorably with the maximum density profile from the VM3 extension (the MSFC density at 1000 kms being less than 1 order of magnitude below the VM3 extended model value). The MSFC mean density profile compares favorably with the older GE Voyager reference atmosphere. The MSFC mean density value at 1000 kms is approximately 1 order of magnitude greater than that obtained from the GE Voyager reference model. The MSFC mean density profile and associated confidence envelopes were found to be consistent with most models presently available.

Estimates of the variations of the atmospheric structure as a function of solar activity were prepared and indicate:

a. The density at altitudes of about 1000 kilometers is likely to exhibit a diurnal (day-night) variation of an order of magnitude.

b. The atmospheric density at 1000 kilometers during a period of high solar activity is likely to be three orders of magnitude greater than it is during a period of low solar activity.

c. Solar cyclic variations of the atmosphere's density at 1000 kilometers of five and six orders of magnitude are expected to result more from uncertainties in the models than from probable variations of the atmosphere itself.

d. The MSFC mean-to-maximum density profiles appear reasonable for periods of high solar activity.

e. The MSFC mean-to-minimum density profiles appear adequate to define the density likely to be encountered during a period of moderate to low solar activity.

6.8 REFERENCES

Chamberlain, J.W., and McElroy, M. B., "Martian Atmosphere: The Mariner Occultation Experiment," Science, 152, No. 3718, April 1, 1966.

Donahue, T. M., "Upper Atmosphere and Ionosphere of Mars," Science, 152, May 6, 1966.

Galbraith, T. L., Personal Communication, GE-MSD, August 22, 1967.

Gross, S.H., McGovern, W.E., and Rasool, S.I., "Mars: Upper Atmosphere," Science, 151, March 11, 1966.

Harris, I., and Priester, W., "Theoretical Models for the Solar-Cycle Variation of the Upper Atmosphere," NASA-TN-D-1444, August 1962.

Hess, D.S., and Pounder, E., "Voyager Environmental Predictions Document," SE-003-BB001-1B28, NASA-JPL, October 1966.

Johnson, F.S., "Atmosphere of Mars," Science, 150, 1965.

Newburn, R., personal communications, NASA-JPL, July 7, 1966.

Smith, N., and Beutler, A.E., "A Model Martian Atmosphere and Ionosphere," University of Michigan, draft copy of paper, April 1967.

Spencer, D., personal communication, NASA-JPL, Feburary 8, 1967.

Vachon, D.N., and Homsey, R.J., Design Environments for Missions to Mars and Venus, GE-TIS-63SD344, December 1963.

Vachon, D. N., "On the Distribution of Density at Orbital Altitudes in the Martian Atmosphere," GE-TM-8126-5, June 1966.

Vachon, D. N., "Proposed Voyager Mars Reference Atmosphere for Planetary Quarantine Studies," GE-PIR-8126-196, Feburary 1967.

Weidner, D. K., "Preliminary Models and Confidence Envelopes for the Mars Atmosphere," Presented at the Planetary Mission Board Meeting, June 16, 1967 and at the Voyager Science Panel Meeting, June 21, 1967, NASA-MSFC, 1967.

Weidner, D. K., and Hasseltine, C. L., "Natural Environment Design Criteria Guidelines for MSFC Voyager Spacecraft for Mars 1973 Mission," NASA-MSFC-TMX-53616, June 8, 1967.

SECTION 7

CLOUDS AND HAZE

SECTION 7

CLOUDS AND HAZE

7.1 INTRODUCTION

The presence of clouds or obscurations over the surface of Mars has important applications in spacecraft design. These applications are quite extensive and are related to a variety of spacecraft subsystems, such as attitude control, scientific experiments package, thermal control, etc. Since the principal interest in design concerns the cloud composition and altitude, these will be provided along with a brief discussion of their other characteristics which may be of interest.

7.2 BLUE HAZE

When Mars is observed at wavelengths of less than 4500 Å, the surface appears blurred by a haze which quite naturally is termed a blue haze. In a previous treatment (Vachon, 1966), two separate blue haze regions were proposed, one lying below 200 kilometers and the other below 10 kilometers. Evans et. al. (1967) suggest that the blue haze lies somewhere between 5 and 200 kilometers, but they do not necessarily suggest the presence of two separate layers. The preference for two separate layers is largely intuitive and favors an upper haze layer which is likened to the Earth's noctilucent clouds. Recently, Palm and Basu (1965) indicated that a correlation appears to exist between the number of meteor showers observed on Earth and the blue haze of Mars. The blue haze has been observed to vanish during certain periods. These periods of "blue clearing" may be of a diurnal nature (Robinson, 1966), with clearing tending to occur around local noon.

In regard to the probable lower layer, it is intuitively expected that this lower region is composed of dust from the surface. Opik (1962) suggests that the optical properties of the blue absorbing haze, and its clearings, are due to variable amounts of dust particles having dimensions on the order of 0.1 micron. If it is assumed that the upper layer is composed largely of material of interplanetary origin, while the lower haze layer is

composed largely of material of planetary origin, many apparent conflicts on the characteristics of the blue haze can be resolved.

7.3 BLUE CLOUDS

The blue clouds are thought to be concentrations of the blue haze by many, while others would suggest that these clouds have characteristics which are somewhat different from the blue haze. For example, Hess and Pounder (1966) indicate that the cloud particle size is on the order of 0.1 micron, while Evans, et. al. (1967) suggest a particle size near 2 microns in diameter.

Evans et. al. (1967) indicate that blue clouds "occur most frequently from 15 to 25 km, and may occur up to 100 km in the atmosphere." It may be possible to resolve the disagreement on particle size estimates by interpreting the estimate of Evans et. al. (1967) as being more representative of the lower altitude blue clouds. The droplet size estimate of Hess and Pounder (1966) as well as Opik (1962) would then be interpreted as representative of the upper altitudes of blue clouds and the blue haze.

In general, the blue clouds are expected to be similar to the cirriform clouds of Earth and to be composed of transparent droplets or particles.

7.4 WHITE CLOUDS

White clouds are frequently observed near the edge of the disc, in polar regions, and near the sunrise and sunset terminator. The polarization of the clouds indicates that they are likely composed of ice crystals of about 1 micron in size, (Evans et. al., 1967; Hess and Pounder, 1966). The possibility does exist that these clouds may be composed of CO_2 rather than H_2O. In general, the hypothesis of H_2O clouds is favored since one can find an immediate analogy to the cirriform clouds of the Earth. Schorn, et. al. (1967) indicate that from their study of photographic data, white clouds are more frequent in occurrence during spring than at any other time. On the basis of this preferential time of occurrence, they suggest that the clouds result from an increase in the H_2O content

associated with the receding north polar cap and prior to the forming of the south polar cap. This concept is supported by Wells (1967), who found a definite correlation between the maximum frequency of observed white clouds and the maximum rate of mass transfer from each pole. Wells concludes from this correlation that the white clouds and polar caps are composed of the same substance, whether CO_2 or H_2O.

The altitude of the white clouds has been estimated as below 30 kilometers (Vachon 1966); 15 to 25 kilometers (Hess and Pounder, 1966); and 15 to 50 kilometers (Evans et. al., 1967).

7.5 YELLOW CLOUDS

Although a rather detailed discussion of yellow clouds has already been presented in Section 4.4 of this report, it is in order to summarize the pertinent characteristics.

The particle size of yellow clouds is estimated as ranging from 1 to 100 microns by Hess and Pounder (1966) and from 1 to 20 microns or more by Evans et. al. (1967). The estimate of particle size is heavily influenced by the mechanism responsible for the generation of these clouds.

The altitude of the yellow clouds is estimated as being 3 to 30 kilometers by Hess and Pounder (1966), while Evans et. al. (1967) indicate that yellow clouds occur more frequently at an altitude range of 5 to 9 kilometers.

The introduction of dust clouds and projections, discussed in Section 4.4, would provide a means of accommodating both estimates.

7.6 CONCLUSIONS

Based on observed cloud motions, there appear to exist preferential regions over which the white and yellow clouds occur, as well as preferential time periods during which they are most likely to be observed. An analysis of a selected data sample of observed motions

of clouds, which are thought to exist at different altitudes on Mars, indicates that even a limited sample of observed motions of white and yellow clouds may provide a means of assessing the horizontal and vertical circulation characteristic of the atmosphere.

7.7 REFERENCES

Evans, D. E., Pitts, D. E., and Kraus, G. L., "Venus and Mars Nominal Natural Environment for Advanced Manned Planetary Mission Programs," NASA SP-3016, Second Edition, 1967.

Hess, D. S., and Pounder, E., "Voyager Environmental Predictions Document," SE-003-BB001-1B28, NASA-JPL, October 1966.

Opik, E. J., "Atmosphere and Surface Properties of Mars and Venus," Progress in the Astronautical Sciences, Ed. S. F. Singer, Vol. I, North Holland Publ., 1967.

Palm, A., and Basu, B., "The Blue Haze of Mars," Icarus 4, pp. 111-118, 1965.

Robinson, J. C., "Ground-Based Photography of the Mariner IV Region of Mars," Icarus 5, pp 245-247, 1966.

Schorn, R. A., Spinrad, H., Moore, R. C., Smith, H. J., Giver, L. P., "High-Dispersion Spectroscopic Observations of Mars, II. The Water-Vapor Variations," Astrophysical J., 147, February 1967.

Vachon, D. N., "Design Environments for Missions to Mars," GE-TM-8126-8, August 1966.

Wells, R. A., "Some Comments on Martian White Clouds," Astrophysical J., 147, March 1967.

SECTION 8

CHEMICAL KINETICS AND COMPOSITION

SECTION 8

CHEMICAL KINETICS AND COMPOSITION

8.1 INTRODUCTION

In order for some experiments which have been suggested for Martian atmosphere exploration to be successful, it is important to have well founded predictions of the atmospheric composition as a function of altitude. The major component indicated by available data is carbon dioxide. However, at high altitudes where solar flux in the effective wavelength range of from 1300 to 1650Å is available, the carbon dioxide is largely dissociated. It is therefore not sufficient to know that the Martian atmosphere is largely CO_2 and that N_2 is present. Rather, the major species to be expected at each altitude should be known. The fraction of CO_2 dissociated at various altitudes depends not only upon the solar flux but also on a number of reactions, some of which involve minor species. Only a thorough chemical kinetics investigation involving such minor species and many reactions can establish these primary features.

In this study, the possible importance of a number of minor species and many reactions was tested. Previous studies used only an extremely simple chemical system with the result that the compositions so determined may be somewhat erroneous because of these simplifications. The present study has been conducted to be as complete in its chemical kinetics as necessary to avoid this problem. Provisions have been made for adding other features in the future whereby the present study can be made more comprehensive.

8.2 ATMOSPHERIC DATA

The predictions of the atmospheric composition must be based on available data and must agree with them within their limits of uncertainty. Such available data have been described and discussed in detail (e.g.; Fjeldbo et.al., 1966 a, b, Chamberlain, 1962; Chamberlain and McElroy, 1966; Spinrad et.al., 1966; Owen, 1966; and Edelson, 1967). These data are limited primarily to pressure, spectra, and electron density measurements. The information acquired from these measurements give direct usable estimates of pressure as a

function of altitude, pressure scale height, electron density as a function of altitude, and total CO_2 content. From these, indirect estimates of number density, temperature, and certain other quantities have been made. The latter estimates involve certain assumptions which introduce considerable uncertainty in the derived quantities. Since some of these quantities are used in the calculations to be described, these calculations will involve similar uncertainties. It is possible that disagreement between the predicted composition resulting from this study and data obtained in experiments to be conducted on the Martian atmosphere will help in reducing the uncertainty in the derived quantities used as inputs in this study.

The data which are used in the calculations are: the number density as a function of altitude; the relative elemental composition; and of lesser importance, temperature. The number densities were taken from Fjeldbo et al., 1966.

Since the CO_2 content of the Martian atmosphere, as determined by spectral measurements, appears to be nearly as large as the total density derived from the pressure measurements, the composition of the atmosphere has been assumed to be at least 80% CO_2 and perhaps as much as 100% CO_2. For cases where the composition consists of less than 100% CO_2, the remaining material is usually assumed to be nitrogen. The latter assumption was accepted in performing the calculations, but a further study with other gases as the remaining material would seem in order. The elemental compositions assumed for the calculations were:

a. 0.8 C; 1.6 O; 0.4 N
b. 0.9 C; 1.8 O; 0.2 N
c. 1 C; 2 O

The total density as a function of altitude is shown in Figure 8-1.

The solar flux incident at the top of the Martian atmosphere was obtained by modifying the corresponding values obtained for the Earth, through use of correction factors (Allen, 1963) to account for the different heliocentric distances.

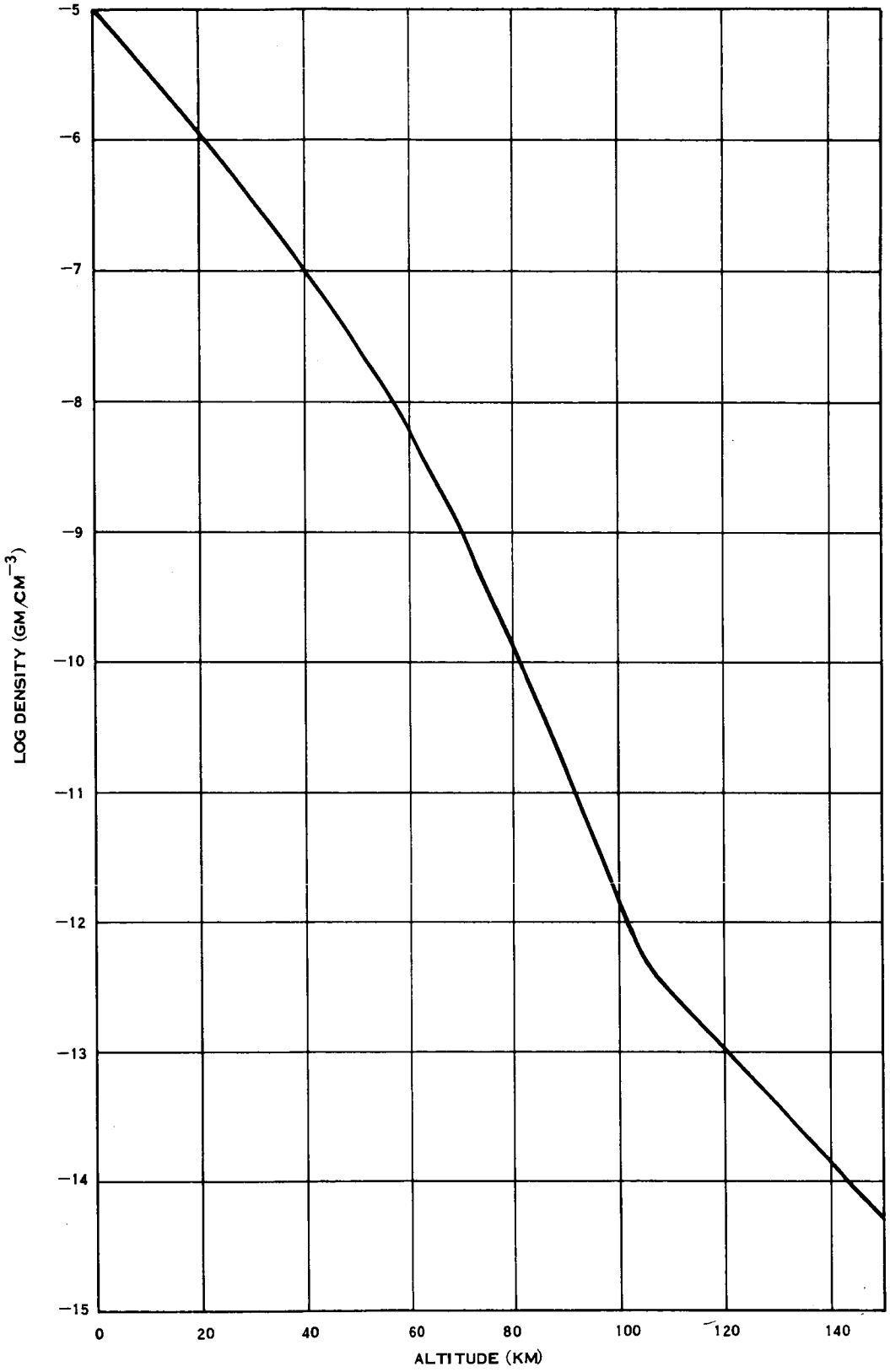

Figure 8-1. Density of Martian Atmosphere as a Function of Altitude

8.3 CHEMICAL SYSTEM AND CHEMICAL KINETICS

8.3.1 CHEMICAL SPECIES

Calculations have been made of the steady-state concentrations as a function of altitude. The concentrations are those of eighteen species comprised of: seven neutral species, free electrons, seven positive ions, and three negative ions. The specific species considered were:

CO_2	CO_2^+	O^-
N_2	N_2^+	O_2^-
N	N^+	O_3^-
CO	CO^+	e
O	O^+	
O_2	O_2^+	
O_3	NO^+	

The concentrations calculated were steady-state concentrations for an average solar flux and for a flux increased by a factor of 2.3 at all wavelengths. (Time-vaying concentrations should be calculated using normal flux variations; however, such calculations were considered to be outside the scope of the present study.)

The calculations included the various photochemical processes and the other chemical reactions which appreciably affect the concentrations of the major species of interest. The attenuation of the flux through the atmosphere was calculated along with the changes in concentrations resulting from the photochemical processes.

8.3.2 THE CHEMICAL PROCESSES

As noted previously, the flux at the top of the Martian atmosphere was calculated by comparing it with that at the top of the Earth's atmosphere. Calculations were started at 150 km, an altitude sufficiently high that the attenuation above it would be negligible. The total number density was determined at this altitude from the calculations described in Section 8.3.1. At this and at each succeeding lower altitude, the rates per reacting particle of each of the various photoionization and photodissociation processes were determined by integrating the product of the solar flux and the effective cross section over the wavelength range of importance. These integrals are then first-order rate constants since each, when multiplied by the appropriate concentration, gives the rate of the process. These and the other chemical processes were then used to determine steady-state concentrations. These concentrations would be expected to be reached only after considerable time. At altitudes where diffusion can play a role, steady-state conditions would actually never be reached. (The consideration of diffusion is another modification which should be carried out in the future, but which is considered outside the scope of the present study.)

Forty-four reactions were included in the chemical kinetics calculations, and included photoionization, photodissociation, photodetachment, three-body neutral-neutral recombinations, neutral rearrangement, dissociative ion-electron recombination, three-body electron attachment, dissociative attachment, associative detachment, ion-ion recombination, positive-ion charge transfer and charged rearrangement, and negative-ion charge transfer and charged rearrangement reactions. These are listed in Table 8-1 along constants used in the study.

The rate constants used were taken from various reference sources. Some of them are known with an uncertainty of perhaps 20 percent, but others are only estimated. Obviously, this will introduce uncertainties in the calculations. A major source of uncertainty in these rate constants is the temperature effect. This is due to lack of accurate data on the temperature variation of the rate constants and to the uncertainty in the temperature itself. All rate constants were evaluated at 200°K although the temperature may be appreciably

lower at some altitudes. Since the value of rate constants at lower temperatures, especially those of the order of $100^{o}K$, is not known, the use of values at $200^{o}K$ for all altitudes appeared reasonable.

After the concentrations of the eighteen species are calculated at each altitude, the rates of six other reactions not included in the iterative calculations, are calculated to permit an estimation of their importance and the effect of their omission. The reactions and the rate constants used were:

Reactions		Rate Constants (sec)
$N_2^+ + O^- \longrightarrow$	$N_2 + O$	3×10^{-7}
$N_2^+ + O \longrightarrow$	$N_2 + O^+$	1×10^{-12}
$N_2^+ + O \longrightarrow$	$NO^+ + N$	2.5×10^{-10}
$N^+ + CO_2 \longrightarrow$	$NO^+ + CO$	1×10^{-11}
$O_3^- + CO_2 \longrightarrow$	$CO_3^- + O_2$	4×10^{-10}
$N + O + M \longrightarrow$	$NO + M$	1.3×10^{-32}

Although the system of eighteen species and fifty reactions appears to be rather complex, a closer examination shows that other species and other reactions are also important. For example, the major negative ion at low altitudes is none of the three included in the fifty reactions but rather CO_3^-, formed by the reaction

$$O_3^- + CO_2 \longrightarrow CO_3^- + O_2$$

Table 8-1. Chemical Reactions and Rate Constants Used in the Chemical Kinetics Calculations

Reactions	Rate Constants (sec)
Photoionization	
$CO_2 + h\nu \longrightarrow CO_2^+ + e$	
$N_2 + h\nu \longrightarrow N_2^+ + e$	
$CO + h\nu \longrightarrow CO^+ + e$	
$O + h\nu \longrightarrow O^+ + e$	
$O_2 + h\nu \longrightarrow O_2^+ + e$	
$N + h\nu \longrightarrow N^+ + e$	
Photodissociation	
$CO_2 + h\nu \longrightarrow CO + O$	
$O_2 + h\nu \longrightarrow O + O$	
$O_3 + h\nu \longrightarrow O + O_2$	
Photodetachment	
$O^- + h\nu \longrightarrow O + e$	
Dissociative recombination	
$CO_2^+ + e \longrightarrow CO + O$	2.5×10^{-7}
$N_2^+ + e \longrightarrow N + N$	3.0×10^{-7}
$NO^+ + e \longrightarrow N + O$	5.0×10^{-7}
$O_2^+ + e \longrightarrow O + O$	2.9×10^{-7}
Ion-ion recombination	
$CO_2^+ + O^- \longrightarrow CO_2 + O$	3×10^{-7}
$CO_2^+ + O^- \longrightarrow CO + O + O$	3×10^{-7}
$NO^+ + O_3^- \longrightarrow N + O + O_3$	3×10^{-7}
$CO_2^+ + O_3^- \longrightarrow CO_2 + O_2$	3×10^{-7}
$O_2^+ + O_3^- \longrightarrow O_2 + O_3$	3×10^{-7}
Attachment	
$O + e + M \longrightarrow O^- + M$	1×10^{-32}
$O_2 + e + M \longrightarrow O_2^- + M$	1×10^{-30}
$O + e \longrightarrow O^- + h\nu$	1.3×10^{-15}
Associative detachment	
$O_2^- + O \longrightarrow O_3 + e$	3×10^{-10}
$O^- + CO \longrightarrow CO_2 + e$	8×10^{-10}

Reactions	Rate Constants (sec)
Charge transfer, positive ion	
$N_2^+ + CO_2 \longrightarrow N_2 + CO_2^+$	9×10^{-10}
$N_2^+ + CO \longrightarrow N_2 + CO^+$	7×10^{-10}
$N_2^+ + N \longrightarrow N_2 + N^+$	1×10^{-12}
$N_2^+ + O_2 \longrightarrow N_2 + O_2^+$	2×10^{-10}
$N^+ + CO_2 \longrightarrow N + CO_2^+$	1.3×10^{-9}
Charge transfer, positive ion	
$CO^+ + O \longrightarrow CO + O^+$	1×10^{-11}
$CO^+ + CO_2 \longrightarrow CO + CO_2^+$	1.1×10^{-9}
$CO_2^+ + O \longrightarrow CO_2 + O^+$	1×10^{-11}
Charged rearrangement, positive ion	
$CO_2^+ + N \longrightarrow NO^+ + CO$	1×10^{-11}
$CO_2^+ + O \longrightarrow O_2^+ + CO$	1×10^{-11}
$O^+ + CO_2 \longrightarrow O_2^+ + CO$	1.2×10^{-9}
$O^+ + N_2 \longrightarrow NO^+ + N$	3×10^{-12}
$O_2^+ + N \longrightarrow NO^+ + O$	2×10^{-10}
Charge transfer, negative ion	
$O_2^- + O_3 \longrightarrow O_2 + O_3^-$	3×10^{-10}
$O^- + O_3 \longrightarrow O + O_3^-$	7×10^{-10}
Three-body neutral recombination	
$CO + O + M \longrightarrow CO_2 + M$	1×10^{-35}
$O + O + M \longrightarrow O_2 + M$	9.8×10^{-33}
$N + N + M \longrightarrow N_2 + M$	1.1×10^{-32}
$O + O_2 + M \longrightarrow O_3 + M$	1.8×10^{-33}
Neutral rearrangement	
$O + O_3 \longrightarrow O_2 + O_2$	7.7^{-16}

This specie was not included in the basic calculations in order to permit simplification. An estimate of the amount of O_3^-, derived from the amount of CO_3^-, is being provided later in this report. Deriving the amount of O_3^- from the amount of CO_3^- is reasonable since the major mechanism by which either is removed is ion-ion recombination

$$X^+ + O_3^- \longrightarrow \text{neutral products}$$

$$X^+ + CO_3^- \longrightarrow \text{neutral products}$$

8.3.3 KINETICS OF INDIVIDUAL SPECIES

As mentioned previously, the concentrations of the important species depend upon numerous reactions some of which involve minor species.

CO_2 is dissociated and ionized by solar flux and is also consumed by several charge exchange reactions. Although it is reformed by the three-body recombination of CO and O, other reactions involving ions (mainly O^+ and various negative ions) provide faster production of CO_2. This is shown schematically in the flow diagram in Figure 8-2. At low altitudes there is little dissociation since the effective flux is absorbed at higher altitudes. At higher altitudes, CO_2 is largely dissociated because the reactions forming CO_2 are slow. At intermediate altitudes, there is a steady-state in which several reactions are important.

The kinetics of CO and of O are shown schematically in Figures 8-3 and 8-4, respectively. The reactions shown are those which appear to be the most important in controlling the various concentrations of interest. The chemical kinetics of N_2 are shown schematically in Figure 8-5.

8.4 METHOD OF CALCULATION

The rates of all the reactions were calculated using any set of trial concentrations which were required only to fit the elemental composition assumed. Then the ratios, for each specie, of the rate at which it is being formed to the rate at which it is being consumed, was

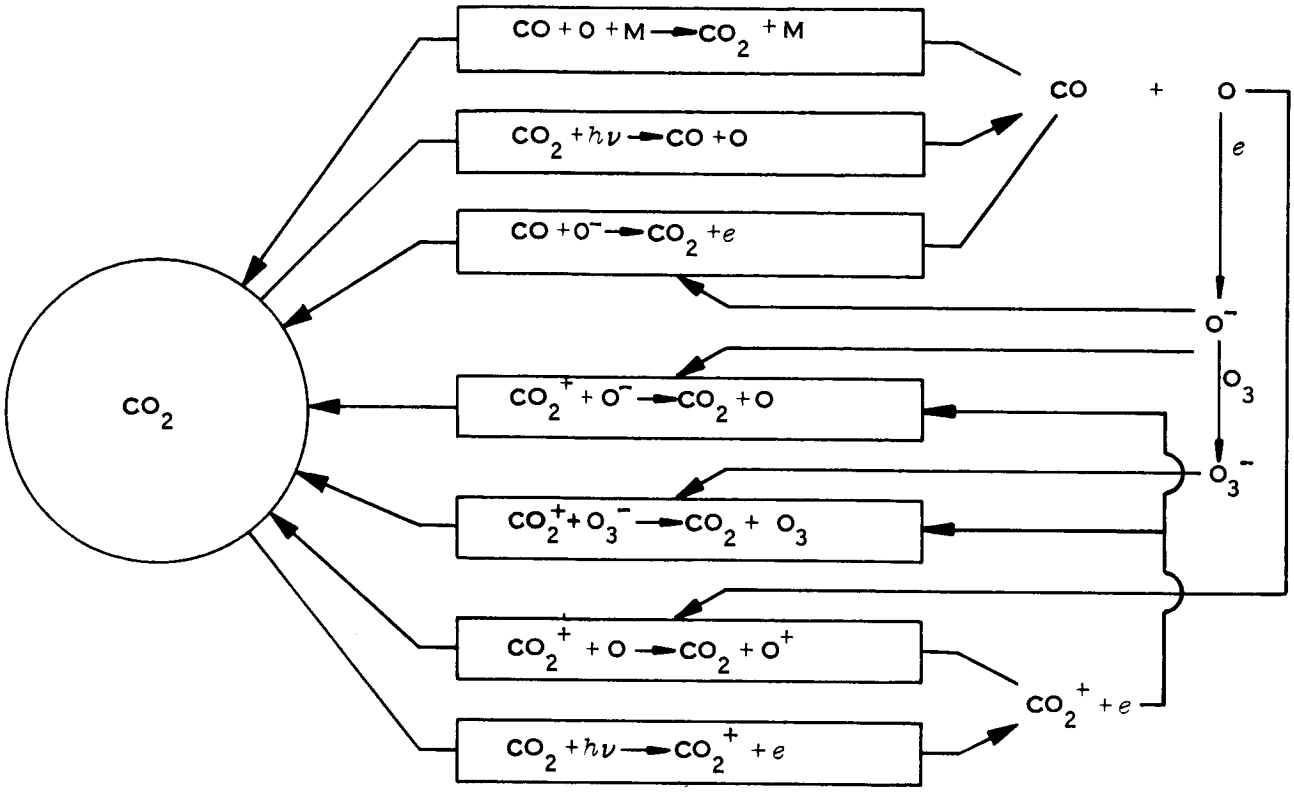

Figure 8-2. Schematic Representation of CO_2 Kinetics in Martian Atmosphere

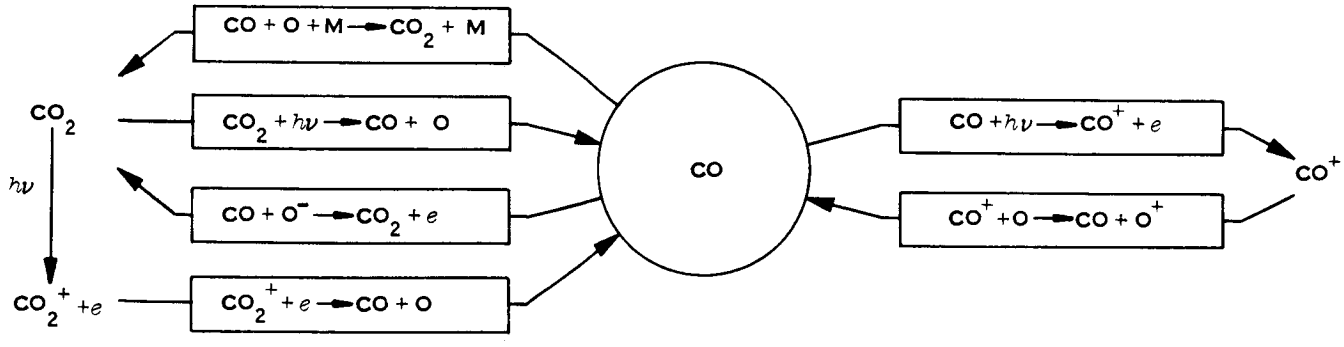

Figure 8-3. Schematic Representation of CO Kinetics in Martian Atmosphere

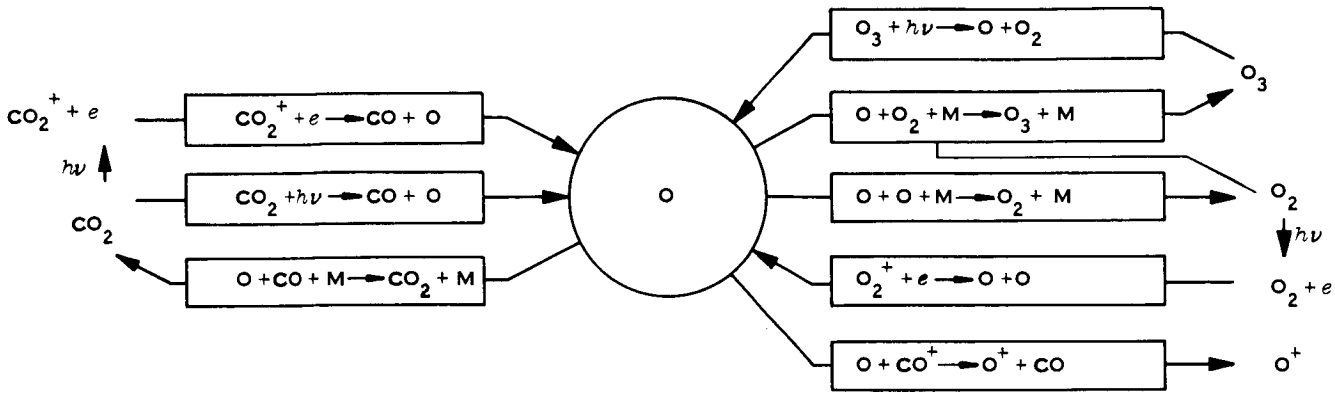

Figure 8-4. Schematic Representation of Chemical Kinetics of Atomic Oxygen in Martian Atmosphere

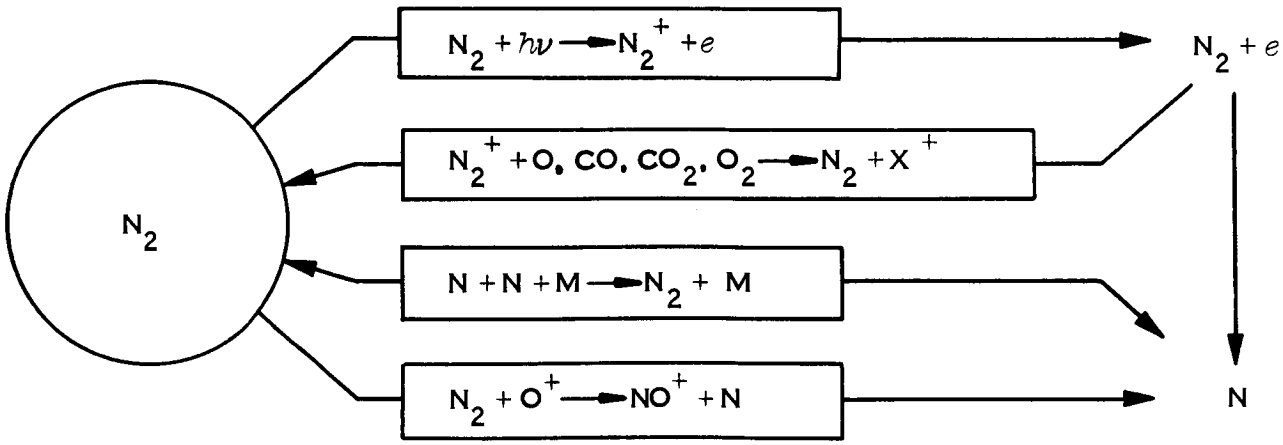

Figure 8-5. Schematic Representation of Chemical Kinetics of N_2 in Martian Atmosphere

calculated. The individual concentrations were then changed to bring them closer to the steady-state values, by making the ratios nearer unity by a factor of as much as 1.5. Several concentrations (including: one carbon-containing species, one oxygen-containing species, one nitrogen-containing species, and one negatively charged species), were calculated by balance so that the total number of atoms and the elemental composition would not be changed. The species so calculated were usually those of the highest concentration. The procedure was then iterated a number of times until the ratios were all very close to unity. The attenuation of flux, as a function of wavelength, was then calculated for a five kilometer altitude interval, assuming the composition and flux attenuation to be constant over that altitude range and equal to that in the middle of the altitude range. The flux so determined, was then used as the initial flux for the calculation of conditions at an altitude five kilometers lower. The procedure was repeated for each 5-kilometer altitude increment down through the atmosphere.

This same calculation was carried out for each of the assumed atmospheres, that is, for each of the three assumed elemental compositions and for two different fluxes.

A flow diagram of the Computer Program is shown in Figure 8-6.

8.5 ATMOSPHERIC COMPOSITION

8.5.1 NEUTRAL SPECIES

The calculated atmospheric composition provides the concentrations of the eighteen species listed in Section 8.3.1.

Figures 8-7, 8-8, and 8-9 graphically give the results for the neutral species.

The calculations predict CO_2 to be more than half dissociated at altitudes above 60 km. This is a somewhat lower altitude than given in other predications (Fjeldbo et. al. 1966 and Chamberlain, 1962), but the data should be reliable because they are calculated from a consideration of the detailed flux and its attenuation through the atmosphere. CO and O are

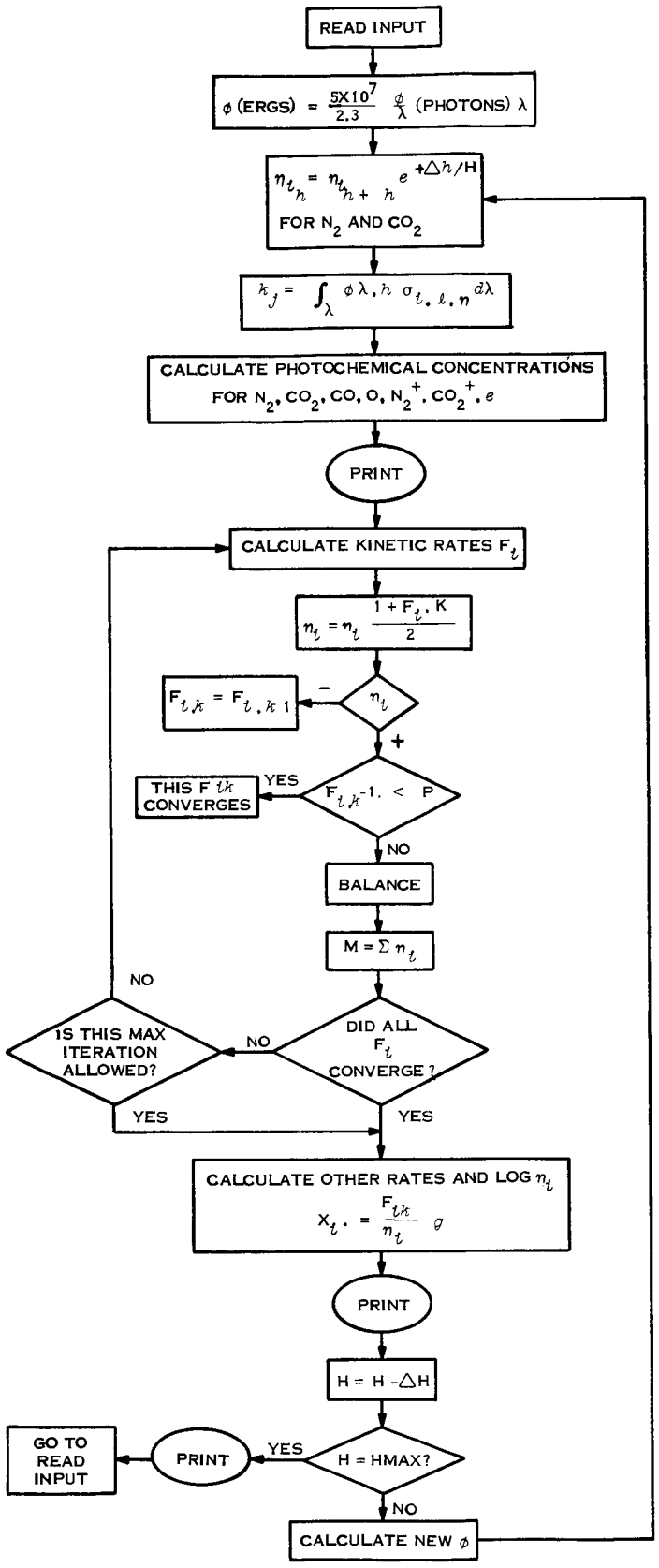

Figure 8-6. Flow Diagram of Computer Program Used for Martian Atmosphere Composition Calculations

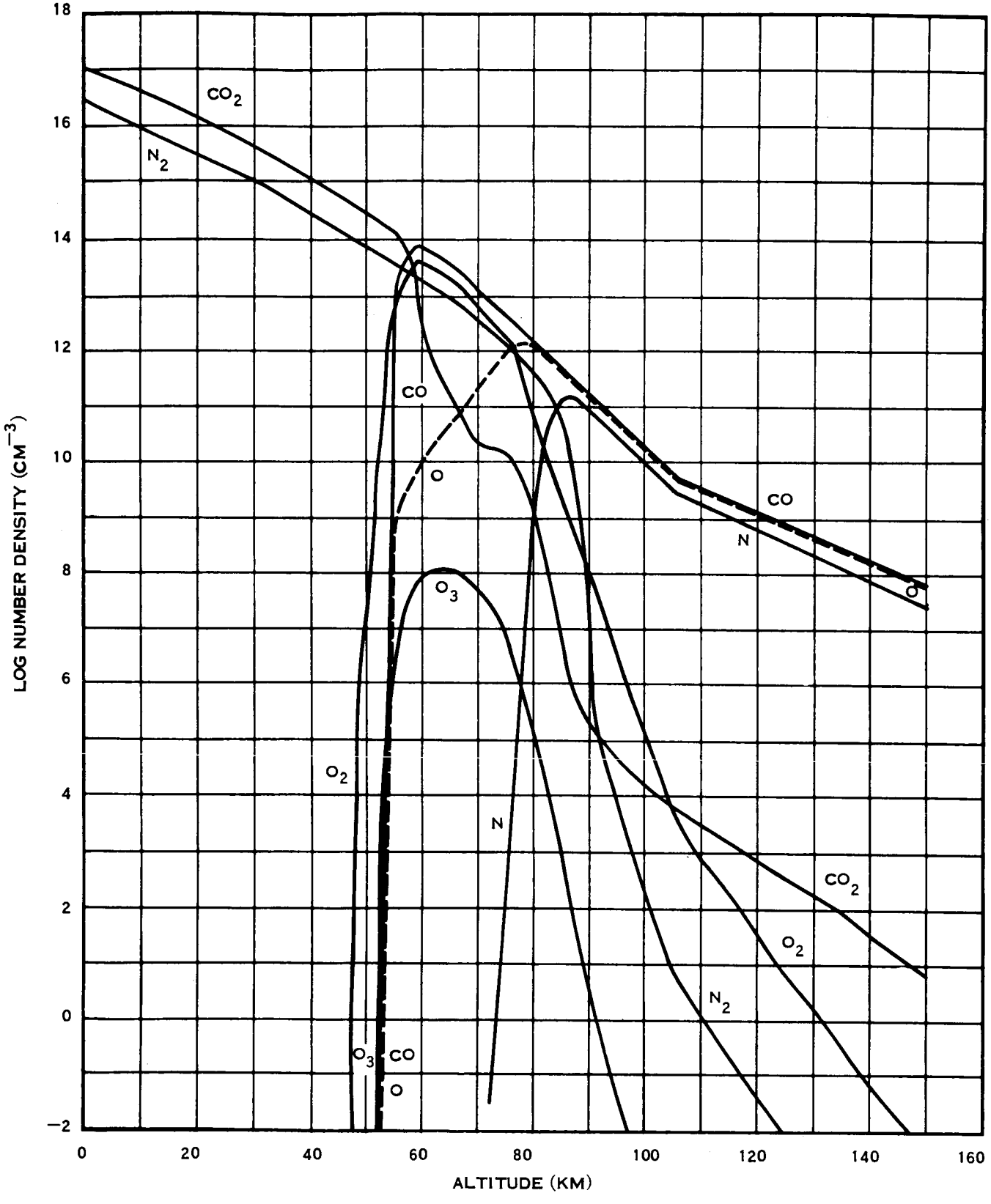

Figure 8-7. Calculated Neutral Species Concentrations (80% CO_2, 20% N_2)

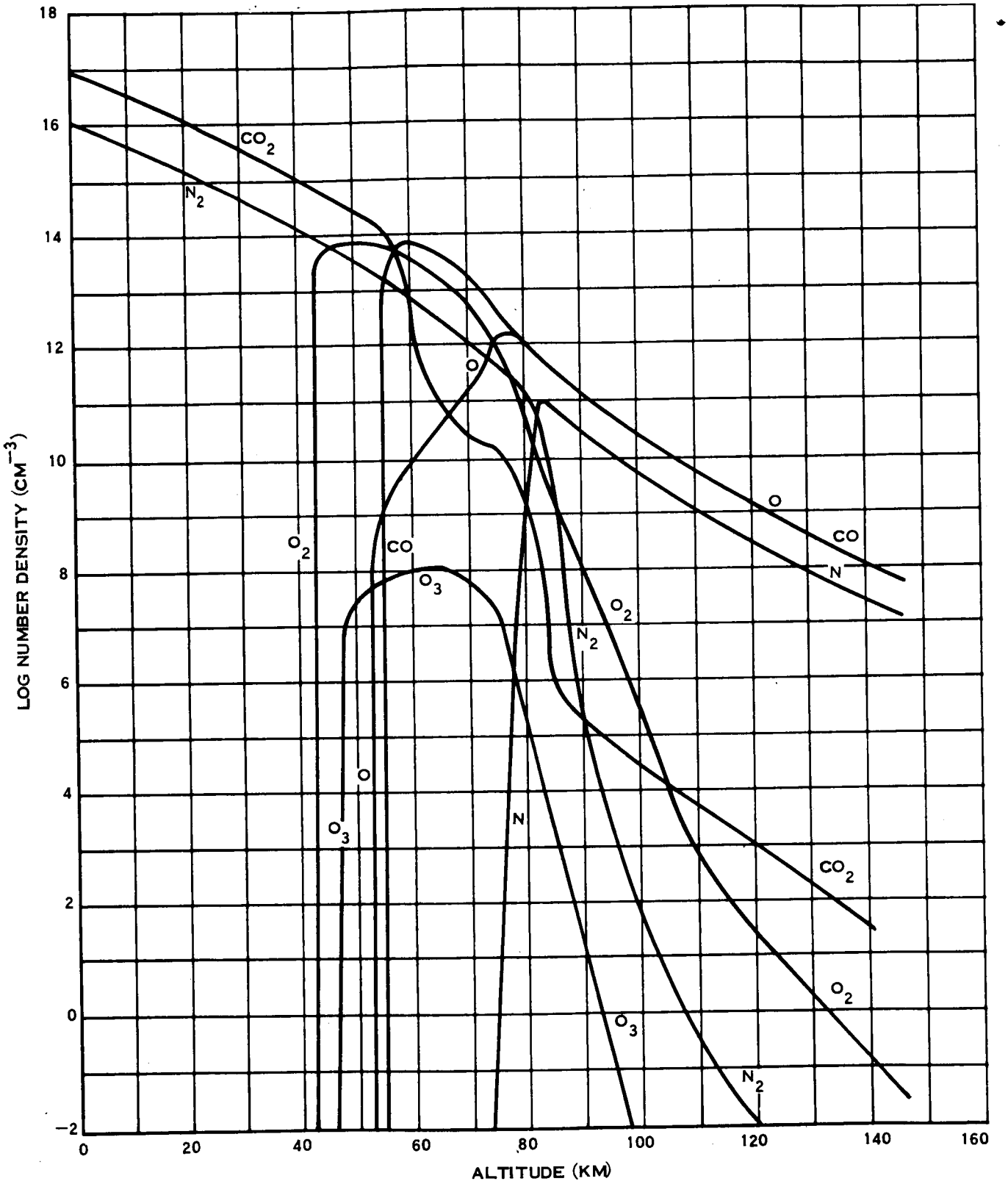

Figure 8-8. Calculated Neutral Species Concentrations (90% CO_2, 10% N_2)

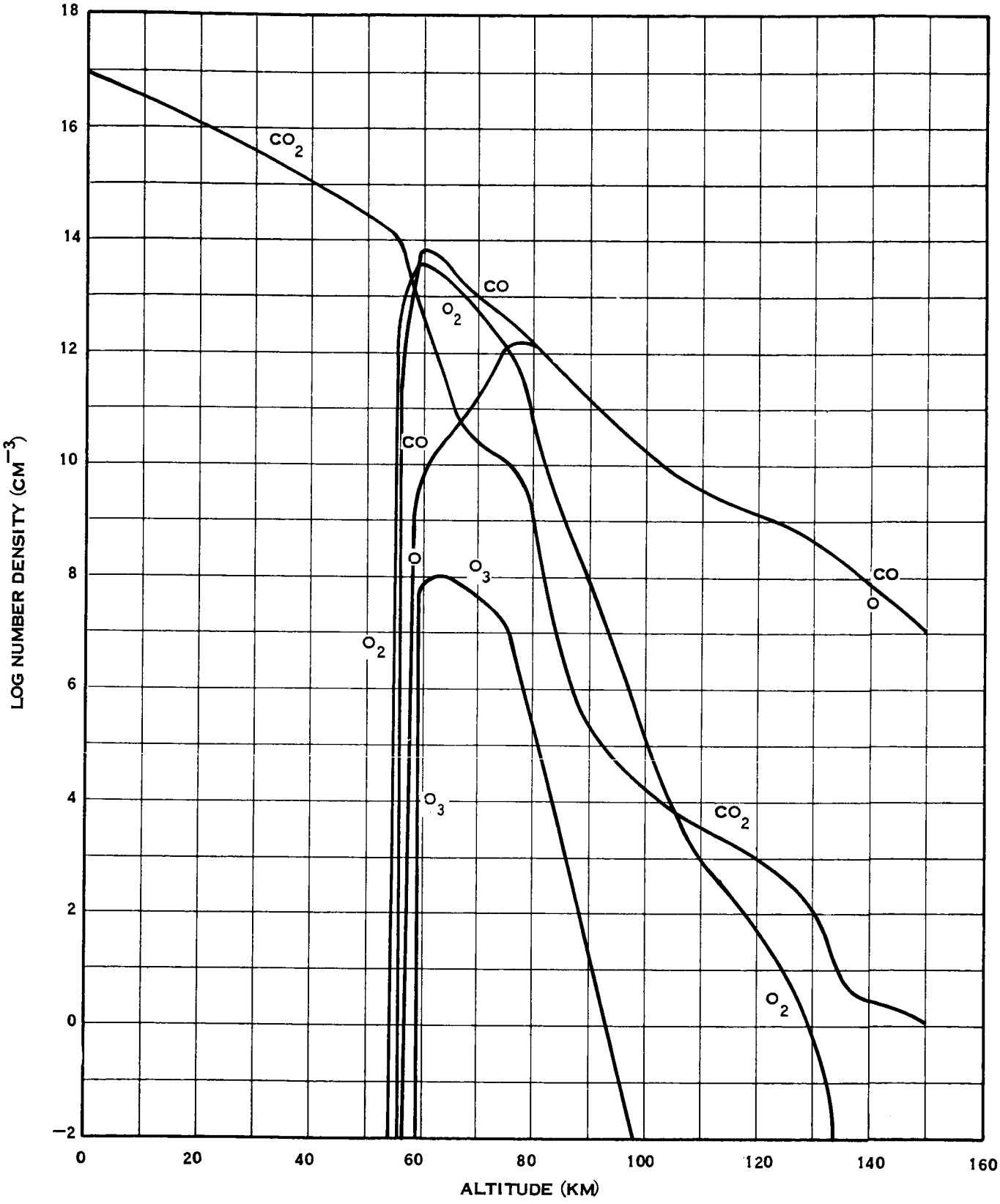

Figure 8-9. Calculated Neutral Species Concentrations (100% CO_2)

the major species initating from CO_2 and have approximately equal concentrations down to about 80 km. Below this, CO continues to increase to a peak at about 60 km while O decreases due to the formation of O_2 which is important in the 50 to 90 km range. Ozone is present in concentrations of as large as about one part per million peaking at about 65 km.

In the atmospheres considered where nitrogen was included, it was found to be largely dissociated above 85 km. Data on reactions not included in the iterative calculations, indicate that nitrogen oxides are not important, although a more complete investigation would be required to eliminate this possibility completely. It appears that some NO may be formed but would be consumed rapidly by the N + NO reaction. The data obtained are sufficient to make a more complete analysis of certain facets of the kinetics such as the nitrogen oxide effects. This should be carried out when time permits.

The three atmospheres considered did not give drastically different results for the neutral species. The preceeding findings appear to hold for all three compositions. There is little variation of the altitude of the peaks or even of their magnitude among the three cases (other than the obvious change in nitrogen content).

8.5.2 CHARGED SPECIES

The results of the calculations of the charged species are less reliable than those of the neutral species. The data obtained showed total charge densities which were much higher than the available experimental data indicate. However, it is believed that the relative concentrations of the charged species are reliable. The data, therefore, are presented in this form; that is, concentration relative to the electron density. The data are shown in Figures 8-10, 8-11 and 8-12. The charged species data below 85 km are not reliable since the electron density is extremely low and all ion kinetics are dependent upon the electron density. Above 125 km there is also some doubt about certain of the species, although in general they appear reasonable.

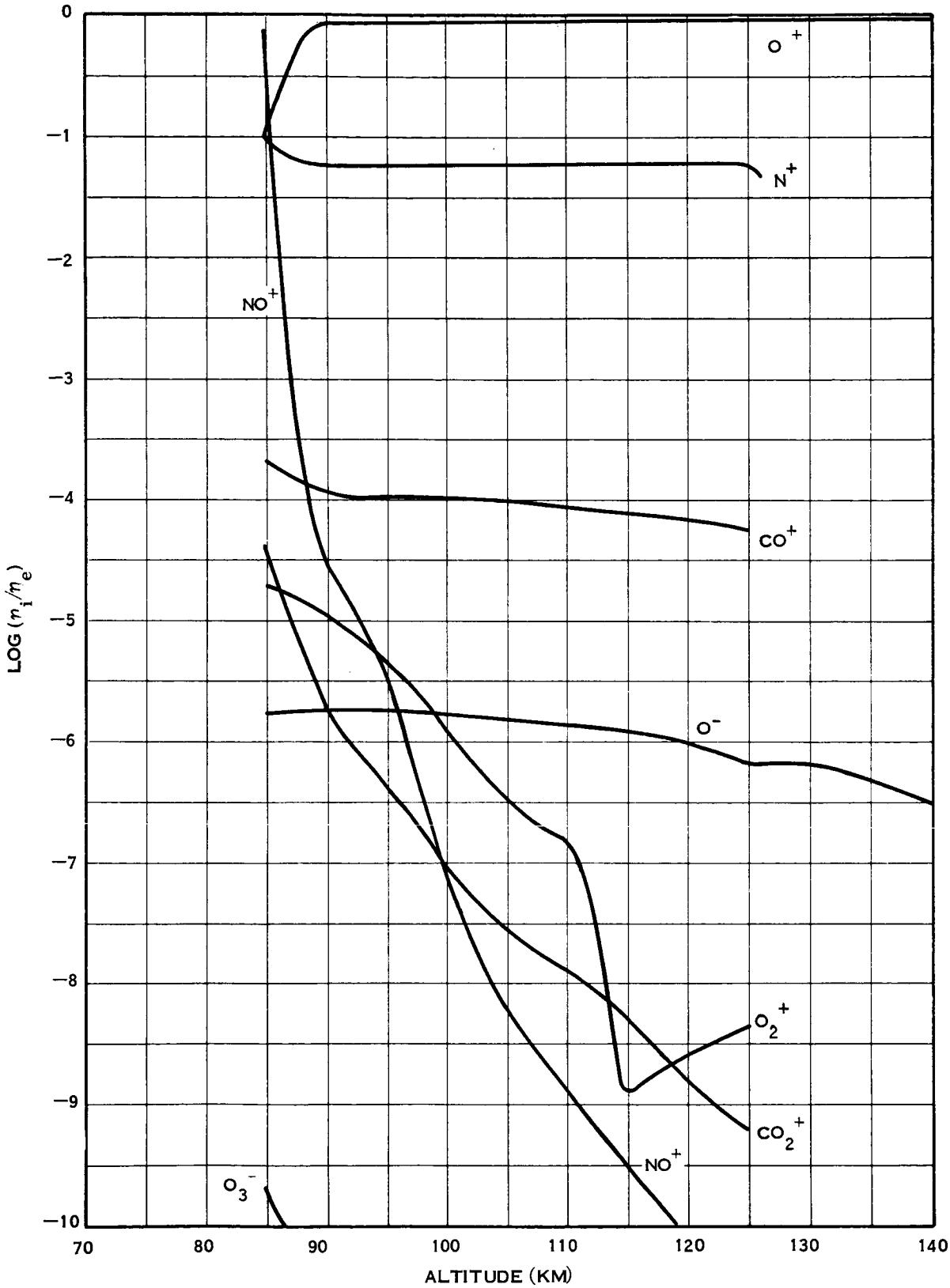

Figure 8-10. Ion Concentrations Relative to Electron Density (80% CO_2, 20% N_2)

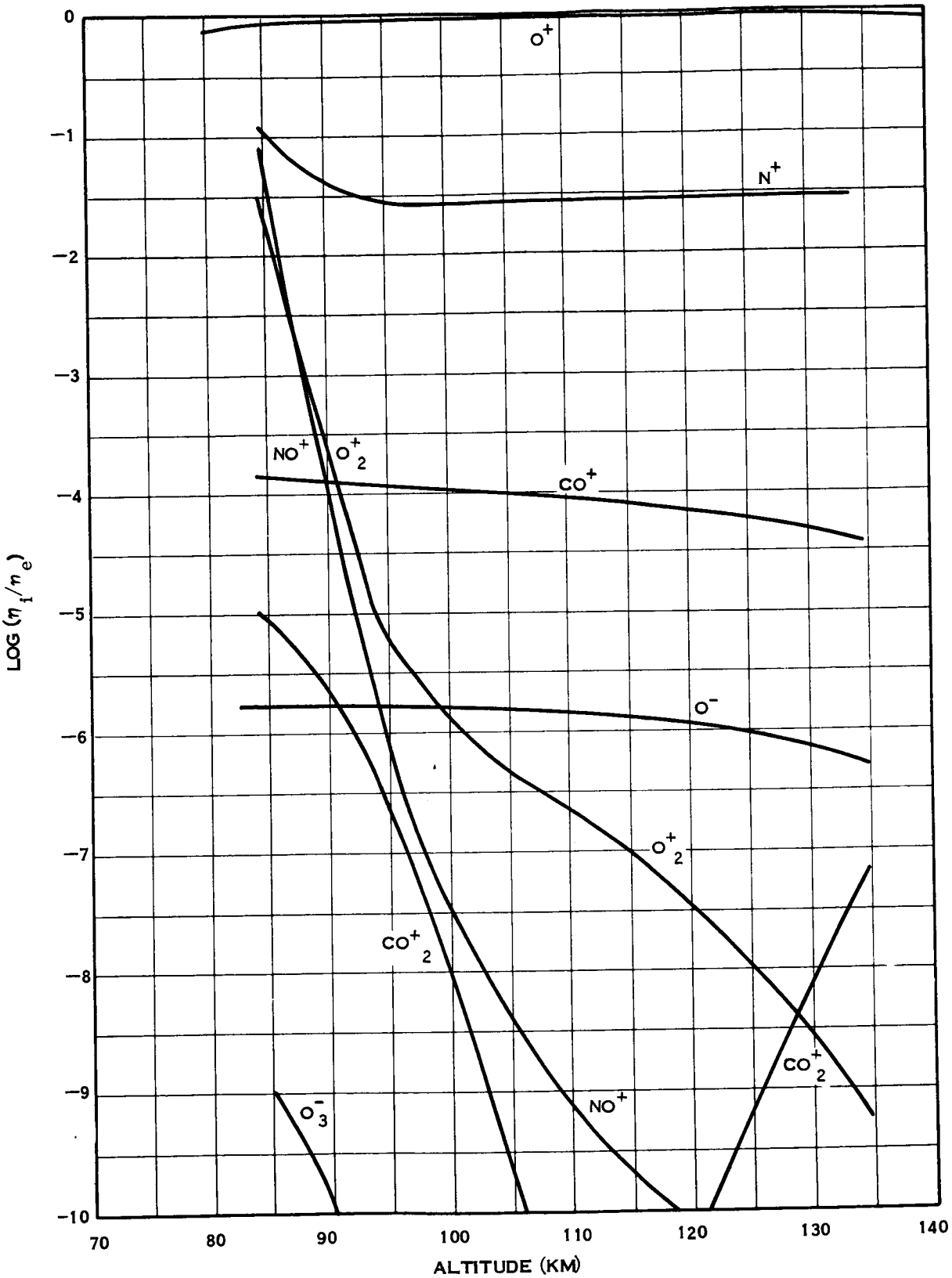

Figure 8-11. Ion Concentrations Relative to Electron Density (90% CO_2, 10% N_2)

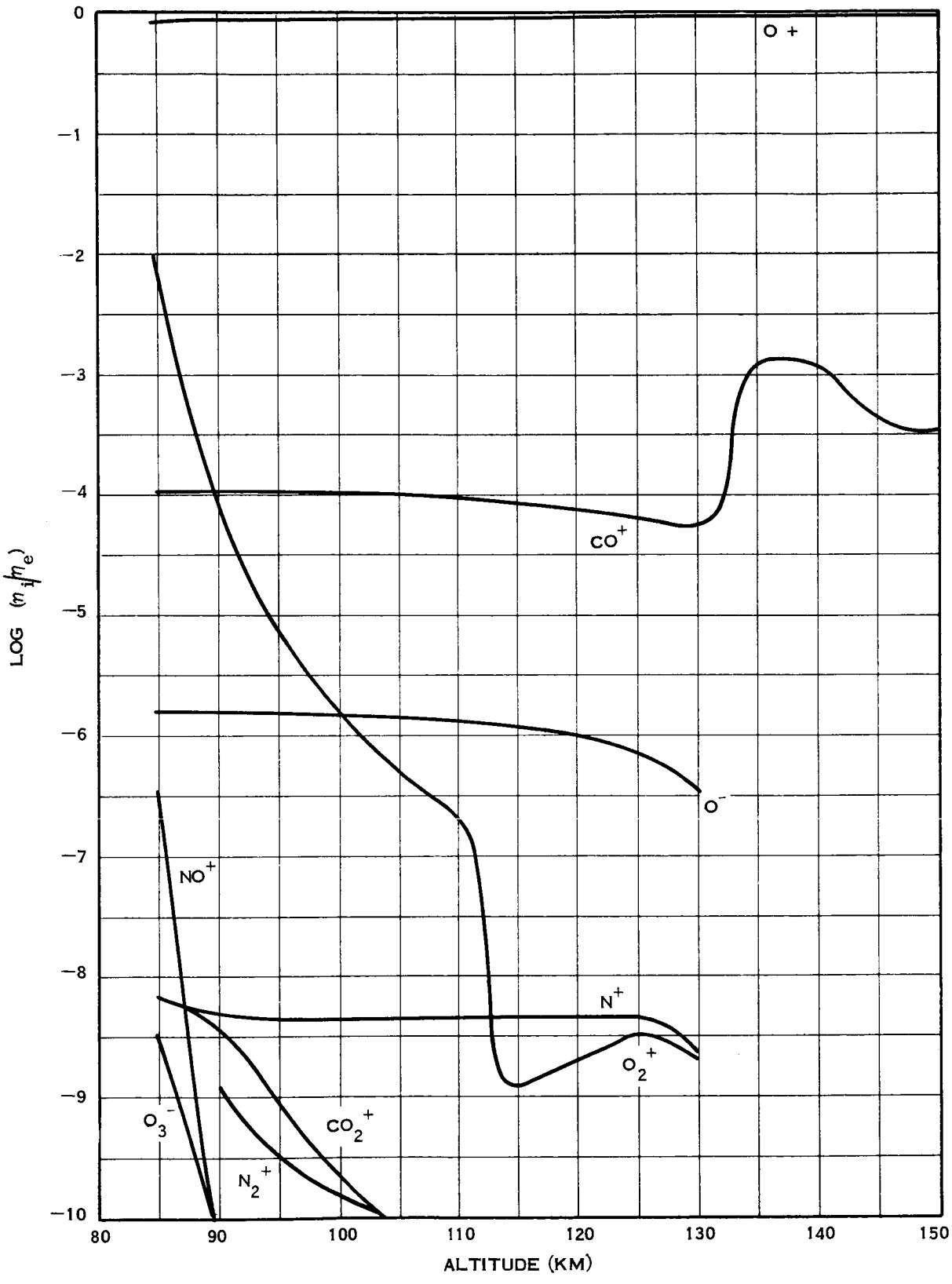

Figure 8-12. Ion Concentrations Relative to Electron Density (100% CO_2 - 0.1 PPM N_2)

Due to the difficulties in obtaining charged species concentrations above 125 km, the location of the electron density peak could not be located with high accuracy. However, in all cases, the electron density dropped off below 125 km and when any data were obtained above this, a decrease was indicated. This would agree with the findings of Fjelbdo, et al, 1966a. It is noted that diffusion would tend to change the electron densities rather than to shift the peak.

In most cases considered, O^+ is the major ion present. With appreciable nitrogen included in the atmosphere, NO^+ does become important at low altitudes and even becomes the predominant ion at 85 km in the 20% N_2 case. The importance of O_2^+ and CO_2^+ was found to increase at low altitudes.

No negative ions become important at altitudes below 85 km; e.g., O^- is present in the largest concentration but only amounts to about 10^{-6} of that of the free electrons. O_2^- is important only in leading to other negative ions, and this is of minor significance. O_3^- is found to build up at low altitudes but not to significant concentrations. It is probable that some negative ions are present at altitudes below 85 km. These, as discussed previously, are mainly CO_3^- (probably over 90 percent) with some O_3^-. However, it is unlikely that the ion densities at lower altitudes are large enough to be important.

8.5.3 THE SOLAR FLUX

The solar flux is attenuated as it passes down through the atmosphere. The flux as a function of wavelength is shown for several altitudes in Figure 8-13 for the 80% CO_2 - 20% N_2 atmosphere and as a function of altitude for several wavelengths in Figure 8-14. The attenuation above 110 km is small. Below this altitude, the flux at wavelengths below 900 Å is rapidly attenuated and is essentially completely absorbed by 85 km. Since this is the most important radiation for ionization, there is little ionization below this, as indicated in Section 8.5.2. The flux between 900 and 1350 Å persists to slightly lower altitudes as is illustrated by the dotted lines which represent a maximum and a minimum in the CO_2 cross section. The flux from 1350 to 1600 Å is effective in dissociating CO_2. Because the absorption coefficients (cross sections) for dissociation are smaller than for ionization, the

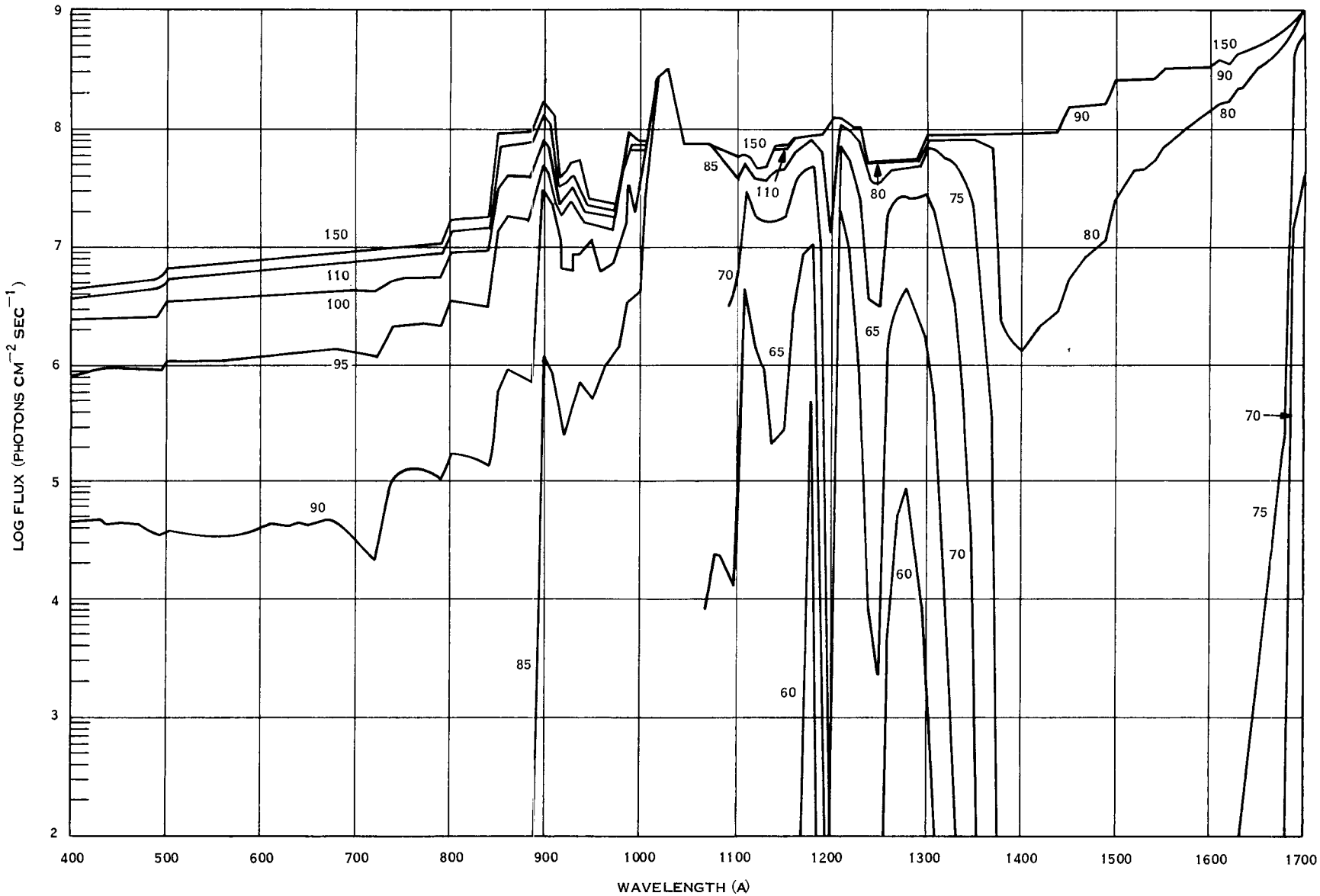

Figure 8-13. Flux at Various Altitudes as a Function of Wavelength (80% CO_2, 20% N_2)

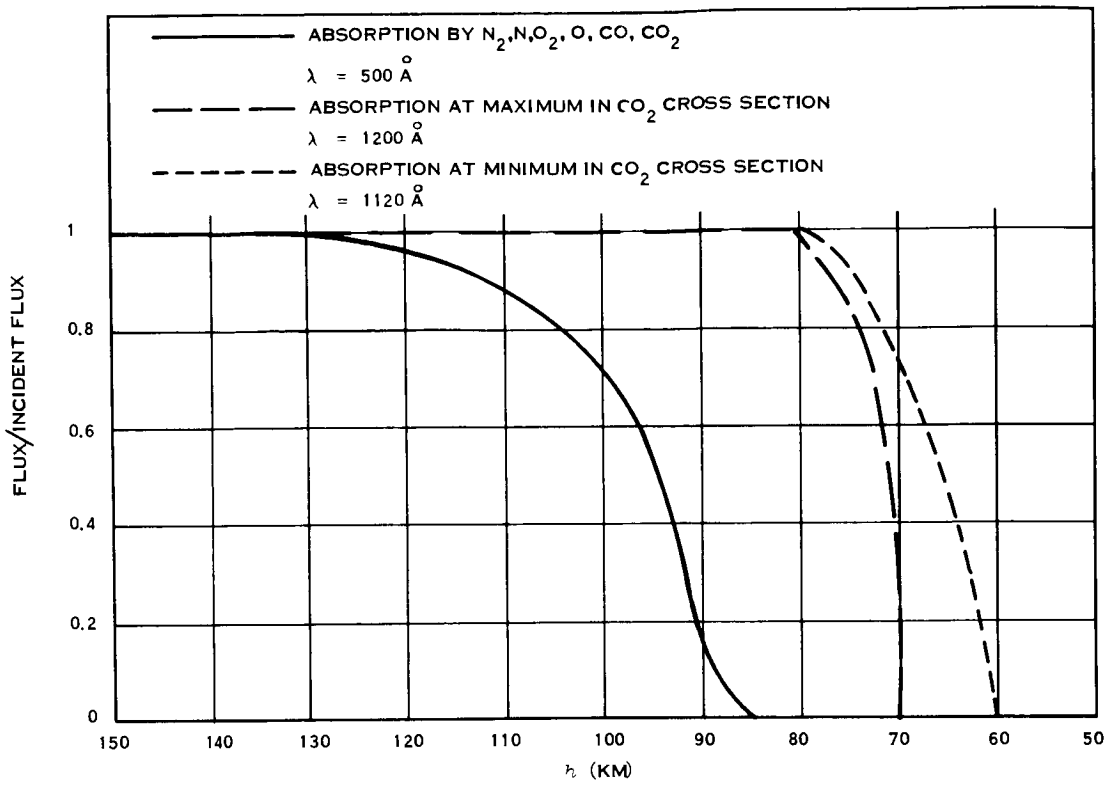

Figure 8-14. Flux/Incident Flux Versus Altitude

effective flux persists to slightly lower altitudes than does the radiation of less than 900 Å, which is completely absorbed by the time it reaches an altitude of a little below 80 km.

The flux attenuation for the other atmospheres is not greatly different from that given above. In the case of the higher flux used, the attenuation was at about the same rate although the curves in Figure 8-13 would be moved to higher intensities; the relative results of Figure 8-14 would not be changed. Thus, examination of the results for the two cases indicates that the degree of ionization and dissociation would be increased for the species O_2, N_2^+, N^+, O^-, NO^+, O^+, CO^+, O_3^- and e but would not change significantly for the species CO, O, CO_2, N_2 N, CO_2^+, O_2^+, O_2^- and O_3.

8.5.4 THE DIFFUSION PROBLEM

Major uncertainties in the preceding calculations arise from the omission of any diffusion processes. Considerable work was carried out on this problem and a method of including diffusion in the calculations has been detailed. The following describes this work.

In addition to photochemical processes, the structure of the Martian atmosphere is controlled by diffusion. At high altitudes, this can be illustrated by noting that, as the pressure decreases the molecular diffusion coefficient increases. Thus, in comparison with the decreasing chemical reaction rates, molecular diffusion becomes dominant. On the other hand, at low altitudes the interaction of the planetary surface with the atmosphere causes winds and related phenomena to smooth chemical variations by turbulent mixing. The following discussion presents a mathematical model of the diffusing Martian atmosphere and qualtitively examines the altitude regions which are controlled by diffusion and chemistry.

In a dynamic atmosphere, the flux of the diffusing species is related to the chemical production rates by the species continuity equations.

$$\frac{dN_i}{dh} = S_i^+ - S_i^- \qquad (8\text{-}1)$$

where

N_i = particle flux of species i (particles/cm^2 sec)

h = altitude

S_i^+ = sum of the rates of all reactions producing species i (particles/cm^3 sec)

S_i^- = sum of the rates of all reactions removing species i (particles/cm^2 sec)

Because charge neutrality is preserved, the summation of N_i over all charged species must be zero. Thus, if there are L species considered in an atmospheric model, there are L -1 independent equations in the set, Equation 8-1, and a charge balance

$$\sum_i Z_i N_i = 0 \tag{8-2}$$

where

Z_i = charge on species i

The Stefan-Maxwell relations as generalized to a multicomponent mixture relate the diffusion fluxes to the concentration, pressure, and electric field driving forces present in the model atmosphere. These equations are well documented in the literature and were obtained from Hirshfelder, et. al., 1954.

$$\sum_j \frac{X_j N_i - X_i N_j}{n D_{ij}} = \frac{d X_i}{dh} + X_i \left(1 - \frac{M_i}{\bar{M}}\right) \frac{d \ln P}{dh} - \frac{X_i Z_i E}{k T} \tag{8-3}$$

$$\sum_i \sum_j \frac{X_j N_i - X_i N_j}{n D_{ij}} = 0 \tag{8-4}$$

where

X_i = mole fraction of species i

n = total number density

D_{ij} = binary diffusion coefficient of species i and j

M_i = molecular weight of species i

$\bar{M}$ = average molecular weight of gas

P = pressure

E = electric field induced by charge separation

k = Boltzmann constant

T = temperature

Charge balance then supplies the equation for the induced electric field.

$$\frac{E}{kT} \sum_j X_j Z_j^2 = -\sum_j \frac{X_j Z_j M_j}{\bar{M}} \frac{d \ln P}{dh} - \sum_j \frac{Z_j}{n} \sum_i \frac{X_j N_i - X_i N_j}{D_{ij}} \tag{8-5}$$

Note that the above equations do not use binary, ambipolar diffusion coefficients since these are not applicable to a multicimponent mixture per se. (Blanc's law must be employed.) However, this effect has been considered by the inclusion of the induced electric field. Several auxiliary relationships are necessary to complete the model; these include the hydrostatic equation:

$$\frac{dp}{dh} = -\rho g = -\frac{p}{H} \tag{8-6}$$

where

ρ = mass density

g = acceleration due to gravity

H = scale height

and the equation of state

$$P = nkT$$

or

$$P = \frac{R}{\bar{M}} \rho T \tag{8-7}$$

Examination of Equations 8-1 through 8-7 indicates a coupled set of differential and algebraic equations, which relate the diffusion fluxes and species concentrations to the solar flux (photochemistry) and the gravitational attractive force of the planet. As mentioned above, the dominant terms in the equations are a strong function of altitude with diffusion controlling the upper atmosphere and chemistry important near the Martian surface. It is of interest to qualitatively determine the altitude region where both effects are of the same order.

Rearrangement of the left hand side of Equation 8-3 results in the approximate expression

$$\sum_j \frac{X_j N_i - X_i N_j}{n D_{ij}} \approx \frac{N_i}{n D_{ij}} \tag{8-8}$$

An approximate flux for species i can be obtained by neglecting the chemical loss terms, S_i^-, and integrating Equation 8-1 over altitude.

$$N_i \approx \int_h^\infty S_i^+ \, dh \tag{8-9}$$

thus combining Equations 8-3, 8-8 and 8-9

$$\frac{d X_i}{dh} \approx \frac{\int_h^\infty S_i^+ \, dh}{n D_{ij}} - \frac{X_i}{H}\left(1 - \frac{M_i}{\bar{M}}\right) \tag{8-10}$$

Examination of the two terms on the right hand side of Equation 8-10, using the results of the previously desceibed nondiffusing atmospheres, indicates that a very sharp distinction between diffusion and chemical dominance is achieved between 85 and 105 km. This is illustrated for electrons in Table 8-2 using the results for the 90% CO_2 10% N_2 atmosphere.

Table 8-2. Comparison of Diffusion and Chemical Dominance

Altitude (km)	Chemistry $\frac{\int_h^\infty S_i^+ \, dh}{n D_{ij}}$	Diffusion $\frac{X_i}{H}\left(1 - \frac{M_i}{\bar{M}}\right)$
85	1.4×10^{-9}	2.8×10^{-13}
90	1.2×10^{-9}	1.1×10^{-9}
95	6.5×10^{-10}	1.1×10^{-9}
100	3.7×10^{-10}	5.1×10^{-9}
105	2.1×10^{-10}	1.9×10^{-8}
110	1.3×10^{-10}	3.7×10^{-8}
115	7.2×10^{-11}	7.2×10^{-8}

Thus, it can be concluded that diffusion will play a major role in determining the profile of the electron density. Note that diffusion will not alter the position of the peak significantly. However the maximum concentration would be expected to decrease.

8.6 CONCLUSIONS

Based on the results obtained for the neutral species, it is found that CO_2 is more than 50 percent dissociated at all altitudes above 60 km. Above this, CO and O are major constituents. Ozone is present in quantities of as much as one part per million. Nitrogen oxides probably do not build up in large concentrations.

Charged species are more difficult to predict. Above 80 km electrons are the only important negatively charged species. Below this, negative ions, especially CO_3^-, become important but none build up to large concentrations. The major positive ions are O^+, N^+ and CO^+ at high altitudes and NO^+ at lower altitudes.

8.7 REFERENCES

Allen, C.W., Astrophysical Quantities, Athlone Press, London 1963.

Bortner, M.H., DASA Reaction Rate Handbook, DASA No. 1948, 1967a.

Bortner, M.H., "A Critical Review of Rate Constants in High Temperature Air," NBS NSRDS Report, to be published, 1967.

Chamberlain, J.W., Ap. J. 136, 582, 1962.

Chamberlain, J.W. and M. McElroy, Science 152, 21, 1966.

Craig, R.A., The Upper Atmosphere, Academic Press, New York, 1965.

Edelson, S., private communication, 1967.

Fjeldbo, G., W.C. Fjeldbo and V.R. Eshelman, J. Geophys. Res. 71, 2307, 1966a.

Fjeldbo, G., W.C. Fjeldbo and V. R. Eshelman, Science 153, 1518, 1966.

Hirshfelder, J.O., Curtiss, C.F., and Bird, R.B., Molecular Theory of Gases and Liquids, John Wiley, 1954.

Loeb, L.B., Basic Processes of Gaseous Electronics, University of California Press, 1955.

Owen, T., Ap. J. 146, 257, 1966.

Spinrad, H., R.A. Schorn, R. Moore, L.P. Giver and H. J. Smith, Ap. J. 146, 331, 1966.